Development of *Rhodosporidium toruloides* NCYC 921 fed-batch cultures for simultaneous production of lipids and carotenoids

Vasco Marques Martins

Thesis to obtain the Master of Science Degree in

Biological Engineering

Supervisors:
Dr. Maria Teresa Saraiva Lopes da Silva, Ph.D.
Prof. José António Leonardo dos Santos

Examination Committee

Chairperson: Prof. Duarte Miguel de França Teixeira dos Prazeres
Supervisor: Dr. Maria Teresa Saraiva Lopes da Silva, Ph.D.
Members of the Committee: Prof. Helena Maria Rodrigues Vasconcelos Pinheiro

June 2015

This page
was intentionally
left blank

Acknowledgments

This work is for my family. Thank you for giving me the opportunity to come this far and the encouragement to keep going forward.

Special thanks go to Catarina. For all the hours you spent by my side, being my strength when I had none. I could not have gotten this far without you, in this work and in life.

To Prof. José Leonardo dos Santos for accepting to be my internal supervisor and for all you taught me in your classes.

To all my professors at Instituto Superior Técnico, for your hard work, knowledge and tools that will aid me through my life.

To all my friends and colleagues, with whom I've shared the past six years and will surely share many more.

To Dr. Teresa Lopes da Silva, for accepting me in this project and as a part of her team. Thank you for your dedication, expert opinion and hard work.

To Dr. Carla Santos, Dr. Alberto Reis, Dr. Luís Duarte, Dr. Paula Passarinho and Margarida Monteiro for their help and knowledge in various aspects of this work. A special thanks goes to Engr. Carlos Barata. For all you taught me, far beyond the scope of this work.

Last but not least, to all who I have shared the past six months at LNEG: Tiago, Marta, Sofia, Diogo, Pedro, Luís, Vera, Joana, Bruno, André, Nuno, Carla, João, Aldo, Ana. You have been friends, colleagues, experts. This work could not have been done without you.

The present work was carried out within the project FCOMP-01-0124-FEDER-019317 (ex-PTDC/AAC-AMB/116594/2010) entitled ‘‘CAROFUEL – New process for a sustainable microbial biodiesel production: The yeast *Rhodotorula glutinis* biorefinery as a source of biodiesel, biogas and carotenoids’’ supported by FCT (Fundação para a Ciência e a Tecnologia) (also supported by FEDER funding through COMPETE – Programa Operacional Factores de Competitividade).

Abstract

In this work the yeast *Rhodosporidium toruloides* NCYC 921 was developed in a dual stage pH control fed-batch culture, designed to improve growth and fatty acids production in the first stage and induce the carotenoid production in the second stage, aiming at implementing a sustainable process for biodiesel production.

Two assays (I and II) were performed in a 7 L benchtop bioreactor to evaluate the impact of different pH values (5.0 and 5.5) in the second stage of fed-batch culture. In these assays, a concentrated glucose solution was used as carbon source. Two assays (III and IV) were performed in a 7 L benchtop bioreactor to determine if a sugar solution obtained from carob pulp was a viable alternative to a defined carbon source such as glucose solution, thus aiming at reducing the process costs. The possibility of scaling up *R. toruloides* cultures was evaluated by performing an assay (V) in a 50 L bioreactor, using a concentrated glucose solution as carbon source.

The highest biomass concentration was obtained in Assay I, with a value of 118.9 $g.L^{-1}$, while the highest biomass productivity was recorded in Assay II (1.52 $g.L^{-1}.h^{-1}$).

The highest carotenoid content (4.44 $mg.g^{-1}$ DCW) and productivity (4.12 $mg.L^{-1}.h^{-1}$) were both obtained in Assay IV, indicating that using carob pulp syrup as carbon source has a beneficial impact regarding carotenoid production.

The highest fatty acid content (30.24% w/w DCW) was obtained in Assay V and the highest fatty acid productivity (0.29 $g.L^{-1}.h^{-1}$) was obtained in Assay I.

Flow cytometry was used to assess the yeast cell viability and carotenoid content throughout the assays.

Keywords: *Rhodosporidium toruloides* NCYC 921; carob pulp syrup; fed-batch cultures; carotenoids; fatty acids; flow cytometry.

Resumo

No presente trabalho procedeu-se ao desenvolvimento de culturas da levedura *Rhodosporidium toruloides* NCYC 921 utilizando uma estratégia de cultura com duas etapas de controlo de pH em regime semi-descontínuo com o objectivo de produzir simultaneamente carotenóides e ácidos gordos, com vista à síntese de biodiesel.

Foram realizados dois ensaios (I e II) num biorreactor de bancada de 7 L, de forma a avaliar o impacto na cultura do uso de diferentes valores de pH (5,0 e 5,5) durante a segunda fase da cultura em modo semi-descontínuo. Para estes ensaios foi utilizada uma solução concentrada de glucose como fonte de carbono. Foram realizados dois ensaios (III e IV) num biorreactor de bancada de 7 L, utilizando xarope de polpa de alfarroba como fonte de carbono. O propósito destes ensaios foi determinar se este xarope é uma alternativa viável à utilização de soluções de açúcares (por exemplo glucose) definidas com o objectivo de reduzir os custos com matéria-prima do processo. Foi ainda avaliada a possibilidade de proceder a um aumento de escala das culturas de *R. toruloides* através da realização de um ensaio (V) num biorreactor de 50 L. Neste ensaio utilizou-se uma solução concentrada de glucose como fonte de carbono.

A concentração de biomassa mais elevada foi obtida no Ensaio I, atingindo o valor de 118,9 $g.L^{-1}$. Já a maior produtividade em biomassa foi obtida no Ensaio II, apresentando um valor de 1,52 $g.L^{-1}.h^{-1}$.

O maior conteúdo em carotenóides e produtividade foram ambos obtidos no Ensaio IV, com valores de 4,44 $mg.g^{-1}$ biomassa seca e 4,12 $mg.L^{-1}.h^{-1}$ respectivamente, indicando que a utilização de xarope de polpa de alfarroba contribui positivamente para a produção destes compostos.

O maior conteúdo em ácidos gordos foi obtido no Ensaio V (30,24% m/m biomassa seca) enquanto a maior produtividade em ácidos gordos foi obtida no Ensaio I (0,29 $g.L^{-1}.h^{-1}$).

Recorreu-se à citometria de fluxo para determinar a viabilidade celular e o conteúdo em carotenóides nos diversos ensaios.

Palavras-chave: *Rhodosporidium toruloides* NCYC 921; xarope de polpa de alfarroba; culturas em regime semi-descontínuo; carotenóides; ácidos gordos; citometria de fluxo.

Contents

This page
was intentionally
left blank

Figures

Tables

This page
was intentionally
left blank

Equations

This page
was intentionally
left blank

Abbreviations and symbols

14:0	Myristic acid
14:1ω5	Myristoleic acid
16:0	Palmitic acid
16:1ω9	Palmitoleic acid
18:0	Stearic acid
18:1ω9	Oleic acid
18:2ω6	Linoleic acid
18:3ω3	Linolenic acid
20:0	Arachidic acid
22:0	Behenic acid
24:0	Lignoceric acid
Ara	Arabinose
ATCC	American Type Culture Collection
ATP	Adenosine triphosphate
BTL	Biomass to liquid
Ca-EDTA	Calcium Titriplex®, dihydrate
Car_{cont}	Total carotenoid content, mg carotenoids.g dry biomass^{-1}
CFDA	Diacetate of carboxifluorescein
CPS	Carob pulp syrup
CTC	5-cyano-2,3 ditolyl tetrazolium chloride
DAD	Diode array detector
DCW	Dry cell weight
$DiOC_6$(3)	3,3'-dihexyloxacarbocyanine iodide
DMSO	Dimethyl sulfoxide
DNSA	3,5-dinitrosalicylic acid
DO	Dissolved oxygen
ECR	Energy consumption rate per capita
ETG	Ethanol to gasoline
FA_{cont}	Total fatty acid content, g fatty acid.g dry biomass^{-1}
FAEE	Fatty acid ethyl ester
FAME	Fatty acid methyl ester
FC	Flow cytometry
FDA	Fluorescein diacetate
FFA	Free fatty acids
Fru	Fructose
FSC	Front scatter
Furf	Furfural
Gal	Galactose
GC	Gas chromatography
GDP	Gross domestic product
GHGs	Greenhouse gases
Glu	Glucose
HFCs	Hydro fluorocarbons
HMF	Hydroxymethylfurfural
HPLC	High performance liquid chromatography
LBG	Locust bean gum
MCI buffer	McIlvaine buffer
m_{FA}	Total fatty acid mass, g
MMbbl/d	Million barrels per day
MTHF	Methyltetrahydrofuran
MUFA	Monounsaturated fatty acid
m_X	Biomass mass, g
NCYC	National Collection of Yeast Cultures
NGL	Natural gas liquids
OD_{600}	Optical density at 600 nm
OECD	Organization for Economic Co-operation and Development
OPEC	Organization of Petroleum Exporting Countries
P_{Car}	Carotenoid productivity, g carotenoids.L^{-1}.h^{-1}

P_{FA}	Fatty acid productivity, g fatty acids.L^{-1}.h^{-1}
PPG	Polypropylene glycol
PUFA	Polyunsaturated fatty acid
P_X	Biomass productivity, g biomass.L^{-1}.h^{-1}
QL	Quality of life index
R^2	Coefficient of determination
RI	Refraction index
rpm	Rotations per minute
SCO	Single cell oils
SFA	Saturated fatty acids
SSC	Side scatter
SSCP	Sugar solution from carob pulp
Suc	Sucrose
t	Time, h
TAG	Triacylglycerol
TS	Total sugars
USA	United States of America
UV	Ultraviolet
wt	Weight
X_t	Biomass concentration at time *t*, g biomass.L^{-1}
Xyl	Xylose
μ	Specific growth rate, h^{-1}
μ_{max}	Maximum specific growth rate, h^{-1}
σ	Standard deviation

1 Introduction

1.1. World energy demand and its implications – an overview

Energy is required to sustain and improve quality of life. The opening line from the work of Pasten and Santamarina [1] is a clear and unequivocal statement: energy consumption rate per capita (ECR) is directly correlated to the quality of life (QL) of a given population. This trend can clearly be seen in the current global situation, as depicted by Figure 1.1.

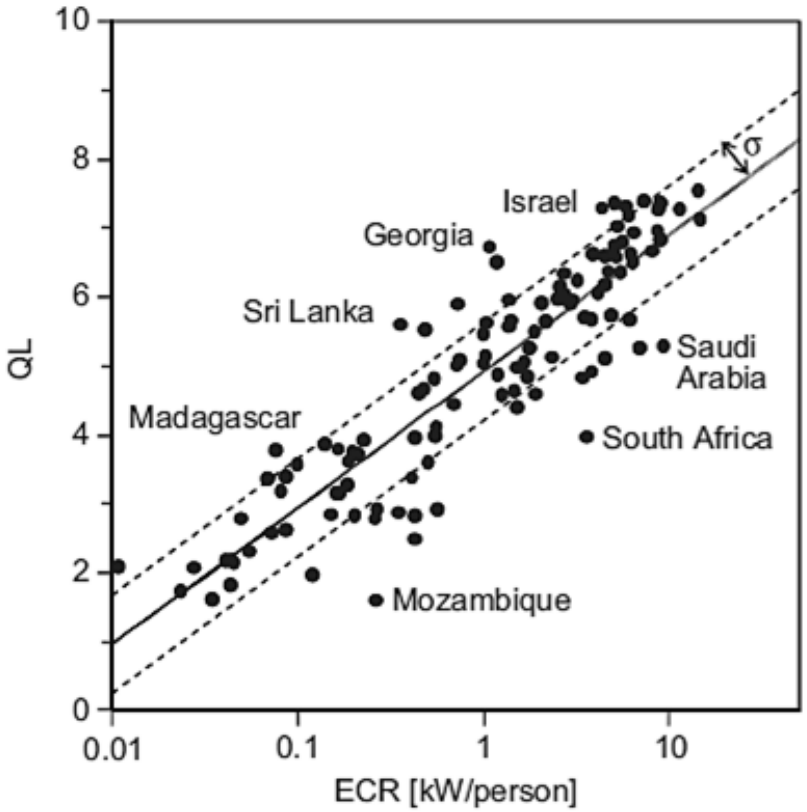

Figure 1.1 – Quality of life index (QL) and energy consumption rate per capita (ECR). Data for 118 countries with populations larger than four million in 2005. The continuous line is the mean trend; dashed lines show the plus and minus one standard deviation (σ) trends. QL is a function of the proportion of the population using improved drinking-water sources, life expectancy at birth, infant mortality rate (deaths/1000 live births) and mean years of schooling for individuals age 25 and older. Adapted from Pasten and Santamarina [1].

A corollary of this dependency is that the global energy needs must rise proportionately to an increase in world population, if the current quality of life status is to be maintained. Likewise, and perhaps more importantly, an increase of the QL in nowadays designated developing countries, in particular for countries outside the Organization for Economic Co-operation and Development (OECD), translates into an increase of ECR. As the QL is directly related to a country's gross domestic product (GDP), previsions regarding this indicator can be translated into subsequent changes to the ECR of said country [2]. The GDP of non-OECD countries is predicted to rise significantly more than that of OECD regions, from 2010 to 2040: for a global GDP rise at an annual average rate of 3.5%, non-OECD countries should increase their GDP by an average of 4.6% per year, compared to a 2.1% per year increase in the case of OECD regions [2]. Based on this scenario, coupled with the projected increase in world population, it

is predicted that the demand for petroleum and other liquid fuels will rise steadily over the next decades, from 87 million barrels per day (MMbbl/d) in 2010 to 119 MMbbl/d in 2040, fueled by the development of non-OECD countries (Figures 1.2 and 1.3) [2].

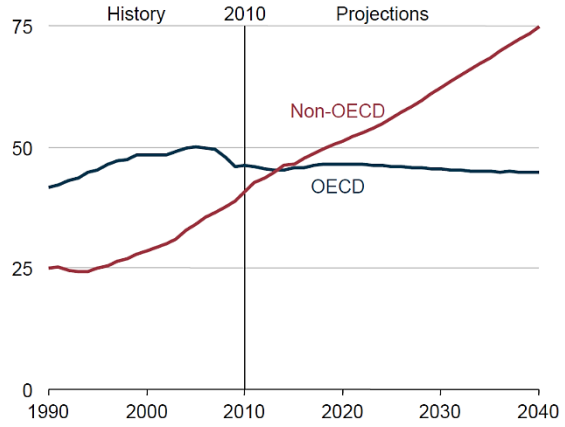

Figure 1.2 – OECD and non-OECD petroleum and other liquid fuels consumption, from 1990 to 2040 (million barrels per day). Reproduced from U.S. Energy Information Administration [2].

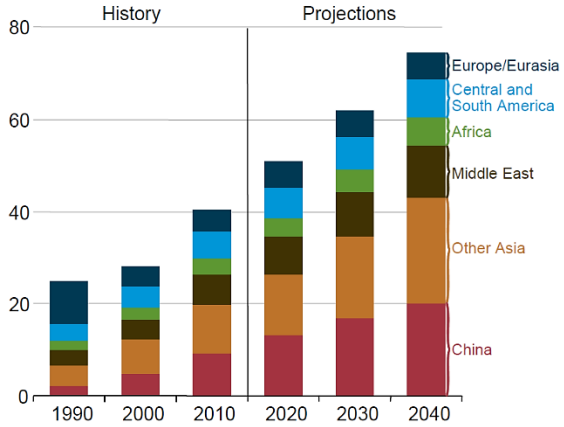

Figure 1.3 – Non-OECD petroleum and other liquid fuels consumption by region, from 1990 to 2040 (million barrels per day. Reproduced from U.S. Energy Information Administration [2].

Despite the growing importance of liquid fuels other than those derived from crude oil (like biofuels and liquid fuels produced from coal and gases), crude and lease condensates will remain the most produced liquid fuels (Figure 1.4) much because of today's global economic policies [2]. In fact, the available literature suggests that this will remain true even in scenarios where the price per barrel of crude (based on prices of North Sea Brent crude oil) is significantly lower than what is observed today (Figure 1.5) [2].

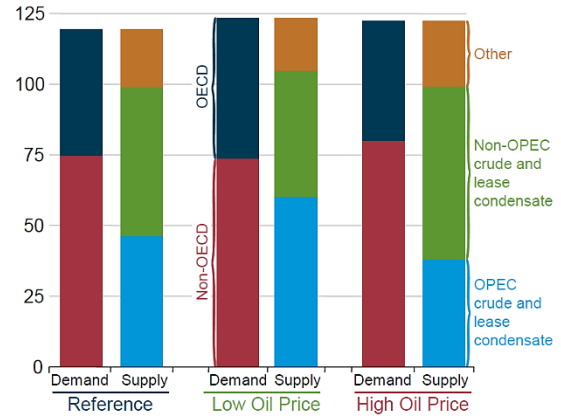

Figure 1.4 – Liquid fuels demand and supply for OECD and non-OECD countries in three cases, from 1990 to 2040 (million barrels per day). Reproduced from U.S. Energy Information Administration [2].

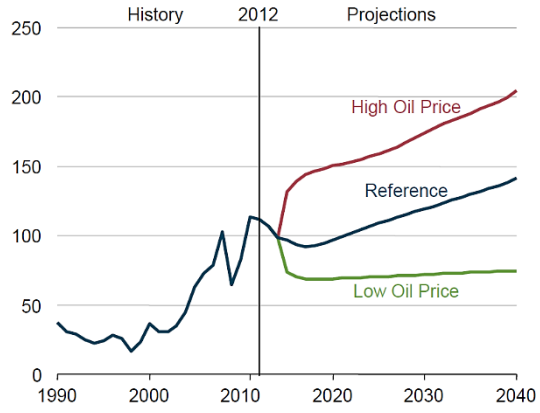

Figure 1.5 – North Sea Brent crude oil spot prices in three cases, from 1990 to 2040 (2012 U.S. dollars per barrel). Reproduced from U.S. Energy Information Administration [2].

Regardless their obvious importance and the fact that they will remain the primary source of energy worldwide for the coming years [2,3], crude and lease condensates cannot be regarded as the fuels that will meet the world's energy needs for the future. To arrive at this conclusion one should look at the importance of the transportation sector in the overall energy demand and the impact that this has had on the environment. Globally, in terms of energy consumption, the transportation sector is second

after the industrial sector, and its energy requirements account for 30% of all energy produced yearly. Of these, 80% is allocated to road transports. It is in this sector that the use of petroleum is most prevalent: nearly 60% of the world's oil demand is destined to the transportation sector and this figure is increasing year by year, with virtually all the energy being derived from crude oil (97.6%) [3]. As this sector continues to expand, it is expected that, by 2030, it will be responsible for nearly three-quarters of the global oil demand [3]. Due to their close relationship, the expansion of the transportation sector will directly impact the supply of crude and although many authors disagree on when peak oil production will occur [4-7], the overall consensus is that reserves are finite and will eventually be depleted.

Other important aspects of traditional liquid fuels are the political and social implications of their extraction and commercialization. Even nowadays, with proved reserves that should be able to meet global demands for at least 50 years [7], trading prices for petroleum are constantly affected the political situations of supplying countries as internal and external conflicts sow instability on the access to provisions [2,7]. Many countries belonging to the Organization of Petroleum Exporting Countries (OPEC) face dire humanitarian crises even today, keeping said countries from realizing the full potential of their oil sectors and possibly failing to meet global needs [2].

One of the main consequences of the continued use of fossil fuels (such as crude and natural gas) is the buildup in the atmosphere of the concentration of greenhouse gases (GHGs). Carbon dioxide (CO_2) comprises roughly 95% of GHGs generated by the transportation sector. The remaining 5% are methane (CH_4) (1%), nitrous oxide (N_2O) (1%) and hydro fluorocarbons (HFCs) (3%) that are emitted by vehicles' air conditioning systems. Because their contribution to global warming has not yet been accurately quantified, ozone (O_3), carbon monoxide (CO) and various aerosols emitted by vehicles are not encompassed in this composition of GHGs [3]. In 2007 and 2008, the transportation sector was responsible for 23% and 22% of global CO_2 emissions, respectively. Due to the growth of the transportation sector, it is expected that the amount of CO_2 released into the atmosphere worldwide will increase by approximately 35% over a 20 year period, from 31.5 billion metric tons in 2015 to 42.4 billion metric tons in 2035 (Figure 1.6) [3].

Given all the aforementioned constraints, it is vital to move beyond traditional energy sources like petroleum and coal and strive to increase the use of alternative energies, being alternative liquid fuels or other energy sources. These alternative energies should overcome some of the limitations of traditional fuels, i.e. they should be renewable, sustainable, efficient, low-cost and with fewer or no net GHG emissions [3,8-10]. Alternative energy sources like wind, solar and nuclear power certainly fall into this category, however they are not suitable for application in the transportation sector which is, as demonstrate above, one of the most important in terms of global energy demand. Presently, the four most important alternative energy sources, suitable for the transportation sector, are biofuels, natural gas, hydrogen and syngas. Of these, biofuels are the most promising alternative to fossil fuels as they are renewable, biodegradable and their combustion generates exhaust gases that have less environmental impact than those of fossil fuels [11]. In fact, it is predicted that biofuel production will experience a significant growth over the next decades (Figure 1.7), mainly due to encouragement from governmental policies that stimulate the production of liquid fuels derived from domestic resources [2].

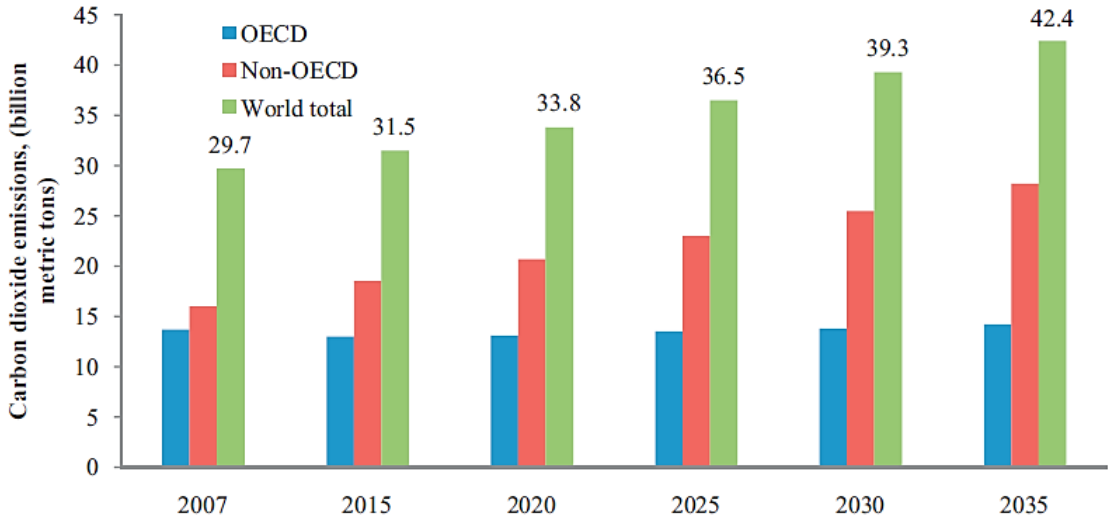

Figure 1.6 – World, OECD and non-OECD carbon dioxide emissions from 2007 to 2035. Reproduced from Atabani *et al.* [3].

It is relevant to point out that the increase in production of natural gas plant liquids is a direct consequence of an increased production of natural gas, therefore only available to countries that already possess this natural resource, whereas biofuels could theoretically be produced by any nation, as long as it produces any sort of waste that can be used as a raw material for biofuel production (see section 1.2.1) [2]. This offers financial and energetic independence for countries with limited fossil fuel reserves, a major advantage as economic motivation is by far the strongest in changing global energy situation [10].

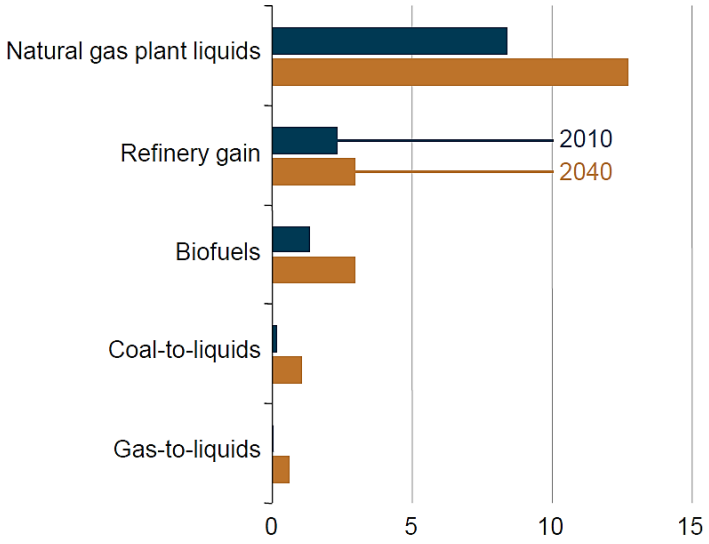

Figure 1.7 – World liquid fuels production, other than crude and lease condensate, by source, for 2010 and 2040. Adopted from U.S. Energy Information Administration [2].

In Europe, steps have been taken in order to increase the use of alternative fuels in the transportation sector, fighting the current oil dependency and limiting GHG emissions. In 2009, Directive 2009/28/EC of the European Parliament and of the Council of the European Union was approved, replacing and amending Directives 2001/77/EC (regarding the promotion of electricity produced from

renewable energy sources in the internal electricity market) and 2003/30/EC (which aims at the promotion of the use of biofuels or other renewable fuels for transport) [12]. With this directive, member-States have agreed to enforce policies in order to assure that, by 2020, national targets are consistent with a 20% share of all energy consumed being from renewable sources and 10% of the energy used in the transportation sector also being from renewable sources [12]. Because these are overall goals for the European Union, each member-State has its own target, under Directive 2009/28/EC. In the particular case of Portugal, where the present work is being developed, the National Plan of Action for Renewable Energies under Directive 2009/28/CE (originally *Plano Nacional de Acção para as Energias Renováveis ao Abrigo da Directiva 2009/28/CE*, [13]) dictates that 31% of all energy consumed should come from renewable sources, with specific goals for electrical energy and the transportation sector: 60% of the first and 10% of the latter should come from renewable sources. These higher goals attest to the importance of renewable energy sources in Portugal as by 2010 40% of electrical energy and 20% of all consumed energy was originated from renewable sources [13].

1.2. Biofuels: deliver us from oil

1.2.1. Biofuels

1.2.1.1. Classification

Biofuels comprise a vast array of renewable fuels derived from biomass, ranging from something as simple as unprocessed wood residues to more technologically advanced fuels like bioethanol and biomethanol, biohydrogen, biomethane and biodiesel [8,14]. According to this technological distinction, biofuels are categorized either as primary or secondary (Figure 1.8) [11].

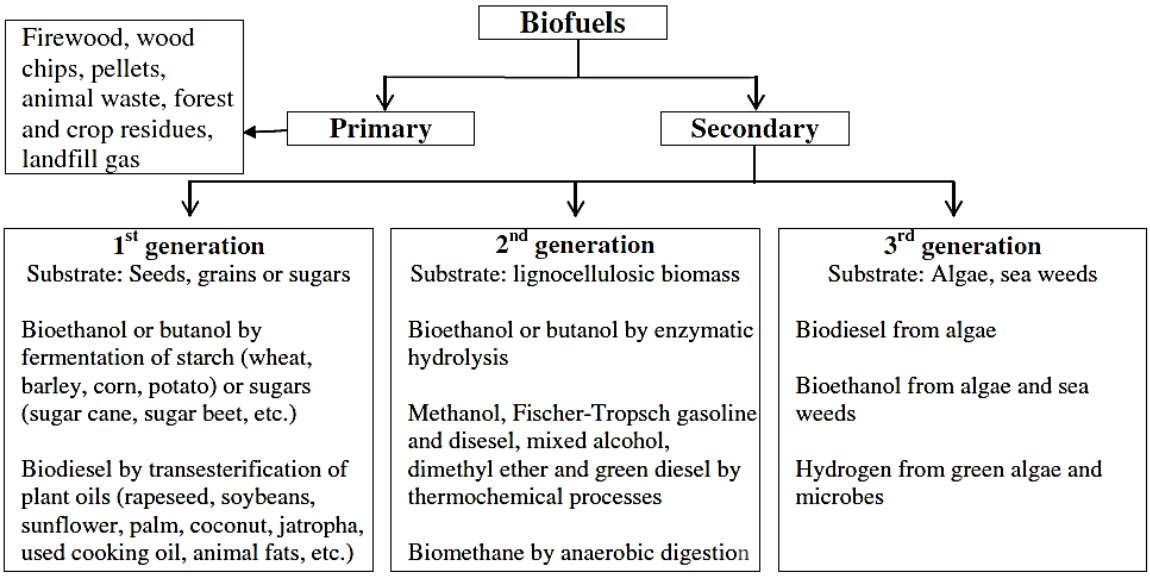

Figure 1.8 – Classification of biofuels. Reproduced from Nigam and Singh [11].

Primary biofuels encompass all biomass that can be directly used as fuel, without any further processing, like wood and lignocellulosic residues from crops, animal waste or gas generated in landfills.

Because they can be used as fuel without any treatment and are generally considered waste, primary biofuels are by far the cheapest of all biofuels. However, their use is limited, particularly in the transportation and industrial sectors. Their use is most prevalent for heating applications or for generating electricity [11].

Secondary biofuels can be considered the result of processing primary biofuels (Figure 1.9). For example, lignocellulosic biomass can be hydrolyzed to obtain a viable substrate for microbial fermentations, a process for bioethanol production. Secondary biofuels are more diverse than the primary biofuels, and can be presented in the form of solids (like charcoal), liquids (like bioethanol and biodiesel) or gases (like biomethane and biohydrogen). Rather than being used on their own, liquid biofuels are commonly mixed with petroleum based fuels so that they can be used in vehicles with standard gasoline or diesel powered engines [8,9]. This practice allows overcoming certain disadvantages of bioethanol and biodiesel: bioethanol has a higher octane value than gasoline, however it produces approximately 70% less energy; biodiesel provides 88% to 95% of the energy of traditional diesels, has better lubricity and a higher cetane value, but increased degradability and higher cloud/pour point that can lead to problems in colder climates [8,15].

Secondary biofuels can be further classified as being of first, second or third generation (Figure 1.8) and this distinction is made according to the raw materials and technologies used in fuel production [8,9,11].

1.2.1.2. First generation

First generation biofuels are the simplest in terms of production. They are derived primarily from foodstuffs and currently represent the vast majority of biofuels produced worldwide [9]. Sugar and starches extracted from sugarcane or sugar beet can be used to produce bioethanol via fermentation and vegetable oils from rapeseed, sunflower or soybean, to name some, can be used to produce biodiesel by transesterification (Figure 1.9) [8,9].

Up today, first generation bioethanol remains the most produced biofuel, with Brazil and the United States of America (USA) as the two leading producers (88% of the total produced volume in 2009) [8]. Perhaps the most pressing issue regarding first generation biofuels is the fuel-versus-food debate. As biofuels gain a greater economic importance, the cost of raw materials is expected to rise, just like in any other market. Increased revenues from crops destined to the biofuel market makes then more desirable to farmers, which could in turn raise the prices of food crops due to a diminishing offer [16,17]. Changing from food to fuel crops also negatively impacts biodiversity as these last ones are sown in detriment of the first [9].

1.2.1.3. Second generation

Second generation biofuels are a possible solution to overcome the fuel-versus-food issue as they are derived from non-edible materials. Both biodiesel and bioethanol can be classified as being of second generation, depending on the feedstock used to produce them [9].

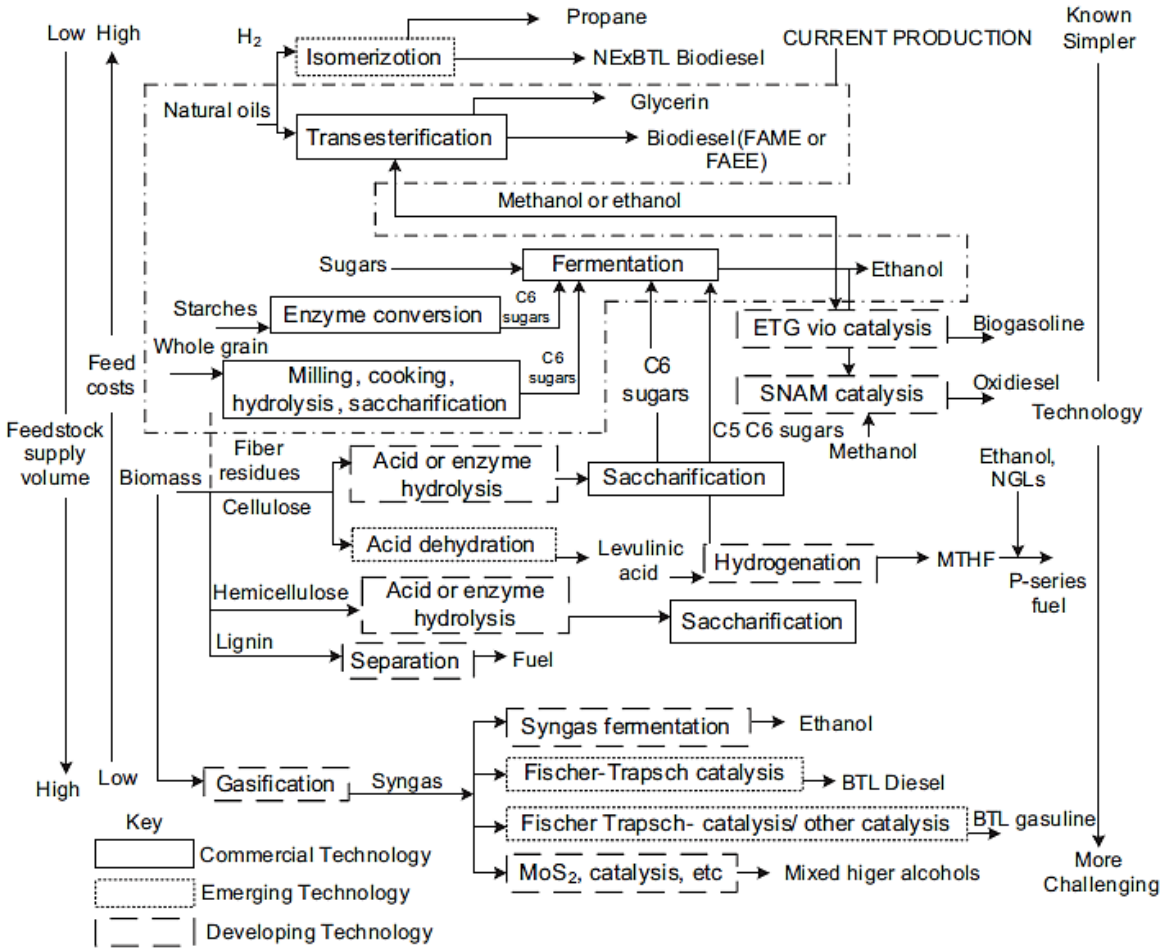

Figure 1.9 – Various technological routes for biofuels production. H_2 – Hydrogen; FAME – Fatty acid methyl ester; FAEE – Fatty acid ethyl ester; ETG – Ethanol to gasoline; NGL – Natural gas liquids; MTHF – Methyltetrahydrofuran; BTL – Biomass to liquid. Reproduced from Nigam and Singh [11].

Second generation bioethanol is produced by processing lignocellulosic biomass, converting the cellulose and hemicellulose present in the raw materials to simple sugars which can then be fermented [8,9]. Alternatively, lignocellulosic biomass can be gasified to produce syngas, which in turn can be used to produce a myriad of other fuels (Figure 1.9) [8]. Lignocellulosic biomass can originate in the food industry (i.e. discarded seed husks and stalks) or from forest residues such as leaves and branches [8,9,18].

Second generation biodiesel is derived from feedstocks like non-edible oilseed plant species or animal fats from the meat industry. Unlike second generation bioethanol, biodiesel produced in this fashion does not require more advanced technologies than those utilized to produce first generation biodiesel, they are simply produced from different substrates [9].

However, second generation biofuels present a few problems. The technology necessary to efficiently convert lignocellulosic biomass to simple sugars is still in its infancy and biofuels produced in this fashion are not yet commercially viable [8]. And although not derived from foodstuffs, some authors [8,18,19] call attention to the fact that non-food crops can still lead to a rise in food prices, due to the

allocation of land and water resources to fuel rather than food crops. Some authors [20] consider that even if oilseed crops were cultivated in all available arable land, the feedstock generated by said crops would not be sufficient to produce biodiesel to cover half of the world's energy demand.

1.2.1.4. Third generation

Third generation biofuels are currently the most technologically advanced ones and have their origin in microorganisms, either being derived from biomass or being produced directly by them [3,21-23]. Classification is based on the raw material utilized to produce the biofuel and the technological advancement associated with this production. For example, ethanol obtained from the fermentation of lignocellulosic substrates is considered a second generation biofuel, whereas biodiesel derived from oleaginous microorganisms, even if cultured on media containing first or second generation substrates, is considered a third generation biofuel [22-24]. This is because the feedstock used in the biodiesel production is the oleaginous microorganisms, not the edible or lignocellulosic biomass. There is also a technological novelty associated with this process as sugar-rich raw materials can be used to produce biodiesel, where before they were exclusively used as substrates for bioethanol fermentations.

Nowadays, several third generation biofuels are being studied and developed [25-28]. In bioethanol production, a promising alternative to use food crops or lignocellulosic biomass is the use of carbohydrate-rich microorganisms such as microalgae rich in starch. These can be saccharified through enzymatic or acid hydrolysis and the resulting sugars used to produce bioethanol via fermentation [28]. Other biofuels, such as biohydrogen and biomethane, can be produced from algal (both micro and macro) biomass [25-27]. The use of photobioreactors to produce microalgae is a particularly interesting perspective as, theoretically, these culture systems can be coupled with existing infrastructures to simultaneously sequester CO_2 and produce algal biomass [26].

Third generation biodiesel also derives from biomass of oleaginous microorganisms as raw material. There are several microbes that accumulate oils (Table 1.1), but not all of them are suitable candidates for biodiesel production. These are microorganisms that present a lipid content higher than 20% of their dry cell weight and these microbial lipids are designated single cell oils (SCOs) [21,29].

Lipid accumulation in microbes usually occurs during the stationary phase of growth, as a result of the exhaustion of a medium nutrient (usually nitrogen) but when there is still a carbon source available [21,22,24]. Under these conditions, population growth is halted as the existing cells can no longer divide and the carbon source is assimilated, converted to triacylglycerols (TAG) and stored, as reserve lipids [21,30]. The lipid composition is dependent on the culture conditions such as temperature, pH and culture age and is different for each type of microorganism (Table 1.2) [21,31-33].

Table 1.1 – Oil content of some microorganisms. Reproduced from Meng *et al.* [21].

Microorganisms	Oil content (% CDW)	Microorganisms	Oil content (% DCW)
Microalgae		**Yeast**	
Botryococcus braunii	25–75	*Candida curvata*	58
Cylindrotheca sp.	16–37	*Cryptococcus albidus*	65
Nitzschia sp.	45–47	*Lipomyces starkeyi*	64
Schizochytrium sp.	50–77	*Rhodotorula glutinis*	72
Bacterium		**Fungi**	
Arthrobacter sp.	>40	*Aspergillus oryzae*	57
Acinetobacter calcoaceticus	27–38	*Mortierella isabellina*	86
Rhodococcus opacus	24–25	*Humicola lanuginosa*	75
Bacillus alcalophilus	18–24	*Mortierella vinacea*	66

Table 1.2 – Lipid composition of some microorganisms. Reproduced from Meng *et al.* [21]. C16:0, palmitic acid; C16:1, palmitoleic acid; C18:0, stearic acid; C18:1, oleic acid; C18:2, linoleic acid; C18:3, linolenic acid.

Microorganisms	Relative amount of total fatty acids (w/w)					
	C16:0	C16:1	C18:0	C18:1	C18:2	C18:3
Microalga	12–21	55–57	1–2	58–60	4–20	14–30
Yeast	11–37	1–6	1–10	28–66	3–24	1–3
Fungi	7–23	1–6	2–6	19–81	8–40	4–42
Bacterium	8–10	1–6	11–12	25–28	14–17	-

Microalgae are good candidates for biodiesel production as they present high oil contents (Table 1.1) and higher photosynthetic efficiencies, biomass productivities and growth rates than traditional energy crops [21]. However, when compared to bacteria and yeasts, microalgae require longer cultivation periods and more complex equipment to sustain growth [21,22,24]. Growing microalgae can also be more challenging as cultures tend to be more prone to contaminations. Bacteria are easily cultured and have the highest growth rates compared to other oleaginous microorganisms, however they have lower average oil contents (Table 1.1). Oil producing bacteria are also scarcer than microalgae or yeasts and the ones that do produce oils generate them in the outer membrane, making extraction a more complicated operation [21].

Because of the aforementioned drawbacks regarding microalgae and bacteria as substrates for biodiesel production, yeasts and fungi have for long been considered more favorable for this application [21,34]. These microorganisms can accumulate high concentrations of lipids (Table 1.1), with usually 90% (w/w) of these being TAG, of which approximately 44% are saturated fatty acids (SFA) [21]. This composition is similar to many plant seed oils, making SCOs from yeast and molds more desirable for biodiesel production as fewer polyunsaturated fatty acids (PUFAs) (which are undesirable for biodiesel purposes, as they are prone to oxidize [35], see section 1.2.2 for more details) are present when compared to SCOs from algae and bacteria [21,36]. In Table 1.2, and throughout this work, fatty acids are identified by their lipid numbers. These take the form *C*:*D*, where *C* is the number of carbon atoms in the fatty acid and *D* is the number of double bonds in said fatty acid. In the case of unsaturated fatty acids (either MUFAs or PUFAs) this number can be followed by the omega (ω) numbering, identifying the carbon atom where the first unsaturation occurs, counting from the methyl end [37].

The use of microorganisms as raw materials presents several advantages over traditional substrates. First and foremost, the fuel-versus-food issue is resolved because microorganisms do not compete with food crops in any way. Granted that microbial cultivations still rely mainly on pure substrates as carbon sources, often derived from food crops, however there has been a concentrated effort to use lignocellulosic wastes and industry by-products as substrates in culture media to obtain biofuels and high-value-added products from microorganisms [23,24,38-40]. Secondly, the production of microbial fuels is far less labor intensive than traditional crops, as many of the processes can be automated, both in terms of monitoring and control. Microbial cultures are also more easily scalable and have shorter life cycles and are not dependent on seasons and climate [21-24]. On the other hand, third generation biofuels are still significantly more expensive than fossil fuels or first and second generation biofuels, mainly due to high production costs and extraction/conversion of the desired products [23].

1.2.2. Biodiesel

Biodiesel is the biofuel resultant from the transesterification of natural triglycerides, from sources such as vegetable oils, animal fats or SCOs [9,10,23]. The most common process converts triglycerides into fatty acid alkyl esters and glycerol through reaction between an alcohol and the triglycerides, usually catalyzed; the utilized alcohol, usually methanol or ethanol, dictates which fatty acid alkyl esters are produced: either fatty acid methyl esters (FAMEs) or fatty acid ethyl esters (FAEEs), respectively (Figure 1.10) [3,9,23,41]. The most commonly used technique is transesterification using methanol, so the alkyl esters used for biodiesel production are usually FAMEs [35].

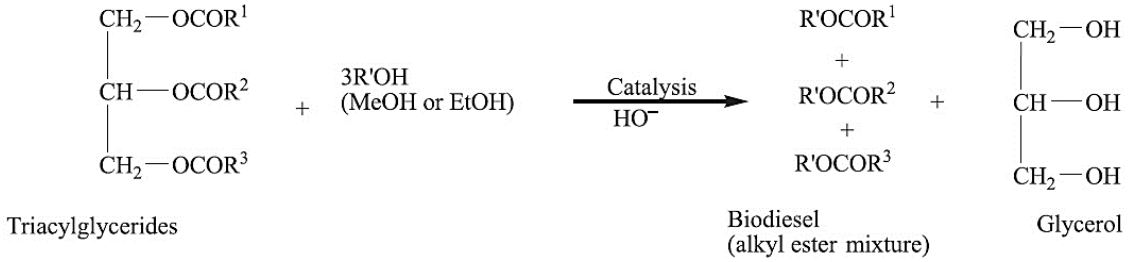

Figure 1.10 – Glycerol production *via* triglyceride transesterification with methanol or ethanol. Reproduced from Meireles and Pereira [41].

In this reaction, the catalyst works by increasing the alcohol's solubility in the oil, promoting more contact between the molecules and speeding up the reaction [3]. Despite being represented as a base in Figure 1.10, catalysts can be either basic or acidic and their selection is dependent on the amount of free fatty acids (FFA) present in the oil: acidic catalysis is more indicated for high amounts of FFA while basic catalysis is the standard for low FFA levels [3,11].

The typical mass balance in biodiesel production is 10–15 kg of alcohol per 100 kg of base oil, yielding 100–105 kg of biodiesel and 10 kg of glycerol [10]. One of the difficulties associated with biodiesel production consists in ensuring that the final product does not contain residual chemicals from the transesterification reaction, being catalyst, alcohol or free fatty acids. This is especially relevant when producing a biodiesel that is intended to be used pure and not as a blend with traditional oil-based

diesel [10]. Because it must be compliant with existing machinery, the biodiesel properties, i.e. density, viscosity, flash point, cold filter plugging point and other, need to be determined in order to ensure that the values of these parameters fall within certain intervals [21]. As biodiesel production rises, standardization becomes increasingly more important in order to assure that the final product meets the desired specifications. In USA, the standard governing biodiesel's specifications is the ASTM Biodiesel Standard D6751, while in the European Union there are different specifications for biodiesel intended for vehicle use (Standard EN 14214) and for heating proposes (Standard EN 14213) [21].

When evaluating a certain biomass as feedstock, its fatty acid composition is particularly important. EN 14214 specifies that the linolenic methyl esters and PUFAs with four or more unsaturations contents are limited to 12% and 1% (w/w of total fatty acids), respectively [42]. This is because these compounds are more prone to oxidation, meaning that a biodiesel rich in them will have poor oxidative stability and quickly become degraded. Another important property is cetane number (CN), a measure of the ignition properties of the fuel. CN increases with the increasing hydrocarbon chain length and decreasing degree of unsaturation. The higher the CN, the better quality biodiesel [35]. EN 14214 specifies a minimum CN of 51 [42]. However, these same FAMEs that, when present, produce good quality biodiesel in regards to CN, impart poor cold-flow properties on the biodiesel (because of their higher melting points), meaning that there must be a balance between SFA, monounsaturated fatty acid (MUFA) and PUFA contents in order to obtain a good quality biodiesel [35].

Biodiesel contributes less carbon or sulfur to the atmosphere than traditional fuels and is thus considered a more environmentally-friendly source of energy (this is of course regarding the fuel usage itself as the entire process, including production, might release more carbon and sulfur) [21]. Nevertheless, the environmental impact of biodiesel is not entirely positive as evidenced by some of the previously mentioned constraints, i.e. the fuel-versus-food dispute and the effect on biodiversity (see sections 1.2.1.2 and 1.2.1.3, respectively). Production of third generation biodiesel is a way of overcoming the aforementioned issues, however production costs are still prohibitively high – microalgae derived biodiesel has a production cost in the range of US$2–US$22 per liter, while biodiesel produced from used cooking oil can have a production cost as low as US$0.21 per liter (2011 prices) [8,43,44]. Even with these challenges, government incentives, subsidies and tax exemptions have ensured that biodiesel production grew steadily (Figure 1.11) and this trend is expected to continue in the foreseeable future [2,7,8].

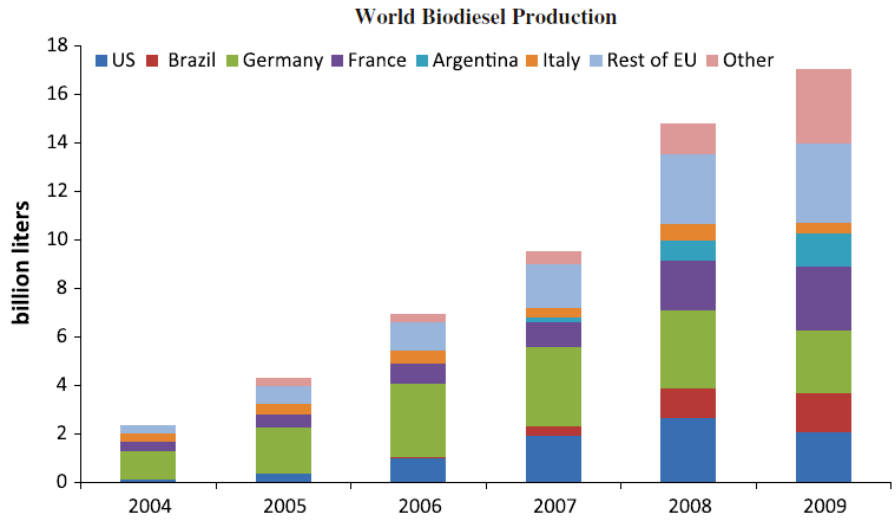

Figure 1.11 – World biodiesel production. Reproduced from Timilsina and Shrestha [8].

1.3. Concomitant production of biodiesel and carotenoids

As previously mentioned, microbial production of biodiesel is not yet an economically viable process as production costs far surpass the market price of the produced biodiesel [24]. However, if the microbial biomass, beyond its high lipid content, is rich in high-value-added products such as carotenoids, (which have many different applications in pharmaceutical, nutraceutical, food and feed industries, with a high market value, see section 1.4), the economics of the process may be greatly improved, as the high-value-added products may sustain the microbial biofuel production. This strategy has gained an added importance in more recent years as several species of algae and yeasts have been found to produce meaningful quantities of both fatty acids (convertible to biodiesel) and valuable by-products, such as carotenoids [21,45,46].

1.4. Carotenoids

Carotenoids are tetra-terpenoid C_{40} pigments containing isoprene residues and a polyene chain of conjugated double bounds (Figure 1.12) [47]. These compounds are naturally occurring in nature and although often considered to be higher plant pigments, they are also synthetized by algae and other microorganisms, like some species of fungi [47,48]. Carotenoids can be either acyclic or terminated by one or two cyclic end groups. Depending on whether they are purely hydrocarbon compounds or contain oxygen atoms in their structure, carotenoids can be further categorized as carotenes or xanthophylls, respectively [48,49].

Carotenoids are the compounds responsible for the yellow and red-orange colors of several different plants and microorganisms and, due to their coloring properties, have been used primarily as additives in the food and feed industries [47,49]. However, when studies carried out in the 1920s and 30s regarding vitamin A demonstrated β-carotene to be a precursor for this vitamin [50], carotenoids gained new importance as key molecules in the functional-foods sector and in medical applications [51]. Due to their strong anti-oxidative properties, carotenoids have been proved to reduce the incidence of

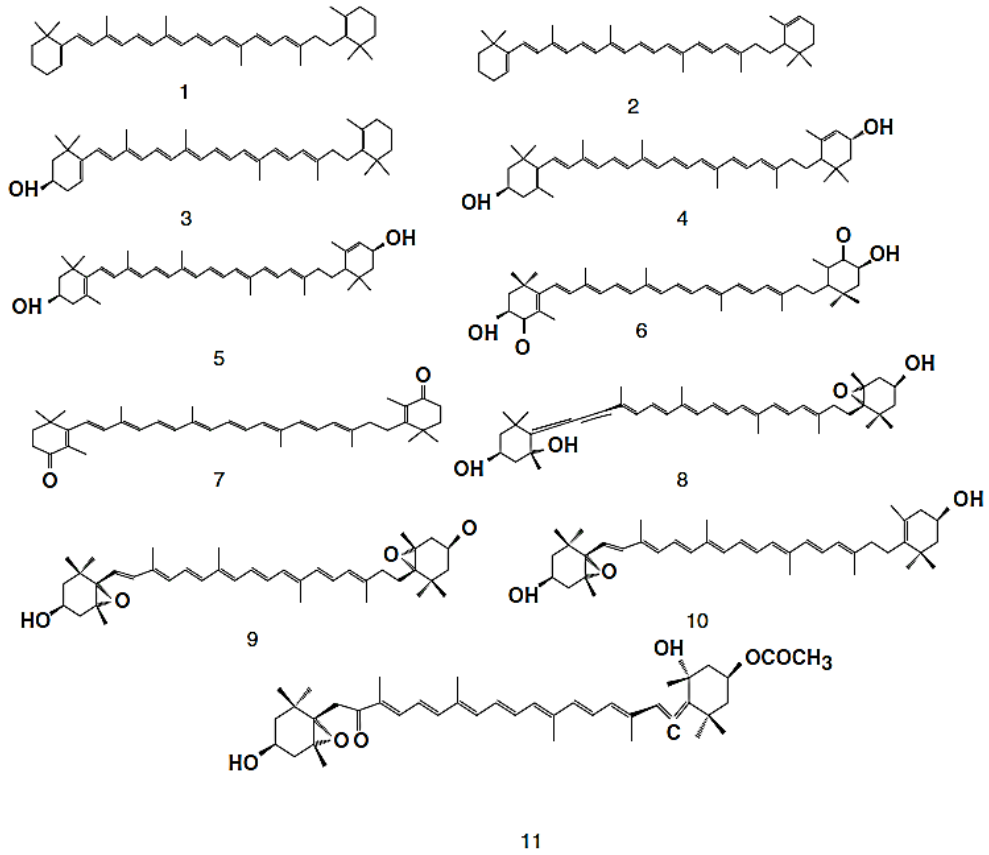

Figure 1.12 – Structures of important carotenoids produced by microorganisms. (1) β-Carotene, (2) α-Carotene, (3) β-Cryptoxanthin, (4) Lutein, (5) Zeaxanthin, (6) Astaxanthin, (7) Canthaxanthin, (8) Neoxanthin, (9) Violaxanthin, (10) Antheraxanthin, and (11) Fucoxanthin. Reproduced from Vachali *et al.* [47].

several diseases, such as cancer [52,53] or type 2 diabetes [54]. Additionally, carotenoid consumption has been linked to reduced incidences of cardiovascular diseases, cataracts, age-related macular degeneration and diseases related to low immune function [48]. The effects on human health of other carotenoids, such as torulene or torularhodin, have yet to be studied because they are not found in foods. However, yeasts containing these pigments are used for animal feeding to produce desirable results like increase in body fat and better nutritional value for the meat. If they are proven to have the same type of antioxidant properties as other carotenoids, torulene and torularhodin could have the same applications of astaxanthin and lycopene, for example. Furthermore, using torularhodin may be advantageous in some formulations as this carotenoid has a carboxyl group that might facilitate the preparation of aqueous solutions. These carotenoids also have applications as pigments [55-57].

From simple colorants to compounds with major health benefits, the shift in how carotenoids are perceived by the general public has brought about a dramatic change in their commercial value. As interest in carotenoids as high-value-added products increases, information regarding market values and trends become more prized and therefore less accessible free of charge. Although specific commercial values are quite difficult to find in the available literature, there are some figures on how the carotenoid market has changed over the past few years and is expected to continue to evolve: in 2003, the European carotenoid market was worth US$348.5 million and projections pointed to a yearly

increase of 2.7%, to reach US$419.6 million in 2010 [58]. The report by Frost & Sullivan [58] specifically mentions that at this time the potential value of carotenoids as nutraceuticals was still largely ignored, meaning that the 2003 market value was based primarily on their use as colorants for food and feeds. Globally, the carotenoid market reached US$1.2 billion in 2010 and is predicted to expand to US$1.4 billion in 2018 [59].

In order to satisfy the growing demand for carotenoids there are three main routes available: (i) carotenoids can be recovered from plant sources where they naturally occur, like apricots and peaches [60], tomatoes [61,62] and others [63], (ii) they can be chemically synthetized [64] or (iii) they can be isolated from carotenoid-producing microorganisms, like algae and yeasts [47,49,57,65]. Of the three, carotenoid production using microorganisms is the most promising alternative, especially taking into consideration the fact that the nutraceutical market is the fastest growing one and products made for this market must be safe to ingest. Chemical synthesis can be attractive as it is an easily scalable and well-defined process. On the other hand, raw materials can be expensive. This method also generates environmentally detrimental by-products that must be disposed of safely, further increasing the overall process cost [64]. Chemical synthesis presents one additional setback that severally limits the application of carotenoids produced in this fashion: as the final product is meant to me edible, it must be assured that it does not contain any harmful chemicals or other substances. This is quite difficult to accomplish when using purely synthetic methods as many of the chemicals employed in the reactions are toxic [64]. This drawback greatly increases the importance of isolating carotenoids from natural sources, as one only needs to utilize industry approved solvents or alternative extraction techniques to produce environmentally friendly food-safe carotenoids [66-68]. However, not all methods are equally efficient and economically relevant. Extracting carotenoids from discarded biomass like fruits and vegetables is currently an expensive and environmentally harmful process as large quantities of solvents are necessary [66]. And although the raw materials are relatively inexpensive as they are primarily by-products of the food industry, the supply of such materials is affected by seasonality, which can lead to restlessness in the markets. Moreover, as most of these raw materials are essentially foodstuffs, it means that carotenoids produced from these sources suffer from the same drawbacks as first generation biodiesel (see section 1.2.1.2). Scalability is also an issue as a scalable production must rest on a scalable supply and traditional carotenoid sources require time and large areas to be grown.

The abovementioned restraints turn the spotlight to carotenoid-producing microorganisms, like algae and some species of yeasts [49]. They benefit from the same advantages as other natural sources of carotenoids and have several others of their own, while at the same time having fewer drawbacks. Food-safe protocols can be applied to extract carotenoids from microorganisms [67], making them desirable to pharmaceutical, nutraceutical and food industries. Because they are grown under controlled conditions and are less affected by seasonality, microorganism-based productions can ensure year-round supplies of carotenoids. These culture systems are also easily scalable, allowing the supply to meet growing demands. Even within this strategy, distinction can be made between algae and other microorganisms such as yeast, with the technological advantage going to this last group [69]. As most species of algae are photosynthetic, culturing must be done in specially designed photobioreactors that

allow continued irradiation. If the light source is artificial than there is a continued energy consumption, making the process less profitable. On the other hand, if the system relies solely on solar radiation for the daytime period, than seasonality reemerges as a constraint. Additionally, the output of such systems can be affected by weather conditions. In general, algae also have slower growth rates when compared to yeasts, making each production run longer and more prone to contamination by faster growing microorganisms like bacteria. Yeasts are therefore a promising alternative as they can be cultured in traditional bioreactors and easily scaled from laboratory to pilot and industrial scales [69]. Because of their higher growth rates, large amounts of biomass can be produced fairly easily and in short amounts of time. Yeasts present the added advantage of being able to be grown under a large variety of carbon and nitrogen sources [69], presenting the possibility of reducing overall production costs by utilizing low-cost and sustainable substrates.

1.5. The oleaginous yeast *Rhodosporidium toruloides*

Rhodosporidium toruloides is an oleaginous yeast and a prolific carotenoid producer [24,45,70]. Formally designated either as *Rhodotorula glutinis* (of which *R. toruloides* is an anamorph) or *Rhodotorula gracilis*, this yeast belongs to the Fungi kingdom, Basidiomycota phylum, Microbotryomycetes class, Sporidiobolales order and *Rhodosporidium* genus [71,72].

The first reports on *R. toruloides* cultivations (or its anamorph) date back to the late 1970s, when Ratledge and Hall [73] published their work on continuous cultures of *R. glutinis* NCYC 154G under nitrogen and phosphate starvation for lipid production. In this work, the yeast was cultured at a pH of 5.5, a value that became a standard for assays performed with this microorganism [74-77]. The same authors carried out a set of different cultivations and determined that oxygen availability played a fundamental role in lipid production and accumulation in *Rhodotorula gracilis* [78]. Pan *et al.* [76] confirmed this with *R. glutinis*. Silva [79] cultured *R. toruloides* NCYC 921 in shake flasks and determined that the optimal pH for biomass and fatty acid production was in fact 4.0, while carotenoid production was maximized at pH 5.0. Based on these results, Dias *et al.* [77] develop a two-step pH process to cultivate *R. toruloides* in fed-batch mode, maximizing biomass, lipids and carotenoid production.

It has been reported that the yeast *R. toruloides* can accumulate intracellular lipids up to 70% (w/w dry cell weight, DCW) (Table 1.1), although most studies report lower lipid contents (from 48% [75] to under 20% [24], with the vast majority of results falling within this range [22,45,70,77]). This indicates that lipid content is highly dependent on the culture conditions as reported by Freitas *et al.* [70]. These authors grew the yeast in shake flasks with glucose as the carbon source; Saenge *et al.* [45] used a palm oil mill effluent as the carbon source added to the growth medium, used to inoculate the yeast *R. glutinis* TISTR 5159 in a 2 L bioreactor; Freitas *et al.* [24] also used alternative carbon sources, such as carob pulp syrup (CPS) and sugarcane molasses, to grow *R. toruloides* NCYC 921, and the assays were carried out in shake flasks; Li *et al.* [75] carried out *R. toruloides* Y4 cultivations in both shake flasks and a pilot-scale (15 L) bioreactor and reported lipid contents of 48 and 67.5%, respectively.

Moreover, the aforementioned works indicate that the yeast's lipid composition is also dependent on the culture conditions and that the most prevalent intracellular fatty acids are palmitic (16:0), stearic (18:0), oleic (18:1ω9), linoleic (18:2ω6) and linolenic (18:3ω3). Beyond these works, there are many others dedicated to the optimization of culture conditions using different strains of this yeast, or its anamorph, *R. glutinis* [39,45,75,77,80,81].

In regards to the production of carotenoids, the majority of pigments produced by *R. toruloides* are β-carotene, torulene and torularhodin [82]. The importance of these and other carotenoids is discussed in the previous section. However, information on *R. toruloides* as a carotenoid producer is still scarce.

The strain *R. toruloides* NCYC 921 was used in the present work due to the capacity to co-produce lipids and carotenoids. It is an obligatory aerobe that naturally inhabits the wood pulp from Coniferae and can grow on a variety of substrates, including (but not limited to) glucose, sucrose, arabinose, xylose, ethanol and glycerol. It was deposited in the National Collection of Yeast Cultures (NCYC) in April 1979 by the American Type Culture Collection (ATCC) [83].

1.6. Culture systems and strategies: batch, continuous and fed-batch cultures

When culturing microorganisms or other cells at the industrial level it is vital to ensure that the selected culture strategy is the most adequate to achieve the desired objective. Moreover, the utilized apparatus must allow monitoring and controlling the culture conditions in order to assure that the final product's specifications are as intended [84]. These requirements mean that the vessel in which microorganisms cultures are carried out is most often the stirred tank bioreactor, henceforth designated simply as a fermenter or bioreactor [85]. This is of course dependent on the type of microorganism that is meant to be cultured.

Running a fermenter in batch mode is the simplest way in which these bioreactors can be used. In this mode, no nutrients or fresh culture medium are added after inoculation. Culture parameters such as pH, dissolved oxygen (DO), temperature and stirring can be controlled. Despite the addition of base and/or acid to control pH and the collection of samples, the volume inside the fermenter is usually considered as a constant, meaning that there are usually no constraints related to the fermenter's capacity. A consequence of this methodology is that biomass, product and nutrient concentrations are time-dependent. In the particular case of medium nutrients, their continued consumption implies that, at some point, the culture will be starved of one or more compounds, after which point population growth will be halted. Usually fermentations in batch mode cannot be maintained for long periods of time for this precise reason. Supplementing the starting medium with higher concentrations of nutrients has its limits, as above certain concentrations problems like inhibition by substrate can occur [86,87]. This mode of operation is most widely used, often when the objective is to produce high amounts of biomass [87].

Alternatively, the fermenter can be run in continuous mode, meaning that the rate by which fresh medium is added to the vessel is matched by the rate by which exhausted medium is extracted. In less

technologically advanced systems, removing exhausted medium implies removing cells as well, meaning that if the feeding rate is too high, the specific growth rate (μ) will not be able to sustain the culture and it will wash out. On the other hand, if the feeding rate is too low, the culture will suffer starvation and cell growth will diminish until an equilibrium is reached between the specific growth rate and feeding/removal rates. At this point, the system will stabilize at the maximum specific growth rate (μ_{max}) [86,87]. This culture system is most often used in bioprocesses like effluent treatment, where producing biomass is not the main objective [88]. It is also suitable for the production of extracellular products or in cases where some extracellular products are toxic to the culture, above certain concentrations.

Fed-batch mode is essentially the bridge between batch and continuous operation modes and can encompass a variety of operational methodologies, like phased or continuous feeding with or without broth removal. Operating a fermenter in fed-batch mode can be the solution to overcome some of the limitations previously mentioned methods: population growth can be sustained by adding fresh medium, meaning that the exponential and stationary phases can be prolonged while a correct formulation of the feeding solution ensures that inhibition by substrate is avoided; the medium added to the fermenter can be changed at any given time, for example to limit one or more nutrients and trigger the activation of secondary metabolic pathways [86,87].

Because the production of fatty acids is usually triggered by nitrogen limitation [21,22] and carotenoids have been shown to be products mainly associated with the stationary phase of the cell population [22,77], fed-batch operation is the mode best suited for the simultaneous production of high amounts of both products when working with *R. toruloides* NCYC 921. This is due to the fact that high biomass concentrations must first be achieved in order to increase lipid and carotenoid productivities and this microorganism is prone to growth inhibition due to substrate from glucose concentrations over 40 $g.L^{-1}$ (data not shown).

1.7. Carob (*Ceratonia siliqua*)

The carob tree (*Ceratonia siliqua*) is an evergreen tree belonging to the Leguminoseae family, Caesalpinaceae subfamily [89]. Native to the Mediterranean region, it can be found in southern countries such as Portugal, Spain, Italy, Greece, Morocco, Turkey, Algeria and Tunisia, where its pods have traditionally been used both for human and livestock consumption, after some degree of processing [90-92]. The fruit of the carob tree, the carob pod, has a brown color and a leathery texture once ripe. It usually measures 10–30 cm in length by 1.5–3.5 cm wide by 1 cm thick and comprises two parts: the pulp, divided in a soft inner region (mesocarp) and an outer layer (pericarp), and the seeds that occur transversally in the pod and are separated by mesocarp from one another [89].

The carob pod is a rather versatile fruit and both the pulp and the seed can be utilized: the pulp can be ground to produce carob powder, usually for human consumption, or used as animal feed; carob has been widely used as a substitute for chocolate due to its similar taste and appearance, having the advantage of being caffeine and theobromine-free; the seeds, more precisely the endosperm, can be

extracted to produce locust bean gum (LBG), a galactomannan with strong gelling properties valued as a natural food additive [91,93]. However, the use of carob presents some limitations. Due to its intense and characteristic aroma, the amount of carob pulp used in animal rations is limited [90]. Human consumption is also limited by the high tannin content of the pod [91]. Utilization of the pulp alone translates into this crop having a relatively low market value for producers, however the increasing demand for natural food additives has, in more recent years, accentuated the economic importance of the carob tree [90]. Consequently, a rise in the production of LBG means an increased surplus of carob pulp, left behind as a by-product of the seed processing.

Unlike with other fruits, carob pulp extract cannot be prepared by subjecting the carob pulp to purely mechanical methods, i.e. pressing, as the water content of the pulp is just 8–9% [94]. The solution to this problem is to treat previously fragmented carob pulp by hot water blanching [90,91,95]. Turhan *et al.* [90] used CPS as a carbon source for bioethanol production and carried out several experiments in order to determine the best extraction protocol. Based on this work, the conclusion was that the optimal extraction conditions were 80 °C, 2 h and a 1:4 carob pulp to water ratio, resulting in a CPS with 115.3 $g.L^{-1}$ of total sugars. Additionally, this work revealed that temperature is the most important parameter amongst the three, with higher sugar extractions being associated with higher temperatures. Despite these findings, Sánchez *et al.* [91] achieved total sugar concentrations of 197.5 $g.L^{-1}$, with 61.36 $g.L^{-1}$ of reducing sugars, by preparing CPS at room temperature. These extractions were carried out for 20 min with carob to water ratios of 1:2.5. This was done based on the evidence that there is nearly 100% total sugars extraction yield from the carob pods that can be obtained in short extraction time periods (< 30 min), even at room temperature. This technique is preferable to others that involve heating steps, as this increases the likeliness of losing some of the extracted sugars by degradation reactions, leading to the formation or extraction of inhibitory compounds like furfural, hydroxymethylfurfural (HMF) and acetic acid [96-99]. More recently, Freitas *et al.* [24] prepared CPS by extracting sugars with a 1:2 carob pulp to water ratio, at room temperature overnight. Although not mentioned in the paper, the total sugar concentration obtained in the CPS was 200 $g.L^{-1}$ and it was successfully used as a carbon source in *Rhodotorula glutinis* NCYC 921 cultivations. Detailed composition of the CPS was not presented in the mentioned work, however it should be similar to the CPS composition detailed in section 4.1.1 as the same preparation protocol was followed.

1.8. Flow cytometry

Flow cytometry (FC) is a laser-based technology that allows the simultaneous analysis of the chemical and physical characteristics of particles in a fluid. Depending on the FC apparatus and setup, FC can be used for cell counting, cell sorting, protein engineering and biomarker detection, amongst other applications [100]. FC is of particular importance to process modeling as it allows real time process control, a strategy that yields far more reliable and accurate results than traditional analytical techniques, which are usually performed on samples taken during the course of an experiment or process, but only give the results some time afterwards [14].

1.8.1. Apparatus and techniques

The flow cytometer is an equipment that comprises a series of integrated systems for cell and cellular function analysis, namely: a radiation source, either a laser or a mercury lamp; a flow cell; optical filters; light detectors, comprising photodiodes and photomultiplier tubes (Figure 1.13), and a data analysis unit [14].

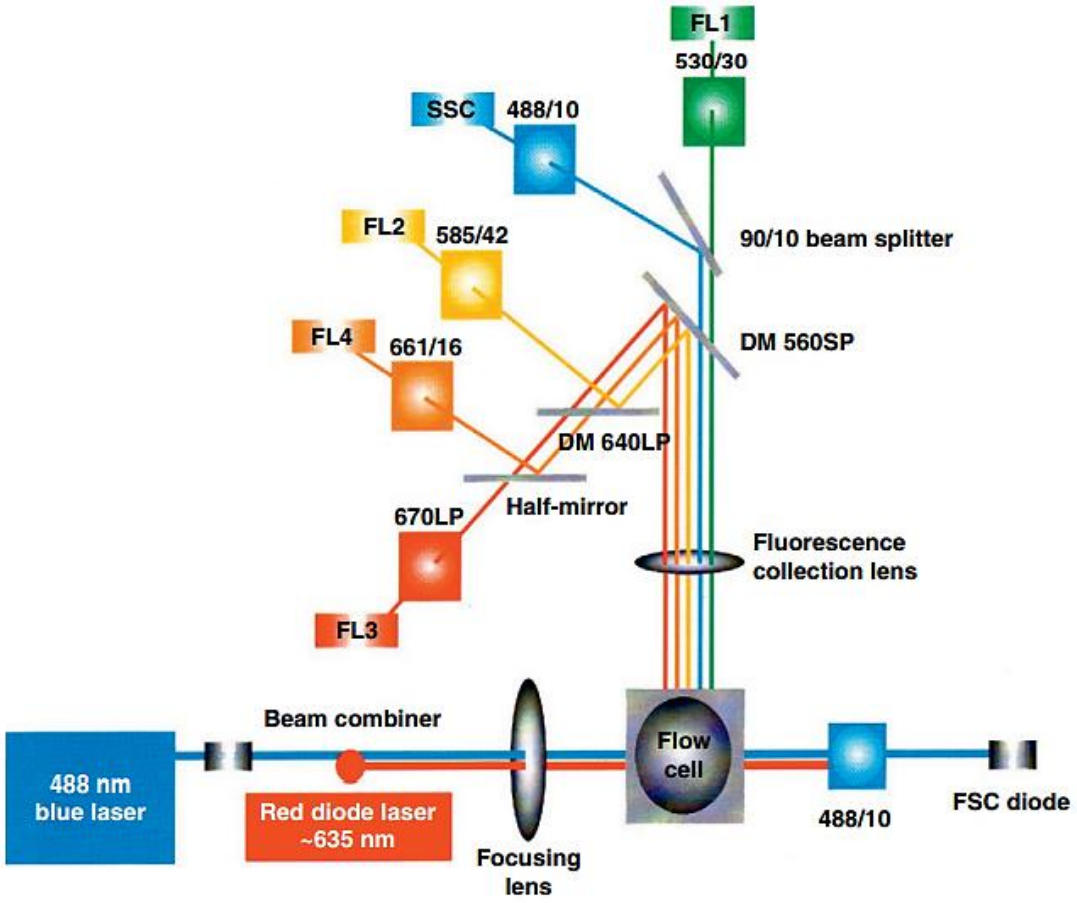

Figure 1.13 – Optical diagram of the FACScalibur benchtop flow cytometer (Becton-Dickinson Biosciences, Franklin Lakes, New Jersey, United States of America). Key: FSC – forward scatter detector; SSC – side scatter detector; FL1, FL2, FL3, FL4 – fluorescence detectors; DM – dichroic mirror; SP – shortpass filter; LP – longpass filter. The FSC is a photodiode and SSC, FL1, FL2, FL3 and FL4 are photomultiplier tubes. Figure adapted from da Silva *et al.* [14].

The flow cytometer's sampling system is based on hydrodynamic focusing. Cells, or other particles to be analyzed, are suspended in a saline solution, making up the sample. This is then aspirated by the flow cytometer and passed through the flow cell in between two layers of rapidly moving fluid, designated sheath fluid. With the sheath fluid running at laminar flow, the sample stream can be made to pass through the flow cell in such a way as to ensure that a single particle intercepts the laser (or light stream) at a time [14,101]. The sample flow is perpendicular to the light source and once a particle crosses the light stream it scatters the incoming light, which in turn is picked up by cytometer's scattered light detectors: one for forward scattered (FSC) light, placed in the same plane of the incoming radiation, and one for side scattered (SSC) light, placed at a 90° angle from the light source. Light arriving at the FSC detector has passed unobstructed through the sample, thus giving information regarding the size of the particles being analyzed. On the other hand, the radiation picked up by the

SSC sensor has been deflected by the particles in the sample, giving information on the particle's granularity. In the case of those particles being cells, light can be scattered by their internal components, providing valuable information regarding said cell's internal complexity. The combined information from both detectors can be used to identify different populations of particles present in the same sample, such as yeast cells from bacteria and debris [14].

The incoming radiation can also be used to excite fluorescent molecules present in the sample, such as dyes and probes. The resulting fluorescence, having a different wavelength than the flow cytometer's light source, is measured by the flow cytometer's fluorescence detectors (FL1 through FL4), each one being sensitive to a specific wavelength [14]. Different dyes and probes can be used to gain information on the cell's physiological condition (Figure 1.14).

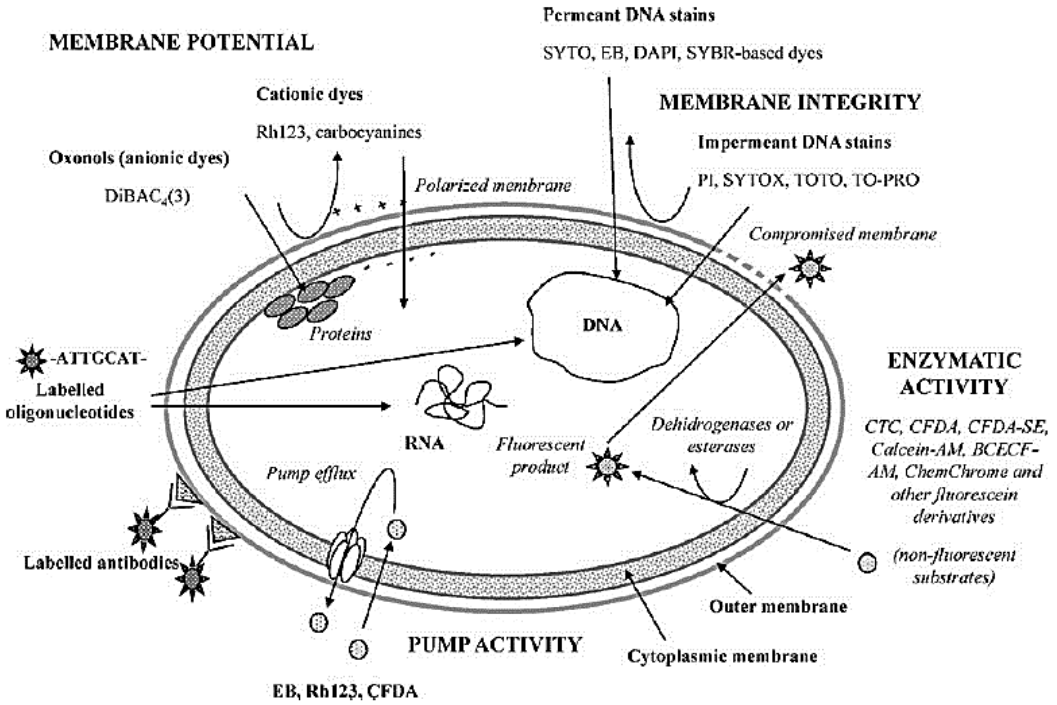

Figure 1.14 – Scheme of different cell target sites and probes for fluorescent labelling. Reproduced from Díaz *et al.* [101].

In the particular case of the flow cytometer used in the present work (FACScalibur benchtop flow cytometer from Becton-Dickinson Biosciences, Franklin Lakes, New Jersey, USA), two radiation sources are available: a blue argon laser (488 nm) and a red diode laser (635 nm). The FSC and SSC detectors both work in the same wavelength as the blue argon laser (488±10 nm). As for the fluorescence detectors, FL1 is sensitive to radiation in the green region of the visible spectrum (530±30 nm), FL2 measures yellow radiation (585±42 nm), FL3 is sensitive to red radiation (> 670 nm) and FL4 detects orange radiation (661±16 nm) [102].

1.8.2. Determination of membrane potential

Biological membranes define the finite space that is referred to as a cell. In the case of eukaryotic cells, they are responsible for creating distinct and defined environments within the cell. Far from being

passive barriers, biological membranes are the structures that allow cells to precisely control the chemistry inside its boundaries. A key function of biological membranes, whether they are the cytoplasmic membrane or the membrane of a cellular organelle, is their ability to generate a chemical or ionic gradient, or potential, from the outside to the inside of the enclosed space [103]. In the particular case of the mitochondrial membrane, this potential is related to the biological synthesis of adenosine triphosphate (ATP) [104]. When the potential across a membrane decreases to zero, ions can permeate it freely and can no longer be utilized to drive biological reactions. Consequently, the maintenance of membrane potentials is indicative of healthy, live cells and is therefore a key parameter in the establishment of cell viability [14,101,105].

The assessment by FC of whether cells are maintaining a membrane potential or not is usually done by exposing the cells to charged lipophilic dyes. These dyes can permeate the cellular membrane and once inside the cell they accumulate according to their charge. Generically, cationic dyes such as carbocyanines accumulate inside polarized cells and are therefore used to stain viable cells, whereas anionic dyes like oxonols stain inactive or depolarized cells [101].

The compound 3,3'-dihexyloxacarbocyanine iodide ($DiOC_6(3)$) is a positively charged lipophilic dye that emits green fluorescence [106]. As with other carbocyanines [107], $DiOC_6(3)$ permeates the cellular membrane of polarized cells. However, it has the particular characteristic of emitting much greater levels of fluorescence once it binds to the mitochondrial membrane, when compared to the signal generated by binding to the cytoplasmic membrane, making possible to use this dye to specifically evaluate the polarization of the mitochondrial membrane [24,106]. This allows differentiating between polarized and depolarized cells.

1.8.3. Assessment of metabolic activity

The fact that a cell has its biological membranes depolarized to some extent is not sufficient to establish cell death, although it is a clear indication that the cell has lost some of its activity and has been subjected to some degree of stress [101,105]. One other way to obtain information on cell viability is to perform metabolic activity assays, which can easily be carried out using FC [14,101].

Dyes used to measure metabolic activity are generally not fluorescent compounds. Instead, they are cleaved or modified in some other way to produce fluorescent by-products which are then detected by the FC apparatus. One such dye is CTC (5-cyano-2,3 ditolyl tetrazolium chloride): it is reduced by dehydrogenases to fluorescent CTC-formazan precipitates, indicating that the respiratory chain is active [101]. Because CTC can be toxic to cells if it is allowed to accumulate inside them, some authors have suggested that CTC staining can only be used to assess metabolic activity in the most actively respiring cells [108]. Esterase activity can also be detected by FC as a cell viability parameter. In this case, staining with fluorescein and fluorescein derivatives has become the standard methodology [109,110]. Being neutral, these dyes can permeate the cell membrane by diffusion. Once inside the cell, they are cleaved by esterases into fluorescent products that are retained if the cell has intact membranes. If the cytoplasmic membrane is not intact, both non-hydrolyzed substrate and products are released and thus these cells will not appear to be stained [101]. Fluorescein diacetate (FDA) and diacetate of

carboxifluorescein (CFDA) are two dyes commonly used to assess esterase activity, with CFDA being the better choice as FDA usually provides weaker fluorescence signals and its products are poorly retained by bacteria [111]. CFDA is better retained by cells, however the fluorescent products resulting from CFDA cleavage have been reported to be actively extruded from *Saccharomyces cerevisiae*, meaning that this dye has its limitations and staining might not be efficient [101]. An alternative to CFDA is carboxyfluorescein diacetate succinimidyl ester (CFDA/SE) as it results in fluorescent products better retained by cells. Yet this dye has been reported as unable to yield robust results when used to stain several strains of freshwater bacteria [112]. This means that the use of these dyes must be done under rigorous protocols and it should be first confirmed that they are suitable for the intended analyses. For example, despite the reports of extrusion by *S. cerevisiae*, Freitas *et al.* [70] have successfully used CFDA to stain the yeast *R. toruloides*.

Finding evidence of metabolic activity in a cell population is a clear indication that said cells are not dead, however special attention must be paid when dealing with populations that have been subjected to severe damage or that are dormant [101]. In the first instance, damaged cellular membranes might prevent fluorescent products from remaining inside the cell, thus lowering the fluorescence levels and leading to false negatives. Similarly, if cells are dormant their metabolic activity may be too low to be detected, again leading to the wrong conclusion regarding cell death. The presence of active ion pumps in the cellular membrane may also interfere with results if the fluorescent products are excreted [101]. On the other hand, determination of metabolic activity can yield false positives due to the fact that enzymatic activity is, in many cases, independent of cell energetics. Even if the cell is inactive in the sense that it can no longer synthesize new products in order to sustain its functions, previously synthesized enzymes can remain active for a period of time and produce a positive result [113].

1.8.4. Determination of membrane integrity

Membrane integrity is regarded as the best and most definitive method to determine whether a cell is viable or not. This is a direct consequence of the importance of the role played by cytoplasmic membranes in maintaining a controlled cellular environment [103]. A cell with a compromised cellular membrane cannot produce or sustain electrochemical gradients essential to maintain its activity. Furthermore, a compromised membrane means that the cellular contents will be exposed to extracellular medium and will eventually decompose [101]. Compared to the above-mentioned analysis, determination of membrane integrity is a more robust method to conclude is a cell's viability has been compromised because membrane depolarization can be reversed (when the membranes are intact) and failure to establish metabolic activity might simply indicate that the cells are dormant or that the cytometry protocol is not adequate [114].

The most common way to assess membrane integrity is to use dye exclusion methods [107]. This methodology involves the use of dyes with one or multiple charges that cannot permeate the cellular membrane unless it is compromised. Once inside the cell, these dyes bind to nucleic acids and become fluorescent [101]. These dyes include SYTOX stains [115], cyanines [116], propidium iodide (PI)

[70,101] and ethidium bromide (EB) [117]. Amongst these, PI is the stain most commonly used to assess membrane integrity, despite reports indicating that it can accumulate inside viable bacteria during exponential growth phase [101,118]. EB is a less preferable dye because it has a single positive charge, which allows the dye to permeate intact cell membranes and thus yielding false positives [117].

Figure 1.15 presents a summary of how information regarding membrane potential (see section 1.8.2), metabolic activity (see section 1.8.3) and membrane integrity can be used to determine a cell's viability and vitality.

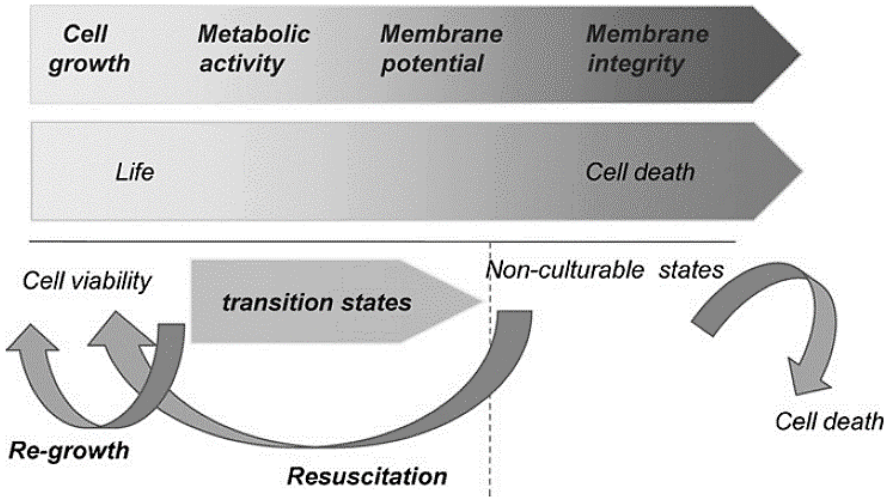

Figure 1.15 – Functional criteria to determine different levels of cell viability and vitality. Multiparametric analysis allows to redefine the term of cell viability based on cell metabolism (enzymatic activity and membrane potential) and membrane integrity detection. Reproduced from Díaz *et al.* [101].

1.8.5. Flow cytometry for bioprocesses: applications and perspectives

Because of its versatility, FC can be a valuable tool for a myriad of applications in various fields, from the food and beverage industries, to pharmaceuticals and medical applications, environmental analysis and bioprocess intensification and control [101].

In the food industry, FC can be used to detected microorganisms responsible for spoilage or that in any way alter the organoleptic properties of both raw materials and final products [119,120]. In the beverage industry, especially in alcoholic beverages production, FC has been used to monitor and control the process of beer [121,122], wine [110,123] and cider production [124]. Information gathered through the use of FC can be used in this setting to optimize and select yeast starter cultures [101].

Flow cytometry has also been used in the pharmaceutical industry, mainly at the research level, where has been proven to be a powerful tool to assess susceptibility of different microorganisms to drugs and antibiotics [125,126]. Furthermore, it has also been used in cell characterization and to study gene regulation and expression [127].

Regarding environmental analysis, FC can be used to rapidly analyze water samples and assess the effectiveness of disinfection techniques like UVA irradiation [128], chlorination [129] or ozonization

[130]. In fact, FC is steadily becoming a standard analytical method in cell quantification and viability assessment for environmental and aquatic systems [113].

An interesting perspective is to use FC to provide additional data for process and kinetic modelling. Because of their simplicity and ease of use, mathematical models of cell cultures tend to be based on average values of the population, mainly due to the techniques that are employed when gathering that information [101]. This includes measurements of total biomass concentration, substrate consumption and product formation, amongst others. However, because these values report to the average state of the cell population and do not provide information on the single cell level, such mathematical models can turn out to be inaccurate [131]. Flow cytometry can be a valuable tool in constructing more accurate cell population models because of the influence that cell heterogeneity is believed to have in the outcome of fermentations, even when done in controlled laboratory conditions [132]. Despite still being in its infancy, application of FC in kinetic modeling is yielding promising results: Cipollina *et al.* [133] successfully demonstrated that FC can be used to build and validate a morphological model to describe the growth of a yeast population, based on cellular heterogeneity; Camacho *et al.* [134] used FC analysis to construct a model to predict the emergence of apoptotic, irreversibly damaged, dead cells and cell debris from viable cells as a result of shear stress in cultures of the marine sponge *Axinella damicornis*; Alcon *et al.* [135] built a structured model for *Candida bombicola* growth that takes into account the effects of temperature, nutrients, oxygen and other such variables, again supported be FC measurements.

This last example [135], together with similar studies undertaken by other authors [136,137], set the tone to what can become a major breakthrough in monitoring, modelling and controlling biological industrial processes. Being able to assess the state of individual cells in a culture and determining what is the proportion of viable to non-viable is of the upmost importance when trying to engineer a process that ensures the best possible product specifications. Flow cytometry allows for “next-to-real-time” measurements that can provide information on when is the best time to harvest cells, when to change culture conditions to induce product synthesis or how to optimize feeding strategies in fed-batch cultures [101]. da Silva *et al.* [14] have presented a review on how FC can be used to improve the production of different types of biofuels and recently several works regarding biodiesel production have been published that present FC as an unmatched tool in optimizing culture conditions [24,70,77,102].

Furthermore, FC can also be utilized to quantify intracellular products of commercial interest much quicker and yielding better, more reliable results than conventional analytical techniques. An example of this type of application is the quantification of total carotenoid content in yeast cells in next-to-real-time, developed and optimized by Freitas *et al.* [70] and used by Freitas *et al.* [24] and more recently by Dias *et al.* [77]. This protocol was also used in the present work to quantify total carotenoid content throughout the various performed Assays, instead of more cumbersome and labor intensive traditional techniques used for carotenoid detection [102].

2 Objectives

The main objective of this work was to optimize the concomitant production of carotenoids and lipids by the yeast *Rhodosporidium toruloides* NCYC 921 using CPS as a carbon source. This work was carried out in a 7 L (5 L working volume) benchtop fermenter operating in fed-batch mode.

As a secondary objective, the possibility to scale up fermentations with the above mentioned yeast was evaluated by carrying out a cultivation in a 50 L pilot scale fermenter (35 L working volume), operated in fed-batch mode. For logistical reasons, this assay was performed using glucose as the carbon source.

Flow cytometry was employed to monitor the yeast cultures in real time, screening for indicative parameters of cell viability (membrane potential and integrity and enzymatic activity) and total carotenoid content. These results were supplemented by measuring the culture's biomass concentration, dissolved oxygen content and residual sugars. The total fatty acid content of the yeast cells was also monitored throughout the yeast cultivation.

Different methods of preparing CPS and their impact on the final sugar concentration of the syrup were evaluated in order to understand how the extraction protocols affect cellular growth during fermentations.

3 Materials and Methods

3.1. Equipment and Reagents

Reagents and other miscellaneous products used throughout the work are listed in Table A.1, which can be found in Annex I.

The equipment used in this work is presented throughout the text, whenever necessary.

3.2. Disclosure

Originally, the aim of this work was to develop and optimize *R. toruloides* NCYC 921 cultures using CPS as a low-cost substrate instead of a defined carbon source (glucose). However, several setbacks throughout the work (including equipment failure, contamination of inocula and cultures and delays in the delivery of reagents and equipment) meant that it could not be executed to its full extent and only two cultivations were performed using CPS.

Two additional objectives were set to compensate for this situation: (i) the possibility of scaling-up the cultivations with glucose as carbon source by using a 50 L bioreactor; (ii) characterization of the CPS used in the performed assays, as well as an evaluation of the impact of storage conditions and different sugar extraction methods on CPS composition. These last experiments were performed after both cultivations with CPS, so the optimal conditions regarding CPS preparation relative to sugar extraction were not those employed in the Assays (see section 3.5.1).

3.3. Microorganism

The microorganism used for this work was the oleaginous yeast *Rhodosporidium toruloides* NCYC 921, supplied by the National Collection of Yeast Cultures (Norwich, United Kingdom). The yeast was kept in malt extract agar slants at 4 °C. Prior to the inocula preparation, the yeast was transferred to fresh malt extract agar slants which were incubated (NIR 252 Incubator, SANYO Electric Co., Ltd., Japan) for 72 h at 30 °C.

3.4. Inoculum

3.4.1. Inocula for assays in the 7 L bioreactor

The inocula were prepared in baffled Erlenmeyer flasks containing semi-defined culture medium, as described by Pan *et al.* [76], supplemented with a carbon source. The composition of the semi-defined culture medium (without the carbon source) is shown below, in table 3.1. Table 3.2 gives the composition of the trace minerals solution used in the preparation of the semi-defined culture medium [76].

Table 3.1 – Composition of the semi-defined culture medium, as described by Pan *et al.* [76].

Medium component	Concentration ($g.L^{-1}$)
KH_2PO_4	12.5
Na_2HPO_4	1.0
$(NH_4)_2SO_4$	5.0
$MgSO_4 \cdot 7H_2O$	2.5
$CaCl_2 \cdot 2H_2O$	0.25
Yeast extract	1.9
Trace minerals (see Table 3.2)	0.25 $mL.L^{-1}$

Table 3.2 – Composition of the trace minerals solution, as described by Pan *et al.* [76]. The solvent for this solution is 5 N-HCl.

Solution component	Concentration ($g.L^{-1}$)
$FeSO_4 \cdot 7H_2O$	40
$CaCl_2 \cdot 2H_2O$	40
$MgSO_4 \cdot 7H_2O$	10
$AlCl_3 \cdot 6H_2O$	10
$CoCl_2$	4
$ZnSO_4 \cdot 7H_2O$	2
$NaMoO_4 \cdot 2H_2O$	2
$CuCl_2 \cdot 7H_2O$	1
H_3BO_4	0.5

The above-mentioned culture medium was sterilized by autoclaving (Uniclave 88, Portugal).

To prevent excess caramelization, the carbon source, whether glucose or CPS, was autoclaved separately and then added to the remaining components of the culture medium. The carbon source solution was added to the culture medium (Table 3.2) so that the final carbon source concentration was 35 $g.L^{-1}$ before inoculation.

For these Assays, 150 mL of culture medium were inoculated using two slants (see section 3.3) and grown for 24 h at 30 °C and 150 rpm (Unitrom Infors, Switzerland).

3.4.2. Inoculum for the Assay in the 50 L bioreactor

To prepare inocula for the 50 L bioreactor, two 150 mL pre-inocula were prepared as previously described (see section 3.4.1). These were then used to inoculate baffled 5 L-Erlenmeyer flasks containing 1350 mL each of culture medium with a sugar concentration of 35 $g.L^{-1}$, resulting in two 1500 mL inocula that were grown for 24 h at 30 °C and 150 rpm (Unitrom Infors, Switzerland). Both inocula were used to inoculate the 50 L bioreactor.

3.5. Experimental Assays

3.5.1. CPS preparation

Prior to use, crushed carob pulp (Chorondo & Filhos Lda., Faro, Portugal), supplied in plastic bags placed inside burlap sacks, was in the laboratory at room temperature.

CPS preparation for the first assay using this carbon source was done with the same technique as described by Freitas *et al.* [24], with some modifications: (i) fragmented carob pulp was mixed with water in a 1:2 ratio; (ii) extraction was carried out overnight at room temperature (~ 20 °C); (iii) the following day, the water was collected and the wet carob pulp was pressed with a hand-operated hydraulic press to over 150 bar in order to extract more water; (iv) the collected water was centrifuged (Sigma 2-16K, Sartorius, Germany) for 10 min at 9000 rpm and at 5 °C to remove any suspended solids (Figure 3.1). The solution obtained after this step will henceforth by referred to as sugar solution from carob pulp, SSCP; (v) the SSCP was acidified to pH 2.0, placed in open Erlenmeyer flasks and left to hydrolyze overnight at 100 °C (Memmert UM 80, Memmert GmbH+Co.KG, Germany). The product of the hydrolysis is the CPS, which was again centrifuged (Sigma 2-16K, Sartorius, Germany) for 10 min at 9000 rpm and at 5 °C, then sterilized by autoclaving (Uniclave 88, Portugal) after the pH was corrected to 4.0. This process is outlined in Figure 3.2.

Figure 3.1 – Sugar solution from carob pulp, before (on the left) and after (on the right) clarification by centrifugation.

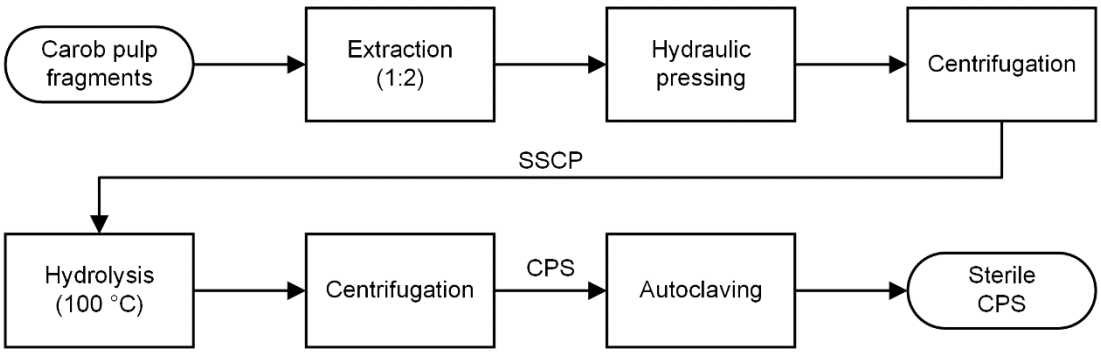

Figure 3.2 – Schematic of the sterile CPS production process for the first assay using this carbon source.

For a second assay using CPS as the carbon source, CPS was prepared as previously described, with one additional step: before hydrolysis, the SSCP was placed in an incubator (Memmert ULE 500, Memmert GmbH+Co.KG, Germany) at 40 °C and left to concentrate until approximately half of the volume had been lost. The concentrated SSCP was acidified to pH 2.0 and left to hydrolyze at 100 °C overnight, then centrifuged (Sigma 2-16K, Sartorius, Germany) for 10 min at 9000 rpm and at 5 °C, to remove any particle or precipitate, as done before to the SSCP. Then the pH of the CPS was raised to 4.0 and it was sterilized by autoclaving (Uniclave 88, Portugal).

In both cases, samples were collected at various stages of the CPS preparation protocol to determine the total sugar content and the concentration of inhibitory compounds (furfural and HMF).

Additionally, two experiments were conducted in order to determine how pulp storage conditions influence CPS composition and how the CPS composition was dependent on the extraction conditions:

1) A second batch of crushed carob pulp (Chorondo & Filhos Lda., Faro, Portugal) was used to produce CPS and determine whether the conditions under which the raw material is stored influenced the CPS composition, as this one was stored in sealed plastic drums and kept at 5 °C;
2) An extraction was performed according to the technique described by Turhan *et al.* [90], by which the extraction of soluble compounds was done with a 1:4 carob pulp to water ratio for 2 h at 80 °C (Memmert ULE 500, Memmert GmbH+Co.KG, Germany). The resulting solution was then hydrolyzed and autoclaved as previously described. This was done with both carob pulp batches stored under different conditions (room temperature and 5 °C).

3.5.2. Cultivations

This work is framed within the national project PTDC/AAC-AMB/116594/2010 – Carofuel – New process for a sustainable microbial biodiesel production: The yeast *Rhodosporidium toruloides* biorefinary as a source of biodiesel, biogas and carotenoids and was based in previous results that specified a set of optimal parameters for the simultaneous production of carotenoids and lipids by the yeast *Rhodosporidium toruloides* NCYC 921 in laboratory-scale fermenters, using glucose as a carbon source and operating in fed-batch [77]. Previous efforts have culminated in the following experimental protocol: *Rhodosporidium toruloides* NCYC 921 cells are cultivated in a two-step pH control fed-batch system, designed to first maximize the yeast biomass growth and lipid accumulation carried out at pH 4.0 and, in a second step, the carotenoid production is induced by changing the feeding nutrient composition and the medium pH to 5.0. The cultivations begin in batch mode, with an initial total sugar content of 35 $g.L^{-1}$ at the time of inoculation; once the available carbon source is exhausted, the cultivation is fed with a solution containing a carbon source and other nutrients (see Table 3.4 for the detailed feed composition) at a variable feeding rate, until the end of the growth phase; once the culture reaches the stationary phase, the pH is altered to 5.0, and the previous feeding is replaced by a carbon source solution, i.e. water with dissolved sugar(s) at a concentration of 600 $g.L^{-1}$, again with a variable feeding rate. Throughout the entire cultivation the temperature is kept at 30 °C. Previous work by this team [77] has shown that the change in pH during the stationary phase may potentiate the production and accumulation of carotenoids during this phase. These were the experimental conditions of Assay I, performed to establish a reference cultivation against which other Assays would be compared (Table 3.3).

Assay II was performed under the same conditions of Assay I, except for the pH of the stationary phase (5.5 instead of 5.0) (Table 3.3). The purpose of this Assay was to evaluate the impact of the medium pH of 5.5 on the yeast carotenoid and fatty acid production since this pH value was used in

earlier works by Ratledge and Hall [73], Yoon and Rhee [74] and Pan *et al.* [76], being considered optimal for growth and lipids production by this strain.

Given the above-mentioned parameters, the next experiments were performed in order to replace the defined carbon source (glucose) by a carbon source present in low-cost substrates, in this case CPS. The use of this carbon source presents several problems, such as (but not limited to) variable sugar contents, in both concentration and ratios, and presence of inhibitory compounds [95,138].

Assay III was carried out under the same conditions as the previous assays, except that a CPS solution with a total sugar concentration of 200 $g.L^{-1}$ was added to the culture (Table 3.3). This sugar concentration was one third lower than the one used in previous experiments. It was observed that such a total sugar concentration resulted in the use of higher feeding rates, which led to the end of the cultivation before the carotenoid production stage, due to the maximum level of the vessel has been reached earlier.

In order to overcome this limitation, the CPS was concentrated, so that lower feeding rates could be used. This concentrated CPS (described in section 3.5.1) was used in Assay IV (Figure 3.3).

Finally, the possibility of scaling up the production was evaluated by caring out a fermentation in a 50 L pilot scale fermenter (35 L working volume). The conditions set for this Assay (Assay V) were the same as for Assay I (Figure 3.3).

Table 3.3 gives a summary of all performed Assays and what parameters were unique to each one. All additional parameters were kept the same throughout the Assays.

Table 3.3 – Conditions of the yeast cultivations performed during this work. TSC, total sugar concentration.

Assay	pH	Scale	Initial volume without inoculum (L)	Carbon source	TSC of the feeding solutions ($g.L^{-1}$)
I	4.0 → 5.0	Laboratory	2.850	Glucose	600
II	4.0 → 5.5	Laboratory	2.850	Glucose	600
III	4.0 → 5.0	Laboratory	2.850	CPS	200
IV	4.0 → 5.0	Laboratory	2.850	Concentrated CPS	550
V	4.0 → 5.0	Pilot	15.00	Glucose	600

Table 3.4 gives the composition of the nutrients solution. Feeding was continuous using a peristaltic pump (520Du, Watson Marlow, USA). The feeding rate was adjusted according to the concentration of residual glucose, ideally kept under 40 $g.L^{-1}$ to avoid growth limitations due to substrate inhibition. Once the culture entered stationary phase (determined by OD readings), the feeding solution was changed a 600 $g.L^{-1}$ solution of glucose in the case of Assays I, II and V or CPS for Assays III and IV. pH was set at 5.0 (or 5.5 in the case of Assay II).

Table 3.4 – Composition of the nutrient solution used for fed-batch.

Compound	Concentration ($g.L^{-1}$)
Yeast extract	20
$MgSO_4 \cdot 7H_2O$	9
Glucose†,‡	600

† - For Assay III, the carbon source was CPS with a total sugar content of 220 $g.L^{-1}$.
‡ - For Assay IV, the carbon source was CPS with a total sugar content of 550 $g.L^{-1}$.

Assays I through IV were performed in a 7 L (5 L working volume) bioreactor, coupled with a dedicated controller to measure and control agitation, DO, temperature, pH and foaming (FerMac 310/60 Bioreactor, Electrolab Biotech, United Kingdom). pH was controlled by adding 5 M sodium hydroxide (NaOH) and 5 M-HCl and measured with a pH probe (Mettler Toledo, Switzerland). Two drops of pure sterile polypropylene glycol (PPG) were added in the beginning of the cultivation to prevent foaming at an early stage. Throughout the cultivation the foam level was monitored and automatically controlled through the addition of a 1:10 aqueous sterilized solution of PPG, whenever foaming was detected. Agitation was done by means of two Rushton turbines and temperature was controlled by heating/cooling system comprising an external heating blanket and an internal cold finger. The temperature probe is an integral part of the FerMac 360 Controller. Improving mixing was further assured by placing a harness with four baffles inside the fermentation vessel. DO levels were monitored with the aid of an oxygen probe (Mettler Toledo, Switzerland). The basic experimental setup for these Assays can be seen in Figure 3.3.

Figure 3.3 – Basic experimental setup for Assays I through IV.

Assay V was performed in a 50 L (35 L working volume) bioreactor (C 809, Biolafitte, France), coupled with a dedicated control module to measure and control temperature and stirring. pH and DO were monitored with the aid of an external control module (MOD 7F, Setric Genie Industriel, France). pH was controlled by adding 10 M-NaOH with the aid of a peristaltic pump (Setric Genie Industriel, France) connected to the control module or 5 M-HCl manually. The pH probe was an Ingold InFit 764-50 (Mettler Toledo, Switzerland) and the DO probe was from the same manufacturer (Mettler Toledo, Switzerland). Foaming was controlled by manually adding drops of PPG. Agitation was done by the means of three Rushton turbines and four lateral baffles and temperature was controlled by the

fermenter's integrated heating/cooling external jacket. The experimental setup for this Assay can be seen in Figure 3.4.

Figure 3.4 – Experimental setup for Assay V.

In Assays I through IV, the DO was maintained at 40% of the air saturation by automatically tuning the agitation speed in order to avoid oxygen limitation. In Assay V, all changes in agitation speed were done manually as the Biolafitte bioreactor was not capable of automatically controlling this setting. Additionally, DO was controlled by changing the internal pressure of the vessel.

Samples were collected periodically and their pH was measured with a benchtop pH meter (Consor C3021, Belgium) to confirm the reading given by the bioreactor's probe. If necessary, corrections were made to the set-point to ensure that the culture was kept at the desired pH value. The residual glucose concentration was promptly estimated in the samples using the glucose Combur-Test® Strips (Roche, Switzerland) and the feeding rate was adjusted according to this information, so that the residual sugar concentration would not increase above 40 $g.L^{-1}$, in order to avoid substrate inhibition. This test reveals the concentration of glucose by means of color change of a sensitive area that was exposed to the culture medium. These strips are sensitive to glucose concentrations between 0.5 $g.L^{-1}$ and 10 $g.L^{-1}$. The optical density of each sample at 600 nm (OD_{600}) (ThermoSpectronic Genesys 20, Portugal) was also recorded. This value would later be used to calculate the culture's biomass concentration (see section 3.7.1). Additionally, in the case of Assays III and IV, biomass growth was accompanied by dry weight measurement because residues present in the CPS could potentially interfere with OD readings. Finally, samples were analyzed by FC to assess cell viability and carotenoid content (see section 3.6.4). The samples were centrifuged (Sigma 2-16K, Sartorius, Germany) for 10 min at 9000 rpm and at 5 °C to separate the biomass from the supernatant and both fractions were frozen at -18 °C, for further analysis (see sections 3.6.2 and 3.6.3).

3.6. Analytical methods

3.6.1. Determination of the composition of CPS prepared under different conditions by High Performance Liquid Chromatography (HPLC)

Samples collected during CPS preparation were analyzed by HPLC (Agilent 1100 Series, Germany), using an Aminex HPX-87H (Bio-Rad, California, USA) to detect glucose, sucrose, fructose, galactose, xylose, arabinose, furfural and HMF and an Aminex HPX-87P (Bio-Rad, California, USA) column to screen for acetic acid (CH_3COOH), furfural and HMF. The columns' characteristics and operational conditions are presented in Table 3.5.

Table 3.5 – Main characteristics of Aminex chromatography columns HPX-87H and HPX-87P and their respective operating conditions. RI, Refraction index; UV, Ultraviolet.

Characteristics	Column	
	Aminex HPX-87H	**Aminex HPX-87P**
Dimensions	300 × 7.8 mm	
Mobile phase	H_2SO_4, 0.5 mM	H_2O
Flow rate	0.6 $mL.min^{-1}$	
Volume sampled	5 µL	20 µL
Column temperature	50 °C	80 °C
RI detector temperature	50 °C	55 °C
UV detector wavelength	280 nm	

Concentrations of the above-mentioned compounds were calculated by building calibration curves with standard solutions of each compound, with concentrations ranging from 0.1 to 20 $g.L^{-1}$.

Prior to analysis, all samples were filtered with 0.20 µm filters (Millipore®, Merck Millipore, Germany) and diluted so that the concentrations of the desired compounds fit the calibration curves. All saccharides and acetic acid were quantified using a refraction index (RI) detector while furfural and HMF were quantified using an ultraviolet (UV) radiation detector that is part of the equipment's diode array detector (DAD). Both detectors were used with either columns.

The chromatograms were analyzed using the ChemStation for LC 3D Systems Rev. B.01.03 software (Agilent Technologies, USA).

3.6.2. Quantification of residual sugars

3.6.2.1. Quantification of reducing sugars using 3,5-dinitrosalicylic acid

The reducing sugars present in the supernatant of each sample were quantified using the 3,5-dinitrosalicylic acid (DNSA) method [139].

Briefly, DNSA reagent was prepared by mixing 5 g of DNSA, 8 g of NaOH and 150 g of potassium sodium tartrate ($KNaC_4H_4O_6 \cdot 4H_2O$) in 500 mL of distilled water while applying gentle heat. The DNSA reagent was then filtered and kept in a tinted glass bottle, protected from light.

In test tubes, 0.5 mL of DNSA reagent were added to 0.5 mL of supernatant. This solution was heated by placing the test tubes in boiling water for 5 min and afterwards cooled in an ice bath for an

additional 5 min. 5 mL of distilled water were added to each sample, which were homogenized (MS2 Minishaker, IKA, Germany) before their absorbance at 550 nm was read (ThermoSpectronic Genesys, Portugal), measured against water. All samples were prepared in duplicated.

The quantification of reducing sugars in each sample was done by comparing the absorbance of each sample to a calibration curve prepared by applying the above-mentioned methodology to a series of standards prepared with glucose. A new calibration curve was prepared for every set of samples.

This techniques was used to quantify reducing sugars (glucose) in Assays I, II and V.

3.6.2.2. Quantification of glucose, fructose and sucrose by HPLC

In the samples collected during Assays III and IV, the use of Combur-Test® Strips (Roche, Switzerland) could give false results regarding the amount of residual sugar, because they only detect glucose, and CPS contains additional saccharides. HPLC (Merck-Hitachi LaChrom L-7000 series, USA) was used to detect residual glucose, fructose and sucrose (the main sugars present in CPS).

Before HPLC analysis, samples were centrifuged (Sepatec™ Biofuge 15, Heraeus™, Germany) at 15,000 for 10 min to separate any residual biomass or particulate matter. They were then analyzed with a Sugar-Pak® column (Waters, USA) to quantify the amount of glucose, fructose and sucrose. The column's characteristics and operating conditions are presented in Table 3.6.

Table 3.6 – Main characteristics of the Sugar-Pak® chromatography column and its operating conditions. RI, Refraction index.

Characteristics	Column
	Sugar-Pak®
Dimensions	6.5 × 300 mm
Mobile phase	Ca-EDTA, 50 $mg.L^{-1}$
Flow rate	0.5 $mL.min^{-1}$
Volume sampled	20 µL
Column temperature	75 °C
RI detector temperature	30 °C
RI time interval	0 – 20 min

All three sugars were analyzed using a RI detector and quantified using a calibration curve previously established, with standards ranging from 1 to 25 $g.L^{-1}$. If needed, the samples were diluted to fit within this range.

The chromatograms were analyzed using the Chromeleon™ 6.40 SP6 software (Build 783, Dionex, Thermo Fischer Scientific Inc., USA).

3.6.3. Identification and quantification of fatty acids

Gas chromatography (GC) was the technique chosen to identify and quantify the fatty acids present in the yeast biomass. The use of this technique requires the fatty acids to be converted from their mono, di or triglyceride form into free FAMEs so that they are volatile at the operation temperatures of the GC apparatus. This is achieved by derivatizing them through transesterification, cleaving the

bounds between the fatty acid and glycerol molecules and yielding free FAMEs and glycerol. The extraction of fatty acids and their conversion to FAMEs was done according to the protocol described by Freitas *et al.* [70], which in turn was derived from the work of Lepage and Roy [140].

The applied protocol was the following: 2 mL of a methanol/acetyl chloride solution (95:5, v/v) were added to 0.100 g of previously freeze-dried biomass (Heto PowerDry LL3000 Freeze Dryer, Thermo Scientific, USA, coupled with a vacuum pump from Vacuubrand, Germany) in order to carry out the transmethylation reaction. To this mixture, 0.2 mL of heptadecanoic acid (17:0) (5 mg/mL, Nu-Check-Prep, Elysian, USA) were added as internal standard. The mixture was sealed in a light-protected Teflon-lined vial under nitrogen atmosphere and heated at 80 °C for 1 h. The vial contents were then allowed to cool to room temperature, diluted with 1 mL water and extracted with 2 mL of n-hexane. The organic phase, containing the methyl esters, was collected and dried over anhydrous sodium sulfate (Na_2SO_4) then stored in vials under nitrogen atmosphere until the moment of analysis.

The samples were analyzed with a SCION GC 436 chromatographer (Bruker, Germany), equipped with a flame ionization detector (FID). Separation was performed on a 0.32 mm × 30 m fused silica capillary column (film 0.25 µm) (Supelcowax 10, Supelco, Bellafonte, Palo Alto, CA, USA) with helium as a carrier gas, at a flow rate of 1.6 $mL.min^{-1}$.

The column temperature was programmed at an initial temperature of 200 °C then increased at 2 $°C.min^{-1}$ to 220 °C. Injector and detector temperatures were 250 and 280 °C, respectively, and the split ratio was 1:20 for 5 min and then 1:10 for the remaining time. The column pressure was 13.5 psi. Peak identification and response factor calculation was carried out using the above-mentioned internal standard.

Each sample was prepared in duplicate and injected twice.

The amount of each FAME present in the sample was calculated according to Equation 1, where $m(FAME)_i$ is the mass of a specific FAME, $A(FAME)_i$ is the respective peak's area, $A(17:0)$ is the area of the peak corresponding to the internal standard and $RF(FAME)$ is the response factor of the FAME. This factor was considered to be equal to 1.

$$m(FAME)_i = \frac{A(FAME)_i}{A(17:0)} \times RF(FAME) \quad (1)$$

3.6.4. Monitoring the yeast total carotenoid content and viability by multi-parametric FC

Total carotenoid content and cell viability were analyzed by FC, using a FACScalibur benchtop flow cytometer (Becton-Dickinson Biosciences, Franklin Lakes, New Jersey, USA) equipped with a blue argon laser (488 nm) and a red diode laser (635 nm). The FSC and SSC detectors work in the same wavelength as the blue argon laser (488±10 nm). Additionally, this equipment has four fluorescence detectors, FL1 through FL4. FL1 is sensitive to radiation in the green region of the visible spectrum

(530±30 nm), FL2 measures yellow radiation (585±42 nm), FL3 is sensitive to red radiation (> 670 nm) and FL4 detects orange radiation (661±16 nm) [102].

Gathered data was analyzed with the program FCS Express 4 Flow Research Edition (De Novo Software, USA).

All buffers were filtered prior to use with a 0.22 µm filtration membrane (TPP® Syringe-Filter 0.22 µm, TPP Techno Plastic Products AG, Switzerland).

3.6.4.1. Total carotenoid content

The yeast total carotenoid content was determined by FC using a correlation between this parameter and the cellular autofluorescence (AF) levels measured by FL1, FL2 and FL3 detectors. This was done in accordance to the technique developed by Freitas *et al.* [70].

Samples were firstly sonicated (Transsonic T 660/H, Elma, Germany) for 10 s in order to ensure that no cell clusters remained. The sample was then diluted in a phosphate buffer (PBS buffer: NaCl, 8.0 $g.L^{-1}$; KCl, 0.2 $g.L^{-1}$; NaH_2PO_4, 1.15 $g.L^{-1}$; KH_2PO_4, 0.2 $g.L^{-1}$; pH 7.3 ± 0.2; Oxoid, England) in order to obtain between 800 and 1000 $events.s^{-1}$. All samples were prepared in duplicate.

The correlation between total carotenoid content (Car_{cont}) (mg carotenoids.g dry $biomass^{-1}$) and AF levels measured by FC was established by Sousa [141] and based on the work of Freitas *et al.* [70]. The complete protocol is quite extensive and can be found in detail in the referenced works [70,141]. Briefly, carotenoids were extracted from lyophilized biomass samples collected throughout the cultivation and identified and quantified via HPLC. These results were then compared with the values of AF measured by FC in channels FL1, FL2 and FL3. The best correlation was found between the total carotenoid content and AF measured in FL2 and is expressed by Equation 2.

This correlation was obtained from data gathered during a cultivation done in the same conditions as described in Assay I, with the following changes: pH was set to a fixed value of 5.5 and agitation rate was constant and set to 600 rpm.

$$Car_{cont}\ (mg.g^{-1}\ DCW) = 0.01036 \times (AF\ FL2) - 0.2877, \qquad R^2 = 0.9214 \tag{2}$$

3.6.4.2. Cell viability

Cell viability was determined by assessing membrane integrity, membrane potential and enzymatic activity (esterases). The methodologies for each analysis are presented and discussed below. Controls performed by Freitas *et al.* [70] are also presented in order to elucidate how data obtained by FC can give information on cell viability.

3.6.4.2.1 Membrane integrity and potential

Membrane integrity was assessed by determining whether or not cells would incorporate PI (Invitrogen, USA). For membrane (cytoplasmic and mitochondrial) potential, the analysis was carried

out with $DiOC_6(3)$ (Invitrogen, USA). These analysis were performed simultaneously in a double-staining protocol, as developed by Freitas *et al.* [70].

Samples were previously sonicated (Transsonic T 660/H, Elma, Germany) for 10 s, and diluted in PBS buffer (Oxoid, England) until about 800 – 1000 events.s^{-1} were passing through the flow cell.

PI was prepared as a 1 mg.mL^{-1} solution in filtered distilled water and $DiOC_6(3)$ was prepared as a 10 µg.mL^{-1} solution in dimethyl sulfoxide (DMSO). These dyes were added to the sample in volumes corresponding to final concentrations of 1 µg.mL^{-1} and 0.1 ng.mL^{-1}, respectively.

$DiOC_6(3)$ was added to the diluted sample which was then thoroughly mixed. PI was added to the mixture after a 5 min incubation, the sample was once again mixed and read immediately after.

The signal corresponding to the PI fluorescence (623 nm) was read in the FL3 detector following excitation at 488 nm. $DiOC_6(3)$ is excited at 484 nm and its fluorescent signal has a wavelength of 501 nm, which is detected by the FL1 detector.

3.6.4.2.2 Enzymatic activity

CFDA was used to find evidence of enzymatic activity. This was once again done using a double-staining protocol with PI as the second stain, as described in the work by Freitas *et al.* [70].

The samples were first sonicated (Transsonic T 660/H, Elma, Germany) for 10 s, and diluted in McIlvaine (MCI) buffer solution (citric acid, 100 mM; Na_2HPO_4, 200 mM; pH 4.0). The dilution is the required to achieve a count of 800 to 1000 events.s^{-1}.

CFDA was prepared as a 10 mg.L^{-1} solution in acetone and added to the diluted sample at a concentration of 0.05 mg.L^{-1}. PI was prepared as a 1 mg.mL^{-1} solution in filtered distilled water and added to the diluted sample to reach a concentration of 1 µg.L^{-1}. CFDA was added first. The sample was thoroughly mixed and left to incubate for 30 min. After the 30 min incubation, PI was added and the mixture was left to incubate for another 10 min, with readings taking place at the 40 min mark.

PI fluorescence was measured at the FL2 channel while CFDA fluorescence was read at the FL1 channel (517 nm), following excitation at 488 nm.

3.6.4.2.3 Controls and correlations [70,141]

The controls for both double-staining protocols ([$DiOC_6(3)$+PI] and [CFDA+PI]) were done by Freitas *et al.* [70]. Briefly, samples taken from *R. toruloides* NCYC 921 cultures at two different stages (one during exponential growth phase, with no nutrient limitations, and one in late stationary phase, under nutrient starvation) were stained following the previously mentioned protocols. The results (Figure 3.5) give insight into the physiological pattern of the population and present the necessary information for interpreting the results obtained in the present work.

In the case of [$DiOC_6(3)$+PI] staining, “healthy” cells (i.e. with polarized and intact membranes), appear in the upper left quadrant of the density plots (Figure 3.5, (I) and (II), subpopulation B

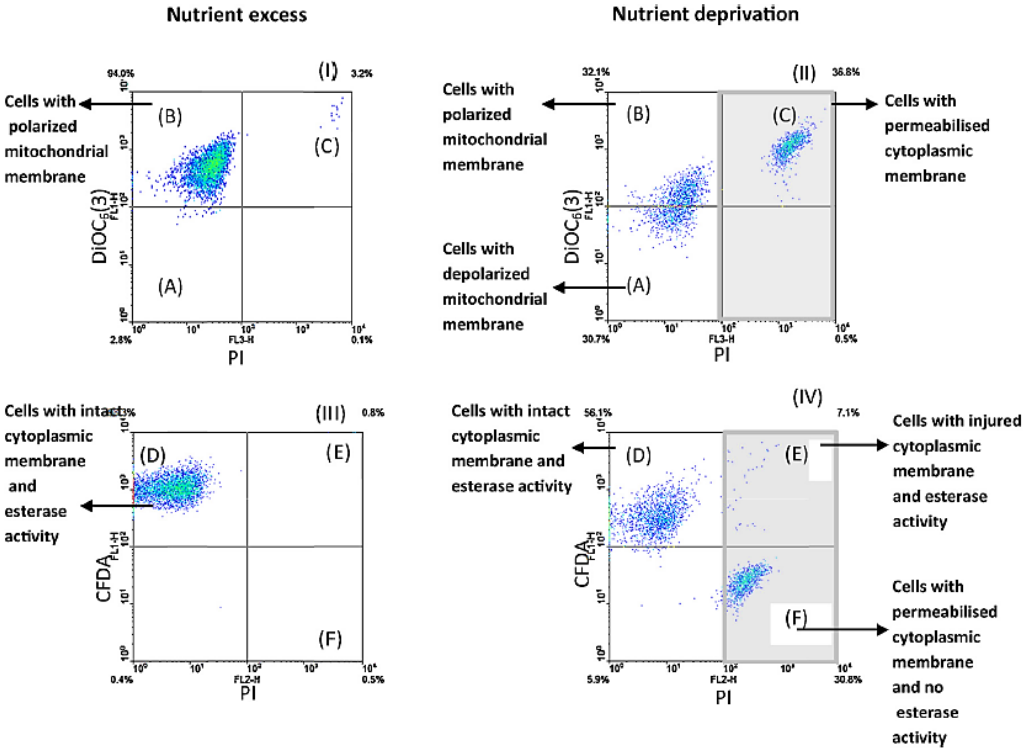

Figure 3.5 – Flow cytometry controls for population identification. [$DiOC_6(3)$+PI] and [CFDA+PI] staining mixtures were used. (I and III) Density plots concerning cells growing under nutrient excess conditions (exponential phase). (II and IV) Density plots concerning cells growing under nutrient starvation conditions (late stationary phase). Grey shadow quadrants correspond to PI^+ cells. Reproduced from Freitas *et al.* [70].

[$DiOC_6(3)^+$,PI^-]). Cells with intact and depolarized cytoplasmic and mitochondrial membranes are located in the left bottom quadrant (Figure 3.5, (I) and (II), subpopulation A [$DiOC_6(3)^-$,PI^-]), while cells with permeabilised membranes are located in the right top quadrant (Figure 3.5, (I) and (II), subpopulation C [$DiOC_6(3)^+$,PI^+]). Regarding [CFDA+PI] staining, cells that show evidence of enzymatic activity and have their membranes intact appear in the upper left quadrant of the density plot (Figure 3.5, (III) and (IV), subpopulation D [$CFDA^+$,PI^-]). Cells with permeabilised cytoplasmic membrane that still present esterase activity appear in the upper right quadrant (Figure 3.5, (III) and (IV), subpopulation E [$CFDA^+$,PI^+]) and cells with damaged cytoplasmic membranes and no esterase activity appear in the lower right quadrant (Figure 3.5, (III) and (IV), subpopulation F [$CFDA^-$,PI^+]). Despite not being present in Figure 3.5, a subpopulation G ([$CFDA^-$,PI^-]) can also be established, comprising cells with intact cytoplasmic membranes and with no esterase activity. If present, this population will appear in the lower left quadrant of (III) and (IV) in Figure 3.5.

3.7. Fermentative and kinetic parameters

3.7.1. Biomass concentration [142]

Assessment of biomass concentration throughout each Assay was done by using the correlation between biomass dry weight and OD_{600} established by Parreira [142]. The established correlation is described by Equation 3 and is valid for OD_{600} values under 0.600.

$$OD_{600} = 0.7062 \times [Biomass] + 0.4338, \qquad R^2 = 0.9986 \qquad (3)$$

3.7.2. Biomass productivity

Biomass productivity (P_X), given in $g.L^{-1}.h^{-1}$ was calculated according to Equation 4, where X_t is the biomass concentration at time t, in $g.L^{-1}$, X_0 is the initial biomass concentration (at t=0 h, inoculation), in $g.L^{-1}$, and t_t is the time, in hours, at which a given sample is taken, counting from the moment of inoculation.

$$P_X = \frac{X_t - X_0}{t_t} \qquad (4)$$

3.7.3. Fatty acid productivity and content

The total fatty acid content (FA_{cont}, g fatty acids.g dry biomass^{-1}) is given by Equation 5, where m_{FA} is the sum of the mass of all fatty acids present in said sample and m_X in the mass of sampled dry biomass.

$$FA_{cont} = \frac{m_{FA}}{m_X} \qquad (5)$$

Fatty acid productivity (P_{FA}, g fatty acids.$L^{-1}.h^{-1}$) at a given time is calculated by multiplying FA_{cont} and P_X, according to Equation 6.

$$P_{FA} = FA_{cont} \times P_X \qquad (6)$$

3.7.4. Carotenoid productivity

Carotenoid productivity (P_{Car}, mg carotenoids.$L^{-1}.h^{-1}$) is calculated in an equivalent way to P_{FA}, by multiplying Car_{cont} and P_X (Equation 7).

$$P_{Car} = Car_{cont} \times P_X \qquad (7)$$

4 Results, Analysis and Discussion

4.1. CPS preparation

The concentrations of sugars (sucrose, glucose, xylose, arabinose and fructose), HMF and furfural of the SSCP and CPS used in Assays III and IV were determined by HPLC and are presented below. The impact of storage conditions and extraction protocol on the composition of SSCP and CPS were also evaluated.

The samples of SSCP and CPS collected at different stages of CPS preparation are presented in Table 4.1.

Table 4.1 – Tested samples of SSCP and CPS. C/w, carob pulp to water ratio; From #, obtained after possessing the solution from were sample # was collected; Assay, assay in which the CPS was used.

Sample ID	Storage conditions of carob pulp	Stage	C/w	Extraction temperature and time	Observations	Assay
A	Laboratory, room T	SSCP	1:2	Room T, overnight	–	III/IV
B	–	CPS	–	–	Hydrolyzed, from A	III
C	–	Sterile CPS	–	–	Autoclaved, from B	III
D	–	Concentrated SSCP	–	–	Concentrated, from A	IV
E	–	Concentrated CPS	–	–	Hydrolyzed, from D	IV
F	–	Sterile concentrated CPS	–	–	Autoclaved, from E	IV
G	Closed containers, 5 °C	SSCP	1:2	Room T, overnight	–	–
H	Closed containers, 5 °C	SSCP	1:2	Room T, overnight	2nd extraction	–
I	–	CPS	–	–	Hydrolyzed, from G	–
J	–	Sterile CPS	–	–	Autoclaved, from I	–
K	Laboratory, room T	SSCP	1:4	80 °C, 2 h	–	–
L	Closed containers, 5 °C	SSCP	1:4	80 °C, 2 h	–	–

4.1.1. CPS for Assay III (samples A, B and C)

Figure 4.1 presents the concentration of sucrose, glucose, xylose, arabinose, fructose, total sugars, HFM and furfural present in the products obtained in each step of CPS preparation for Assay III. Labeling is done according to Table 4.1.

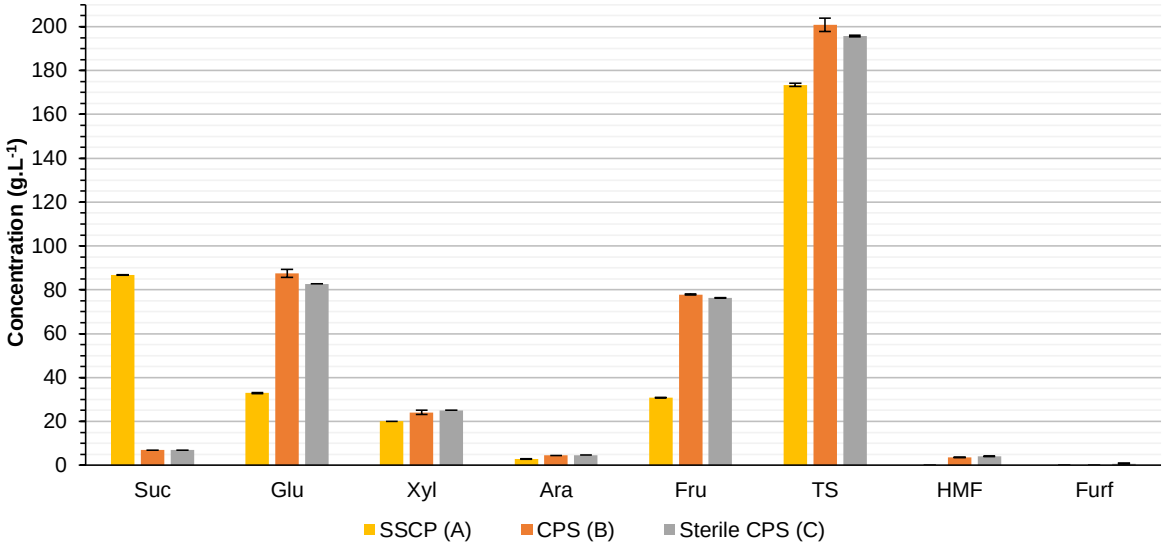

Figure 4.1 – Concentration of sucrose (Suc), glucose (Glu), xylose (Xyl), arabinose (Ara), fructose (Fru), total sugars (TS), hydroxymethylfurfural (HMF) and furfural (Furf) in each step of CPS preparation for Assay III. The black bars represent the standard deviation for each sample. (#), sample identification according to Table 4.1.

Sucrose concentration was initially 87 $g.L^{-1}$ (SSCP, A), dropping to 7 $g.L^{-1}$ after hydrolysis (CPS, B) and suffered no measurable change during autoclaving (sterile CPS, C). Concentrations of glucose and fructose were initially 33 $g.L^{-1}$ and 31 $g.L^{-1}$, respectively. The concentrations of both compounds increased after hydrolysis, to 87 $g.L^{-1}$ and 78 $g.L^{-1}$, respectively. Both sugars had a minor decrease in concentration during autoclaving, to 83 $g.L^{-1}$ and 76 $g.L^{-1}$, respectively. Formation of inhibitory compounds (HMF and furfural) only occurs after the solution has been subjected to heating. HMF concentration in the CPS was 3.6 $g.L^{-1}$, increasing to 4.1 $g.L^{-1}$ after autoclaving. Furfural was only formed during this last step with a concentration of 0.7 $g.L^{-1}$.

The concentrations of xylose remained stable throughout CPS production, increasing from 20 $g.L^{-1}$ to 25 $g.L^{-1}$. Arabinose concentrations increased from 2.9 $g.L^{-1}$ to 4.6 $g.L^{-1}$.

Adding all quantified sugars in the sterile CPS yields a total sugar content of 195.6 $g.L^{-1}$, a result similar to that achieved by Freitas *et al.* [24]. However, this result falls short in regards to the amount of sugars extracted comparing to other works that also described the CPS preparation, as they obtained sugar solutions with identical concentrations while using higher water to carob pulp ratios [90,91]. Reference to the composition of CPS following sterilization can be found in the work of Sánchez *et al.* [91], mentioning 197.5 $g.L^{-1}$ of total sugars and 61.36 $g.L^{-1}$ of reducing sugars, from an aqueous extraction performed with a carob pulp to water ratio of 1:2.5. The sterile CPS produced in the present work and used in Assay III had 195.6 $g.L^{-1}$ of total sugar, as previously mentioned, and 159.0 $g.L^{-1}$ of reducing sugars.

Acetic acid was also detected in the sugar solution, at a concentration of 0.56±0.01 $g.L^{-1}$. Unfortunately, the HPX-87H column was not available when other samples were analyzed so the identification and quantification of this compound was only possible for sample A. However, because acetic acid is a product of the degradation of hemicellulose (from the acetyl groups of these compounds)

and this reaction is more favorable at low pH, it is expected that the concentration of acetic acid would have increased through each step of CPS preparation [143]. Thus, this acetic acid concentration in the CPS can be underestimated.

4.1.2. CPS for Assay IV (samples A, D, E and F)

Figure 4.2 shows the concentration of sucrose, glucose, xylose, arabinose, fructose, total sugars, HFM and furfural present in the product obtained in each step of CPS preparation, which was used in Assay IV. Labeling is done according to Table 4.1.

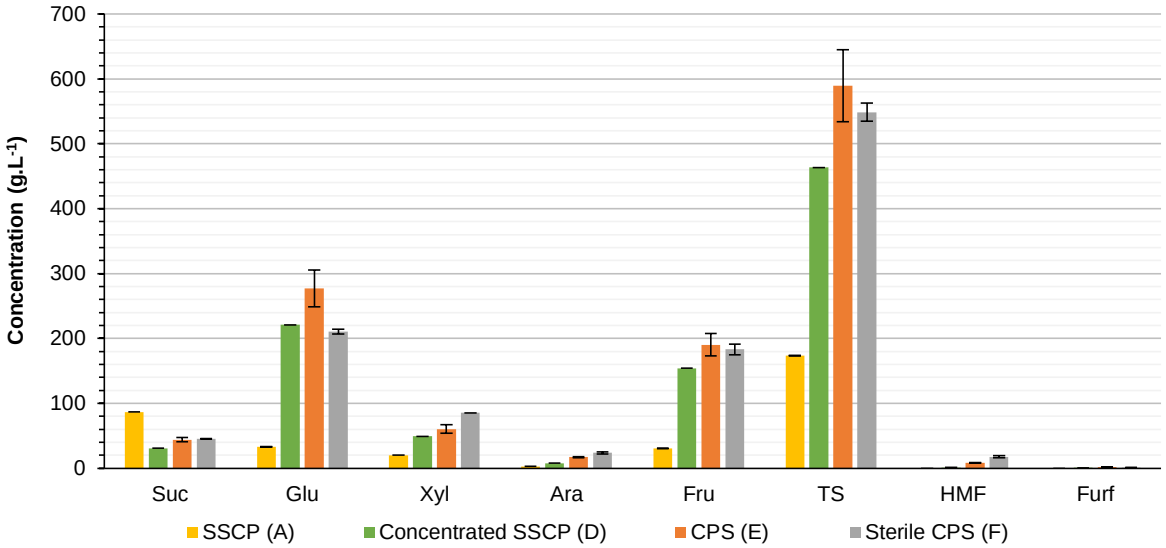

Figure 4.2 – Concentration of sucrose (Suc), glucose (Glu), xylose (Xyl), arabinose (Ara), fructose (Fru), total sugars (TS), hydroxymethylfurfural (HMF) and furfural (Furf) in each step of CPS preparation for Assay IV. The black bars represent the standard deviation for each sample. (#), sample identification according to Table 4.1.

The method employed to prepare the SSCP for this Assay was identical to the previous one and the same batch of carob was used, so the SSCPs are considered identical. Initial concentrations of sucrose, glucose and fructose were 87 $g.L^{-1}$, 33 $g.L^{-1}$ and 31 $g.L^{-1}$, respectively. This SSCP was then concentrated, as described earlier (see section 3.5.1). After this process, sucrose concentration decreased to 31 $g.L^{-1}$, while the concentrations of glucose and fructose rose to 221 $g.L^{-1}$ and 154 $g.L^{-1}$, respectively. This indicates that sucrose had been hydrolyzed to both byproducts, despite the fact that the solution not had been acidified. pH readings revealed that the SSCP had a pH of approximately 4.0 which, combined with the long incubation time and mild heat (~48 h at 40 °C) for sugar concentration, which was sufficient to hydrolyze the sucrose.

Once it was concentrated, the SSCP was acidified to pH 2.0 and left overnight at 100 °C to promote sucrose hydrolysis. However, in this step, the result was not the same as observed earlier (see section 4.1.1): the sugar analysis showed an increase in sucrose concentration, to 44 $g.L^{-1}$. Concentrations of glucose and fructose increased, to 277 $g.L^{-1}$ and 190 $g.L^{-1}$, respectively. Likewise, concentrations of xylose and arabinose also increased, from 50 $g.L^{-1}$ and 8 $g.L^{-1}$ (in the concentrated SSCP, D) to 61 $g.L^{-1}$ and 17 $g.L^{-1}$ in the CPS (E), respectively. During this process the concentrations of HMF and furfural also increased significantly, to 8.5 $g.L^{-1}$ and 1.9 $g.L^{-1}$, respectively. These results

can be explained by the occurrence of hydrolysis of oligosaccharides present in the solution during the pH drop step, as a result of the solubilization of hemicelluloses from the carob pulp [143].

After autoclaving, the sterile CPS presented a sucrose concentration of 46 $g.L^{-1}$, a slight increase from the concentration obtained in the previous step (44 $g.L^{-1}$). Again this can be explained by the occurrence of hydrolysis of oligosaccharides present in the CPS. A significant amount of glucose (~66 $g.L^{-1}$) was lost during the autoclaving step, as a result of caramelization and formation of HMF. Some fructose was also lost during this step, although to a smaller extent (from 190 $g.L^{-1}$ to 183 $g.L^{-1}$). This is accompanied by an increase in the amount of furfural present in the CPS, to a final concentration of approximately 18 $g.L^{-1}$.

These results demonstrate that producing CPS from a concentrated SSCP is possible although some sugars can be lost, either by caramelization or by formation of inhibitory compounds. Despite significant amounts of these latter chemicals can be obtained, CPS produced in this way can still be used to sustain yeast growth, as further demonstrated by Assay IV (see section 4.2.4). The total sugar concentration of approximately 550 $g.L^{-1}$ are close to the carbon source solution utilized in Assays I, II and V, wherein a glucose concentrated solution (600 $g.L^{-1}$ of total sugars) was added during the yeast stationary phase. Indeed, the sterile CPS total sugar concentration used in Assay IV was the highest found in available literature.

4.1.3. Evaluation of the impact of storage conditions on CPS (samples G, H, I and J)

Figure 4.3 shows the concentration of sucrose, glucose, xylose, arabinose, fructose, total sugars, HFM and furfural present in the product obtained in each step of CPS preparation, using a second batch of carob which was stored in closed containers at 5 °C. Additionally, a second extraction was performed to determine how much sugar remained in the discarded carob pulp. Labeling is done according to Table 4.1.

The methodology used to produce CPS from the second batch of carob pulp was the same as the one used to produce CPS for Assay III (see section 3.5.1). The initial sucrose concentration in the SSCP after the first extraction was 100 $g.L^{-1}$, being the highest sugar concentration present in the samples treated in this work. After hydrolysis, sucrose concentration falls to 7.6 $g.L^{-1}$ and further decreases to 5.4 $g.L^{-1}$, after autoclaving. Glucose and fructose concentrations were initially 28 $g.L^{-1}$ and 24 $g.L^{-1}$ and increased to 84 $g.L^{-1}$ and 77 $g.L^{-1}$ after hydrolysis, respectively. Glucose concentration in the sterile CPS was marginally higher, at 86 $g.L^{-1}$. Analysis showed that some fructose was lost during autoclaving, with the final concentration of this sugar being 76 $g.L^{-1}$. Formation of HMF and furfural only occur during autoclaving and are present in the sterile CPS at concentrations of 3.2 $g.L^{-1}$ and 3.5 $g.L^{-1}$, respectively.

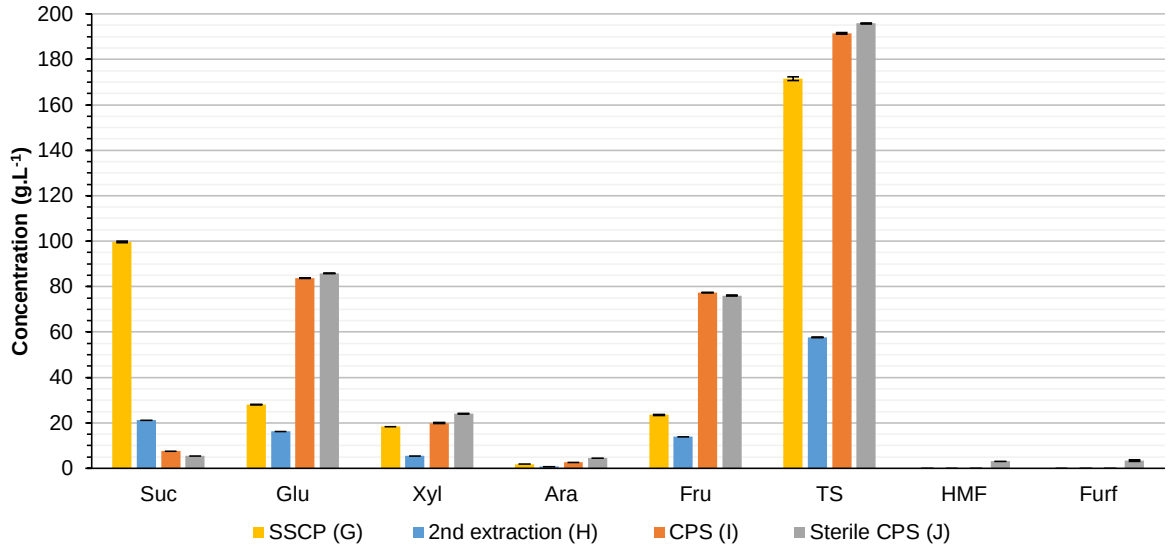

Figure 4.3 – Concentration of sucrose (Suc), glucose (Glu), xylose (Xyl), arabinose (Ara), fructose (Fru), total sugars (TS), hydroxymethylfurfural (HMF) and furfural (Furf) in each step of CPS preparation using a second batch of carob pulp, stored at 5 °C. The black bars represent the standard deviation for each sample. (#), sample identification according to Table 4.1.

The secondary extraction revealed that at least 21 $g.L^{-1}$ of sucrose remained in the discarded carob pulp residues, as well as 16 $g.L^{-1}$ of glucose, 5.5 $g.L^{-1}$ of xylose and 14 $g.L^{-1}$ of fructose, which is 56.5 $g.L^{-1}$ of total sugars. The amount of arabinose was negligible, lower than 1 $g.L^{-1}$.

Comparison between the composition of both SSCPs and sterile CPS (Figure 4.4) suggests that there is no significant difference between the carob pulps stored under different conditions, in relation to the concentration of the identified compounds. In both instances, the sterile CPS had a total sugar content of approximately 200 $g.L^{-1}$.

It would be expected that the carob pulp from the second batch, stored under controlled conditions (at 5 °C), would yield a SSCP, and consequently a CPS, with higher sugar concentrations as it would be less degraded than the carob pulp residues from the first batch, that used carob pulp residues stored at room temperature. A possible explanation for this is the fact that the two batches of carob pulp residues had very distinct granulometries and sizes, with fragments of carob pulp from the first batch (used in Assays III and IV) showing a smaller average size (Figure 4.5). Having a larger surface area as the carob pulp fragments size were smaller, the first batch of carob pulp produced a SSCP with approximately the same sugar concentration as the second batch of carob pulp, although the sugar content of the carob pulp was different (i.e. the sugar extraction yield was higher).

Another possibility to explain these results is that the water could have reached the sugar concentration saturation under the used conditions, in both protocols. The experiments carried out with higher water to carob pulp ratios, presented in the next section, can help further understand this issue.

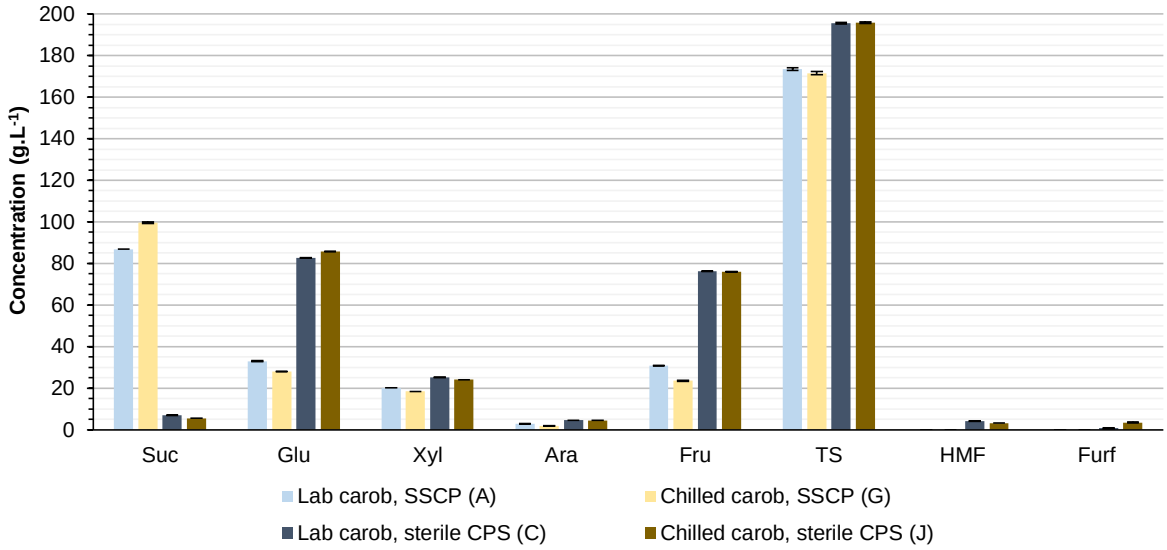

Figure 4.4 – Comparison between SSCP and sterile CPS prepared from both batches of carob. The black bars represent the standard deviation for each sample. (#), sample identification according to Table 4.1. Suc, sucrose; Glu, glucose; Xyl, xylose; Ara, arabinose; Fru, fructose; TS, total sugars; HMF, hydroxymethylfurfural; Furf, furfural.

Figure 4.5 – Carob pulp fragments from the second (on the left) and the first (on the right) batches corresponding to different carob pulp storage conditions.

4.1.4. Extraction according to Turhan *et al.* [90] (samples A, G, K and L)

Figure 4.6 presents the concentration of sucrose, glucose, xylose, arabinose, fructose and total sugars present in the SSCPs prepared according to the methodology of Turhan *et al.* [90] (1:4 w/w carob pulp to water ratio, 80 °C, 2 h) vs. the methodology of Freitas *et al.* [24] (1:2 w/w carob pulp to water ratio, room temperature, overnight), for both batches of carob pulp stored under different conditions. Labeling is done according to Table 4.1.

When interpreting these results it is important to emphasize that, because of the different ratios of carob pulp to water in both protocols, if the same sugar concentration is achieved with the technique that uses more water, this means the twice the amount of sugar was extracted. Taking this into consideration, the results of SSCP preparation from the second batch of carob pulp demonstrate that

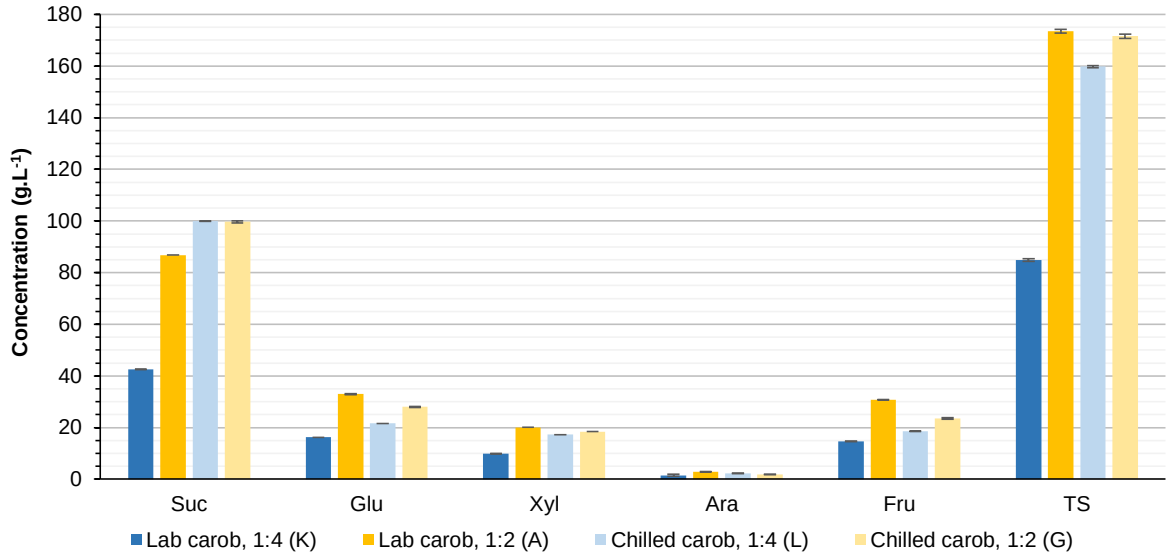

Figure 4.6 – Comparison between sugar solutions prepared by the methodologies of Turhan *et al.* [90] (identified as 1:4) and Freitas *et al.* [24] (identified as 1:2) for both batches of carob pulp. The black bars represent the standard deviation for each sample. (#), sample identification according to Table 4.1. Suc, sucrose; Glu, glucose; Xyl, xylose; Ara, arabinose; Fru, fructose; TS, total sugars.

the technique proposed by Turhan *et al.* [90] is far more efficient in extracting sugars from carob pulp than the first protocol. This can be attributed to a combination of higher extraction temperature (80 °C) and higher water to carob pulp ratio that simultaneously increases sugar solubility and minimizes the risk of achieving saturation.

For the first carob pulp batch, the concentrations of sucrose in the SSCPs were 42.5 $g.L^{-1}$ and 86.5 $g.L^{-1}$ for the 1:4 and 1:2 techniques, respectively. This means that the amount of sucrose extracted was approximately the same with both techniques (85.0 g, 1:4 vs. 86.5 g, 1:2). Glucose concentrations in the SSCPs prepared with the 1:4 and 1:2 techniques were 16.3 $g.L^{-1}$ and 32.9 $g.L^{-1}$, respectively. Fructose concentrations for these techniques were 14.7 $g.L^{-1}$ and 30.7 $g.L^{-1}$, respectively. Consequently, the amounts of glucose and fructose extracted were also identical (32.5 g, 1:4 vs, 32.9 g, 1:2 and 29.4 g, 1:4 vs. 30.7 g, 1:2, respectively).

The difference between both methods was more notorious regarding the second batch of carob pulp (stored at 5 °C): the concentrations of sucrose obtained were approximately the same (99.9 $g.L^{-1}$, 1:4 vs. 99.7 $g.L^{-1}$, 1:2), meaning that the amount extracted with the 1:4 carob pulp to water ratio was twice that of the 1:2 ratio (199.8 g vs. 99.7 g); the 1:4 technique yielded glucose concentrations of 21.6 $g.L^{-1}$ while the result for the 1:2 technique was 28.0 $g.L^{-1}$, meaning that glucose extraction was improved from 28.0 g to 43.2 g; fructose concentrations in SSCPs produced by the 1:4 and 1:2 techniques were 18.7 $g.L^{-1}$ and 23.6 $g.L^{-1}$, respectively, meaning that extraction increased from 23.6 g to 37.3 g; xylose concentrations were 17.3 $g.L^{-1}$ (1:4) and 18.4 $g.L^{-1}$ (1:2) (improved from 18.4 g to 34.6 g) and arabinose concentrations were 2.3 $g.L^{-1}$ (1:4) and 1.8 $g.L^{-1}$ (1:2) (improved from 2.3 g to 4.5 g). These results attest the benefit of applying heat during the extraction step. The same conclusion was found by Turhan *et al.* [90]. Using higher water to carob pulp ratios does mean that the SSCPs obtained will be more diluted. However this experiment may suggest that the sugar saturation

concentration may be reached if the ratios are too low. In addition, CPS may need to be concentrated in order to be used as a substitute of pure sugar solutions (as happened from Assay III to IV), meaning that using higher water to carob pulp ratios allows obtaining more CPS to be produced from the same amount of carob pulp.

Finally, the results presented in Figure 4.6 allow one final comment regarding the impact of carob pulp storage conditions on CPS composition, evaluated in section 4.1.3. Contrary to the results displayed in Figure 4.4, storage conditions appear to play a fundamental role in the composition and quality of the CPS. In Figure 4.6, the extraction results using the 4:1 water to carob pulp ratio method clearly demonstrate that there is a greater amount of extractable sugars in the carob pulp stored under more controlled conditions (5 °C), leading to the conclusion that the first batch of carob pulp was improperly stored and might have induced the raw material degradation. This is supported by research using carob pulp from different regions and even countries that presented far less variability in sugar composition then the 35% to 60% increase found in this experiment [91]. Moreover, the greater amounts of extracted sugars were obtained with carob pulp fragments from the second batch, that were significantly larger in size (Figure 4.5), meaning that the total transfer area was smaller when compared to carob pulp from the first batch.

The total sugar concentration achieve using the 1:4 technique with the first batch of carob was 84.9 $g.L^{-1}$, a value that is smaller than the one previously reported 115.3 $g.L^{-1}$ [90]. However, the same technique applied to the second batch of carob yielded 159.8 $g.L^{-1}$ of total sugars, a 47% increase over the first batch of carob pulp and a 28% increase over the value mentioned in the publication.

4.1.5. Result interpretation

These experiments lead to the conclusion that sugar extraction from carob pulp benefits from conditions that are more aggressive than those utilized to prepare CPS for Essays III and IV. Protocols like the one suggested by Turhan *et al.* [90] yield better sugar extractions because the solution is less likely to become saturated due to higher water to carob pulp ratios being employed. Additionally, the application of heat increases solubility and facilitates the release of soluble compounds from the carob pulp. It is expected that this method also increases the extraction of inhibitory compounds like organic acids. Unfortunately this could not be evaluated because of the lack availability of the HPLC apparatus in the time frame in which these experiments were done. This last hypothesis, together with the fact that the application of heat means that the extraction process will have higher energetic costs, means that the conclusion that one method is preferable to the other is not obvious. A complete cost assessment should be made in order to determine which of the processes is more advantageous.

A second conclusion is that the conditions in which the carob pulp is stored play a major role in the composition of the CPS. Carob pulp that is improperly stored loses humidity and becomes degraded, making difficult the sugar extraction process.

Because these experiments were done only after Assays III and IV were concluded, the conditions found to be optimal for CPS preparation (disregarding the higher energy costs) were not applied when preparing CPS for said Assays.

4.2. Cultivations

Five cultivations of *R. toruloides* NCYC 921 were performed according to the conditions shown in Table 3.3.

4.2.1. Assay I

4.2.1.1. Culture parameters

Assay I was identical to the last experiment performed by Dias *et al.* [77] and its purpose was to serve as a benchmark to which other Assays would be compared. The conditions employed were the ones regarded as optimal to grow *R. toruloides* NCYC 921 with the experimental setup mentioned before (see section 3.5.2).

Figure 4.7 shows biomass concentration and productivity (a), the natural logarithm of the biomass concentration (b), stirring speed and DO (c), the residual glucose concentration (d), total carotenoid content and its productivity (e) and the yeast fatty acid content and its productivity (f) over time for Assay I.

The yeast was cultured in batch mode from t = 0 h to t = 19.7 h (blue vertical traced line), time at which feeding started using a concentrated solution containing a carbon source (glucose) and other nutrients (Table 3.4). This stage was carried out at pH 4.0 and allowed to prolong the growth phase until t = 91.8 h, by which time the pH was changed to 5.0 and the first feeding solution was replaced by a 600 $g.L^{-1}$ glucose concentrated solution (GS) (red vertical traced line) (Figure 4.7).

At t = 18.0 h, the biomass concentration attained 17.52 $g.L^{-1}$, corresponding to a biomass productivity of 0.91 $g.L^{-1}.h^{-1}$. The specific growth rate (μ) achieved in this stage was 0.15 h^{-1}. The culture entered the stationary phase at t = 72.0 h with a biomass concentration of 86.06 $g.L^{-1}$, corresponding to a biomass productivity of 1.18 $g.L^{-1}.h^{-1}$. However, biomass concentration continued to rise after t = 138 h, when the residual glucose concentration increased in the broth (Figure 4.7d), reaching a maximum of 118.90 $g.L^{-1}$ at t = 186.0 h, with a biomass productivity of 0.64 $g.L^{-1}.h^{-1}$. The highest biomass productivity (1.33 $g.L^{-1}.h^{-1}$) was reached during the growth phase, at t = 22.0 h, with a biomass concentration of 30.45 $g.L^{-1}$ (Figure 4.7a). These results are similar to those reported by Zhao *et al.* [80] for their fed-batch assay wherein the residual glucose was kept at 5 $g.L^{-1}$, giving better results than those where the residual glucose concentrations was maintained at 30 $g.L^{-1}$. Maximum biomass concentration was slightly lower in this Assay than the value reported by Dias *et al.* [77] (118.90 $g.L^{-1}$ vs. 126.84 $g.L^{-1}$). Maximum biomass productivity was also lower (1.33 $g.L^{-1}.h^{-1}$ vs. 2.35 $g.L^{-1}.h^{-1}$). One possibility for this is the fact that the yeast used in this Assay had been acquired some time before and suffered multiple passages, which might have compromised its growth characteristics and productivities.

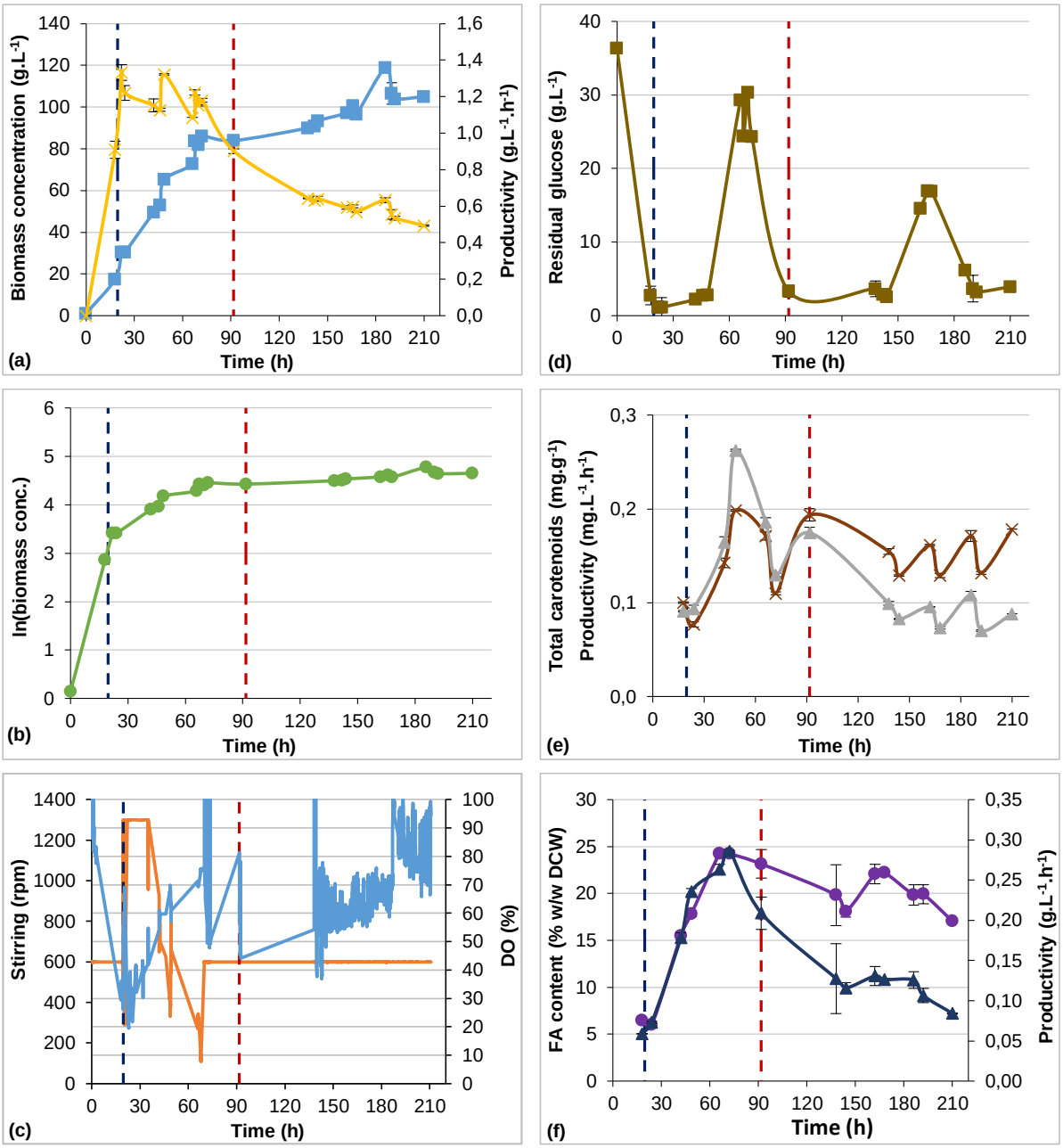

Figure 4.7 – Culture parameters monitored during Assay I. The blue vertical dashed line represents the start of the first stage of fed-batch culture (t = 19.7 h). The red vertical dashed line represents the start of the second stage of fed-batch culture (t = 91.8 h). From top to bottom, left to right: (a), Biomass concentration calculated from OD (■, $g.L^{-1}$) and biomass productivity (x, $g.L^{-1}.h^{-1}$); (b), natural logarithm of the biomass concentration (●); (c), stirring speed (■, rpm) and DO (♦, %); (d), concentration of residual glucose (■, $g.L^{-1}$); (e), total carotenoid content (x, $mg.g^{-1}$ DCW) and total carotenoid productivity (▲, $mg.L^{-1}.h^{-1}$); (f), fatty acid content (●, % w/w DCW) and productivity (▲, $g.L^{-1}.h^{-1}$) over time. The black bars represent the standard deviation for each sample.

Figure 4.7c shows the agitation and DO levels throughout the cultivation time course. Unfortunately there are some gaps in the recordings due to problems with the monitoring software. Even so, the gathered data shows that DO levels were kept above 40% during most of the cultivation, with exception of the end of the batch mode when stirring rates were not dependent on DO readings. When the fed-batch mode was started the parameters were changed to make the stirring rate DO-dependent, allowing it to reach a maximum of 1400 rpm in order to keep DO at a set-point of 60%. At approximately t = 70 h, this dependency led to stirring rates between 300 rpm and 100 rpm, compromising the correct

homogenization of the cultured broth. At this time the stirring rate was once again set to a fixed value (600 rpm) and this setting remained unchanged until the end of cultivation.

Glucose concentration in the culture medium was initially 36.32 $g.L^{-1}$. This value decreased significantly during the batch stage of the cultivation as the biomass concentration increased, with residual glucose concentration attaining a concentration of 2.75 $g.L^{-1}$ at t = 18.0 h. Feeding began at t = 19.7 h and afterwards residual glucose concentration levels started rising, reaching a maximum of 30.34 $g.L^{-1}$ at t = 70.0 h. Feeding was stopped at this time to allow the culture to consume the existing glucose and avoid substrate inhibition. The glucose concentration at which this phenomena may occur is 40 $g.L^{-1}$ (unpublished data, based on previous data gathered within the Project where the present work is inserted), which was never reached during this cultivation. Feeding was resumed at t = 91.8 h with the second feeding solution (GS). Residual glucose concentrations remained steady at under 5 $g.L^{-1}$ until t = 162.0 h, after which point the value began increasing until reaching 16.87 $g.L^{-1}$ at t = 168.0 h. From t = 147.0 h until t = 168.0 h there was an effort to control glucose accumulation in the culture medium by systematically reducing the feeding rates, as it happened between t = 66.0 h and t = 67.5 h. When this action was not sufficient, feeding was interrupted at t = 187.0 h, to allow the culture to consume the existing glucose. Once glucose levels diminished (3.65 $g.L^{-1}$ at t = 190.0 h) feeding was resumed until the end of the culture, at t = 209.7 h (Figure 4.7d).

Total carotenoid content throughout the Assay varied between 0.08 $mg.g^{-1}$ DCW and 0.20 $mg.g^{-1}$ DCW, with this last value equating to a productivity of 0.26 $mg.L^{-1}.h^{-1}$, the highest registered during this assay. Carotenoid content at the end of cultivation was 0.18 $mg.g^{-1}$ DCW, representing a carotenoid productivity of 0.09 $mg.L^{-1}.h^{-1}$. Maximum carotenoid content and productivity were both reached at t = 48.5 h were lower in this Assay than the values reported by Dias *et al.* [77] (0.20 $mg.g^{-1}$ CDW vs 0.29 $mg.g^{-1}$ DCW and 0.26 $g.L^{-1}.h^{-1}$ vs 0.29 $g.L^{-1}.h^{-1}$) (Figure 4.7e).

The yeast's fatty acid content increased steadily during the first stage of fed-batch culture, reaching a maximum of 24.25% before the end of the first stage (t = 66.0 h), a profile similar to that reported by Dias *et al.* [77] (24.42%). Fatty acid content then decreased through the second stage of fed-batch, slightly increasing at t = 162 h, when the residual glucose concentration increased again (Figure 4.7d). At that time, the biomass concentration was also slightly increasing (Figure 4.7a). Indeed growth and fatty acids, which are growth-associated compounds, are dependent on carbon availability [77]. By the end of cultivation the fatty acid content was at 17.03%, equating to a productivity of 0.08 $g.L^{-1}.h^{-1}$ (Figure 4.7f). The maximum fatty acid productivity was 0.29 $g.L^{-1}.h^{-1}$ at t = 72.0 h, 25% lower than the maximum reported by Dias *et al.* [77] (0.40 $g.L^{-1}.h^{-1}$)

Figure 4.8 shows the distribution of the fatty acids comprising the total fatty acid content presented in Figure 4.7f.

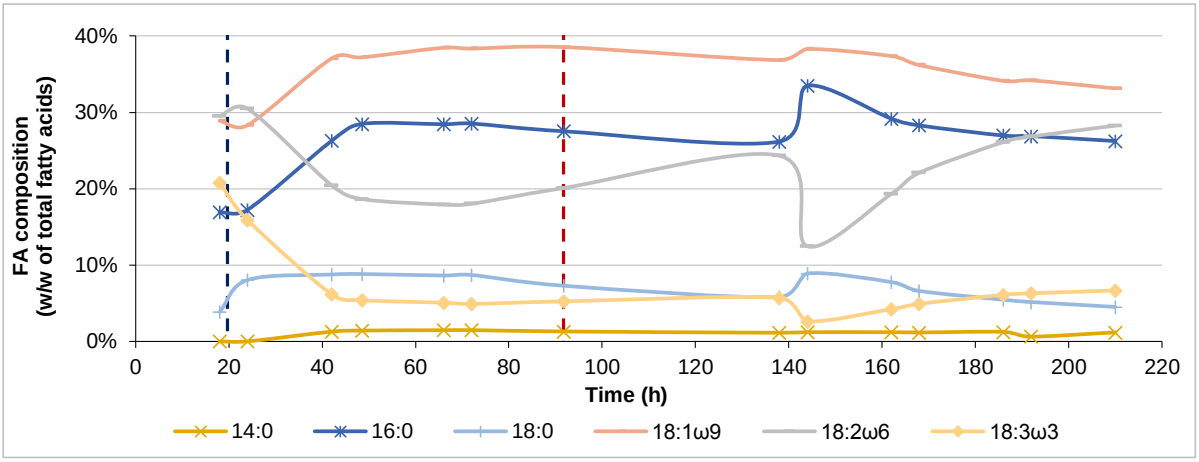

Figure 4.8 – Fatty acid composition in Assay I, quantified as FAMEs. 14:0, myristic acid; 16:0, palmitic acid; 18:0, stearic acid; 18:1ω9, oleic acid, 18:2ω6, linoleic acid; 18:3ω3, linolenic acid. The blue vertical dashed line represents the start of the first stage of fed-batch culture (t = 19.7 h). The red vertical dashed line represents the start of the second stage of fed-batch culture (t = 91.8 h).

The most abundant fatty acids were palmitic (16:0), oleic (18:1ω9) and linoleic (18:2ω6). Of these, the average values of both oleic (35.51% w/w) and linoleic (22.47% w/w) acids are within the range published by Sawangkeaw and Ngamprasertsith [29] (18.0% – 42.0% w/w and 15.0% – 29.0% w/w, respectively). Palmitic acid was present in average in a greater percentage (26% w/w) than the one that is mentioned in the previously cited work (13.0% – 16.0% w/w). The average value of stearic acid (7.02% w/w) is also within range (4.0% – 41.0% w/w). More interesting is the appearance of myristic (14:0) and linolenic (18:3ω3) acids, not reported for this microorganism [29]. Both fatty acids were however identified in the work of Zhao *et al.* [80] (with *R. toruloides* Y4), with the average value of the linolenic acid in this Assay being significantly higher (7.14% vs. 0.7% w/w). During the second stage of fed-batch culture (t = 144.0 h) there is an abrupt descent in the linoleic and linolenic acids percentage, with a concomitant increase in the palmitic and stearic acids. This coincides with a decrease observed in the total fatty acid content (Figure 4.7f) and with a time period during which the residual glucose concentration levels were low (~3 $g.L^{-1}$).

Figure 4.9 shows SFA, MUFA and PUFA percentages of the yeast biomass during Assay I. The profile of SFA percentage over time is similar to that of palmitic acid as it is the most abundant SFA comprising 31.94% w/w of total fatty acids (TFA) at the end of the Assay. Similarly, PUFA profile mimics linoleic acid profile in Figure 4.8, decreasing during the first stage of fed-batch culture, slightly raising from the end of the first stage to the second, and abruptly decreasing at t = 138.0 h, then increasing to 34.92% w/w TFA at the end of cultivation. MUFA profile is stable during the entire Assay, between 30% and 40% w/w TFA. At the end of the Assay MUFAs comprised 33.15% w/w TFA. The average percentages of SFAs, MUFAs and PUFAs were 34.62%, 35.77% and 29.61% w/w TFA, respectively. At the time of the maximum total fatty acid productivity (t = 72.0 h), the SFA content was 38.71% w/w TFA, while MUFAs and PUFAs comprised 38.36% and 22.93% w/w TFA, respectively. SFA proportion was approximately the same value reported by Dias *et al.* [77] for a culture done with the same parameters as this Assay (39.76%).The same authors reported lower MUFA percentages (35.13% w/w

TFA) and a higher PUFA percentage (25.11% w/w TFA). Linolenic acid was approximately the same (4.90% in this Assay vs. 4.50% in the study by Dias *et al.* [77]).

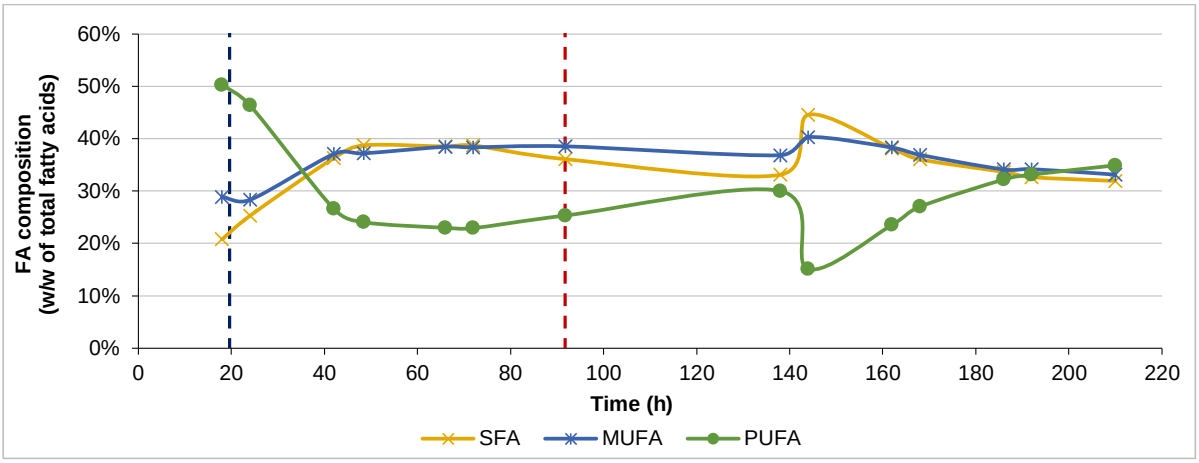

Figure 4.9 – Fatty acid composition in Assay I, quantified as FAMEs. SFA, saturated fatty acids; MUFA, monounsaturated fatty acids; PUFA; polyunsaturated fatty acids. The blue vertical dashed line represents the start of the first stage of fed-batch culture (t = 19.7 h). The red vertical dashed line represents the start of the second stage of fed-batch culture (t = 91.8 h).

4.2.1.2. Cell viability

FC was used to assess cell viability throughout cultivation. Figure 4.10 shows the results of [DiOC$_6$(3)+PI] (a) and [CFDA+PI] (b) staining for Assay I.

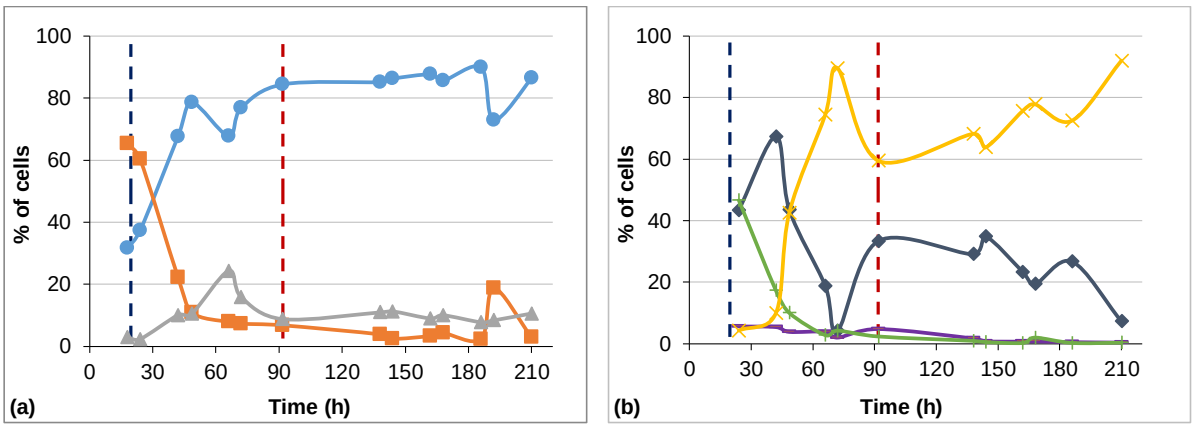

Figure 4.10 – Percentage of cells in each subpopulation, as defined in Figure 3.5, for Assay I. The blue vertical dashed line represents the start of the first stage of fed-batch culture (t = 19.7 h). The red vertical dashed line represents the start of the second stage of fed-batch culture (t = 91.8 h). From left to right: Staining with [DiOC$_6$(3)+PI] (a), subpopulation A (▲) is comprised of cells with depolarized mitochondrial membranes and intact cytoplasmic membranes [DiOC$_6$(3)$^-$,PI$^-$]; Subpopulation B (●) is comprised of cells with polarized mitochondrial membranes and intact cytoplasmic membranes [DiOC$_6$(3)$^+$,PI$^-$]; Subpopulation C (■) is comprised of cells with permeabilised cytoplasmic membrane [DiOC$_6$(3)$^+$,PI$^+$]. Staining with [CFDA+PI] (b), subpopulation D (♦) is comprised of cells with intact cytoplasmic membrane and esterase activity [CFDA$^+$,PI$^-$]; subpopulation E (-) is comprised of cells with permeabilised cytoplasmic membrane that still retain esterase activity [CFDA$^+$,PI$^+$]; subpopulation F (+) is comprised of cells with permeabilised cytoplasmic membranes that do not present esterase activity [CFDA$^-$,PI$^+$]; subpopulation G (x, not present in Figure 3.5) is comprised of cells with intact cytoplasmic membranes and without esterase activity [CFDA$^-$,PI$^-$].

At the end of the batch mode (t = 19.7 h), FC results indicate that the majority of cells (64.31%) had their cytoplasmic membranes damage (subpopulation C), which is indicative of cell stress and unfavorable culture conditions. Cells considered to be healthy represented only 31.64% of the entire

population. Previous works have shown that this result is indicative of nutrient starvation [70,77], as it is expected to occur at the stationary phase, because no nutrients had been supplemented to the culture at that time. Figure 4.7d corroborates this assumption as it indicates that there was almost no residual glucose at the end of the batch period. Once feeding was initiated the fraction of healthy cells (subpopulation B) increased significantly, to 78.57% at t = 48.5 h. At this time, FC shows an increase in the subpopulation of cells with depolarized mitochondrial membranes (subpopulation A), from 10.48% to 24.34% (t = 66 h), meaning that culture conditions were not ideal. Comparison between Figure 4.10 and Figure 4.7d indicates that this rise in subpopulation A was coincident with the observed increase in the concentration of residual glucose, which is indicative that cells were experiencing unfavorable culture conditions and were not consuming the carbon source due to the high feeding rate of the nutrient solution, at that time, leading to its accumulation. Feeding rate was then reduced, to allow the yeast to consume the available glucose. Once the feeding rate was decreased, the residual glucose concentrations dropped and the percentage of cells in subpopulation A decreased to below 10% (t = 91.8 h) and remained low until the end of cultivation. At the end of cultivation (t = 210.0 h) nearly all cells (86.45%) had polarized mitochondrial membranes and intact cytoplasmic membranes, which is an indication that most of the cells were metabolically active.

Similarly to the results of [$DiOC_6$(3)+PI] staining, at the end of the batch phase/beginning of the fed-batch phase, the majority of cells (52.24% at t = 24.0 h) had permeabilised cytoplasmic membranes (sum of subpopulations E and F). Subpopulation D comprised 43.46% of all cells while subpopulation G comprised 4.30%. This latter increased throughout the Assay, reaching a maximum of 91.97% of all cells by the end of the culture (t = 210.0 h). As previously mentioned, this subpopulation comprises cells that have intact cytoplasmic membranes but do not present esterase activity. However, this result cannot be as easily interpreted as the results of PI staining. PI staining yields a conclusive result regarding membrane integrity because PI either stains the cells or not, depending on whether they have intact cytoplasmic membranes. Consequently, the signal in the FL3 channel (in [$DiOC_6$(3)+PI] staining) or in the FL2 channel (in [CFDA+PI] staining) will either be greater or lower than 10^2, respectively (see Figure 4.10 in section 3.6.4.2.3). CFDA staining of a cell population yields a results that is similar to a gradient. The FC protocols used in the present work defined a signal of 10^2 as the threshold between a positive or negative staining result for these dyes, which translates into the profiles observed in Figure 4.10 for subpopulations D and G. Consequently, rather than stating that cells in subpopulation G have no esterase activity, it is more accurate say that they present lower levels of esterase activity than cells in subpopulation D. As esterase activity diminished over time, it is possible to conclude that despite having intact, polarized membranes, the yeast cells were still under some stress.

4.2.2. Assay II

4.2.2.1. Culture parameters

In Assay II the pH of the second stage of fed-batch mode was changed from 5.0 to 5.5 in order to evaluate how this would impact the cells and product synthesis (carotenoids and fatty acids) during the stationary growth phase. The pH of 5.5 is mentioned by Yoon and Rhee [74] and Pan *et al.* [76] as

the optimal for *R. glutinis* growth and lipid production. However, more recent studies mention that this is not the case [77]. Dias *et al.* [77] performed two *R. toruloides* NCYC 921 cultures using the dual stage fed-batch strategy, however both used a pH of 5.0 for the second stage of culture. This Assay aims to evaluate the impact of using a pH of 5.5 in the second stage of fed-batch.

Figure 4.11 shows biomass concentration and productivity (a), the natural logarithm of the biomass concentration (b), stirring speed and DO (c), the residual glucose concentration (d), total carotenoid content and its productivity (e) and fatty acid content and its productivity (f) over time, for Assay II.

The yeast was cultured in batch mode from t = 0 h to t = 18 h (blue vertical dashed line). At this time the first stage of fed-batch was initiated, lasting until t = 48.9 h (red vertical dashed line). In this Assay the pH was changed at t = 65.9 h.

Biomass concentration at the end of the batch stage was 17.21 $g.L^{-1}$, corresponding to a biomass productivity of 0.90 $g.L^{-1}.h^{-1}$. The specific growth rate achieved in this stage was 0.16 h^{-1}. By the end of the first stage of fed-batch culture, biomass concentration rose to 63.64 $g.L^{-1}$ and by the end of the fermentation it reached at 85.00 $g.L^{-1}$, equating to biomass productivities of 1.31 $g.L^{-1}.h^{-1}$ and 0.45 $g.L^{-1}.h^{-1}$, respectively. The maximum biomass concentration was 95.08 $g.L^{-1}$, at t = 89.9 h, during the second stage of fed-batch mode. The highest biomass productivity was achieved during the first stage of fed-batch mode with a value of 1.52 $g.L^{-1}.h^{-1}$ at t = 21.9 h (Figure 4.11a) and was lower than that obtained in Assay I, probably due to the pH of 5.5.

Figure 4.11c shows the variations in DO and agitation speed. Because DO levels were always kept above 40% oxygen saturation there was no need to make agitation DO dependent and stirring speed was kept constant at 600 rpm. DO levels decreased from 100% to 60% during the batch phase of culture and the first stage of fed-batch mode as it was during this period that biomass growth was more significant. Once the second stage of fed-batch was initiated, DO levels raised and stabilized between 70% and 80%, as the yeasts metabolism switched from growth to accumulation of reserve materials.

Glucose concentration was initially 38.02 $g.L^{-1}$ and was completely exhausted by the end of the batch phase. Residual glucose levels remained close to 0 $g.L^{-1}$ throughout the first stage of the fed-batch step, increasing to 3.23 $g.L^{-1}$ when the second stage was initiated. The maximum concentration of residual glucose was observed at t = 185.9 h, with a value of 8.06 $g.L^{-1}$ (Figure 4.11d).

Total carotenoid content was 0.07 $mg.g^{-1}$ DCW at the end of the batch phase. This value rose to 0.13 $mg.g^{-1}$ DCW as the feeding rate was increased during the first stage of fed-batch culture. The value then dropped to 0.10 $mg.g^{-1}$ DCW at the beginning of the second stage of fed-batch culture and rose throughout this stage during which the concentrated glucose solution was added, to a final value of 0.20 $mg.g^{-1}$ DCW, which as the maximum reached in the present Assay. The maximum carotenoid productivity was reached at t = 65.9 h and had a value of 0.19 $mg.L^{-1}.h^{-1}$ (Figure 4.11e).

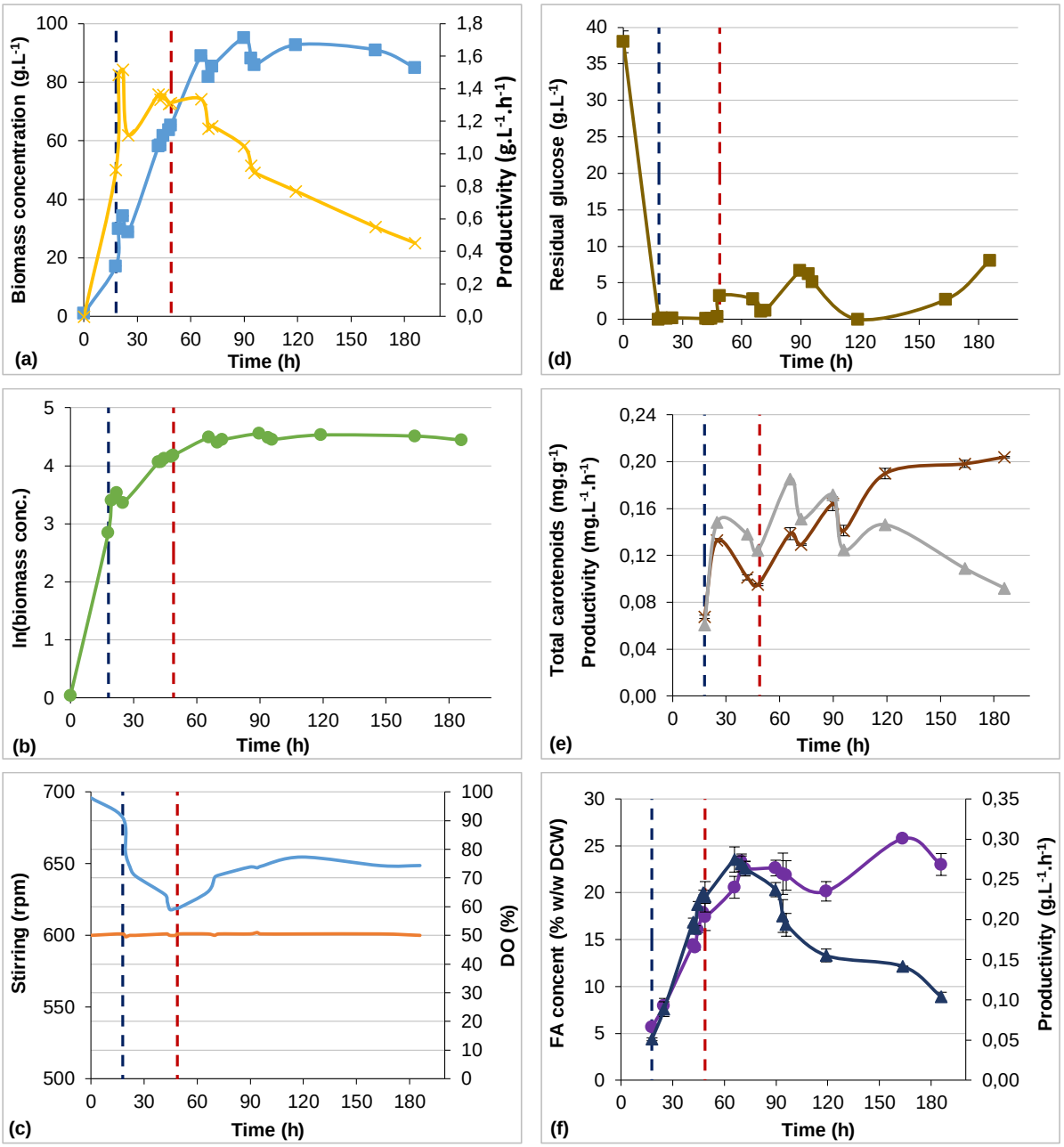

Figure 4.11 – Culture parameters monitored during Assay II. The blue vertical dashed line represents the start of the first stage of fed-batch culture (t = 18.0 h). The red vertical dashed line represents the start of the second stage of fed-batch culture (t = 48.9 h). From top to bottom, left to right: (a), Biomass concentration calculated from OD (■, g.L^{-1}) and biomass productivity (x, g.L^{-1}.h^{-1}); (b), natural logarithm of the biomass concentration (●); (c), stirring speed (■, rpm) and DO (♦, %); (d), concentration of residual glucose (■, g.L^{-1}); (e), total carotenoid content (x, mg.g^{-1} DCW) and total carotenoid productivity (▲, mg.L^{-1}.h^{-1}); (f), fatty acid content (●, % w/w DCW) and productivity (▲, g.L^{-1}.h^{-1}) over time. The black bars represent the standard deviation for each sample.

Fatty acid content was 5.68% at the beginning the first stage of fed-batch mode, rising steadily until t = 69.9 h and reaching 23.32%. However, the maximum fatty acid productivity achieved was observed in the previous sample, taken at t = 65.9 h, with a value of 0.27 g.L^{-1}.h^{-1}. Fatty acid content decreased to 20.14% at t = 119.1 h when the residual glucose concentration also decreased, then increased once again reaching the maximum of 25.76% at t = 163.7 h. By the end of cultivation the fatty acid content was 23.00%, with a productivity of 0.14 g.L^{-1}.h^{-1} (Figure 4.11f).

Figure 4.12 shows the fatty acid profiles during Assay II.

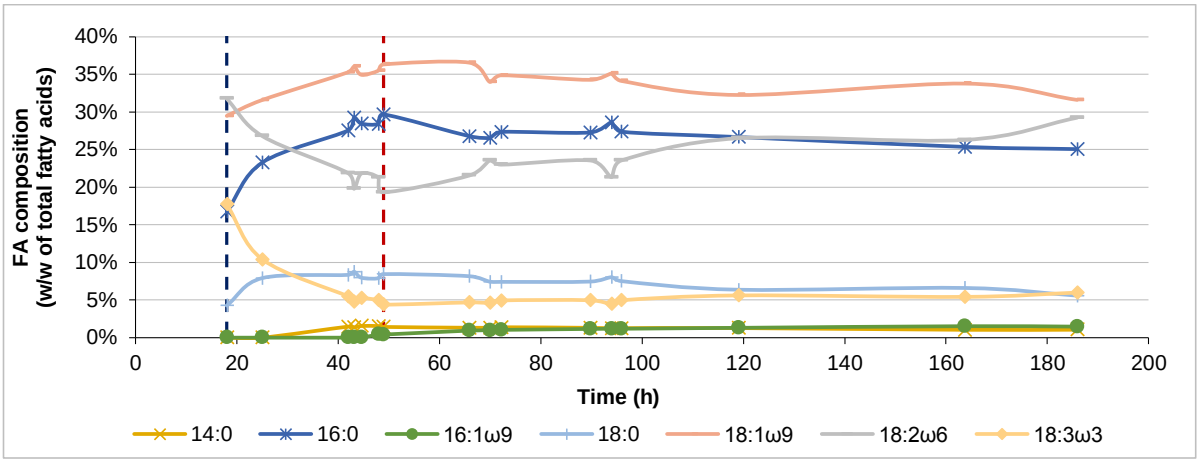

Figure 4.12 – Fatty acid composition in Assay II, quantified as FAMEs. 14:0, myristic acid; 16:0, palmitic acid; 16:1ω9, palmitoleic acid; 18:0, stearic acid; 18:1ω9, oleic acid, 18:2ω6, linoleic acid; 18:3ω3, linolenic acid. The blue vertical dashed line represents the start of the first stage of fed-batch culture (t = 18.0 h). The red vertical dashed line represents the start of the second stage of fed-batch culture (t = 48.9 h).

The most abundant fatty acid throughout this Assay was oleic acid, representing in average 34.11% w/w of the total fatty acid content. This is followed by palmitic and linoleic acids, with average values of 26.53% w/w and 23.83% w/w, respectively. Similarly to what was observed in Assay I, the values of oleic and linoleic acids fall within the intervals published by Sawangkeaw and Ngamprasertsith [29], while palmitic acid surpassed in over 10% the range mentioned in the article. Stearic and linolenic acids have average values of 7.39% and 6.17% w/w respectively, with the first falling within the range published in the aforementioned article for this fatty acid and the second being significantly higher than the value published by Zhao *et al.* [80]. Myristic and palmitoleic acids were present in lower quantities, with average values of 1.16% and 0.73% w/w, respectively. Neither of these fatty acids are mentioned in the work of Sawangkeaw and Ngamprasertsith [29] and both present lower values than those published by Zhao *et al.* [80]. They are however in accordance to data published by Li *et al.* [75] for fed-batch assays carried out in a 15 L bioreactor.

Figure 4.13 shows the proportion of SFAs, PUFAs and MUFAs of *R. toruloides* biomass during the time course of Assay II. SFA and MUFA proportions were stable throughout the entire Assay (between 30% and 40% w/w TFA), with the largest increase in SFA percentage observed during the first stage of fed-batch culture. During the same time period, there was a decrease in PUFA percentage, from 49.49% w/w TFA at t = 18.0 h to 23.72% at t = 48.9 h. PUFA percentage then increased during the second stage of fed-batch culture, having presented a final value of 35.22% w/w TFA at t = 185.9 h. At this time SFA and MUFA percentages were similar to this figure (31.71% and 33.07% w/w TFA, respectively). In this Assay the average percentages of SFA, MUFA and PUFA were 35.17%, 34.83% and 30.00% w/w TFA, respectively. These figures are nearly identical to those obtained in Assay I. At the time of the highest fatty acid productivity (t = 65.9 h), SFA, MUFA and PUFA percentages were 36.27%, 37.49% and 26.24% w/w TFA, respectively. SFA percentage was lower than the value reported by Dias *et al.* [77] for a cultivation done at pH 5.5 (40.00% w/w TFA). The same is true for PUFA

percentage (29.42% w/w TFA). MUFA percentage was higher in this Assay than in the mentioned publication (35.41% w/w FTA).

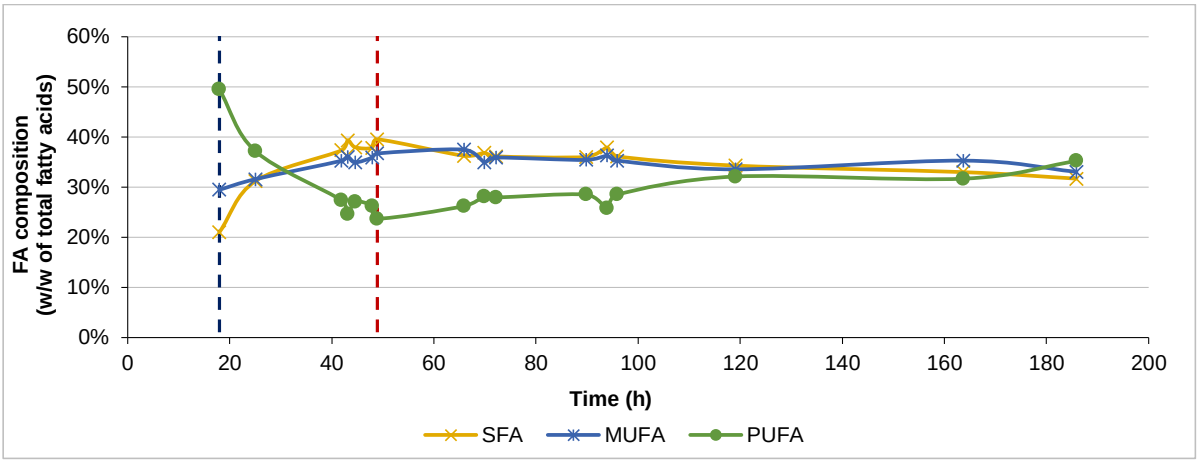

Figure 4.13 – Fatty acid composition in Assay II, quantified as FAMEs. SFA, saturated fatty acids; MUFA, monounsaturated fatty acids; PUFA; polyunsaturated fatty acids. The blue vertical dashed line represents the start of the first stage of fed-batch culture (t = 18.0 h). The red vertical dashed line represents the start of the second stage of fed-batch culture (t = 48.9 h).

4.2.2.2. Cell viability

Figure 4.14 shows the results of [DiOC$_6$(3)+PI] (a) and [CFDA+PI] (b) staining for Assay II.

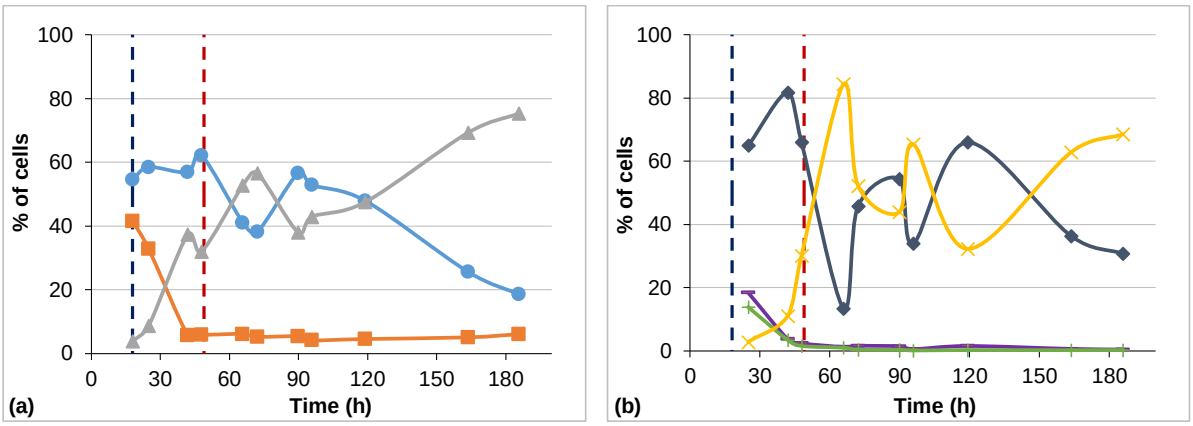

Figure 4.14 – Percentage of cells in each subpopulation, as defined in Figure 3.5, for Assay II. The blue vertical dashed line represents the start of the first stage of fed-batch culture (t = 18.0 h). The red vertical dashed line represents the start of the second stage of fed-batch culture (t = 48.9 h). From left to right: Staining with [DiOC$_6$(3)+PI] (a), subpopulation A (▲) is comprised of cells with depolarized mitochondrial membranes and intact cytoplasmic membranes [DiOC$_6$(3)$^-$,PI$^-$]; Subpopulation B (●) is comprised of cells with polarized mitochondrial membranes and intact cytoplasmic membranes [DiOC$_6$(3)$^+$,PI$^-$]; Subpopulation C (■) is comprised of cells with permeabilised cytoplasmic membrane [DiOC$_6$(3)$^+$,PI$^+$]. Staining with [CFDA+PI] (b), subpopulation D (♦) is comprised of cells with intact cytoplasmic membrane and esterase activity [CFDA$^+$,PI$^-$]; subpopulation E (-) is comprised of cells with permeabilised cytoplasmic membrane that still retain esterase activity [CFDA$^+$,PI$^+$]; subpopulation F (+) is comprised of cells with permeabilised cytoplasmic membranes that do not present esterase activity [CFDA$^-$,PI$^+$]; subpopulation G (x, not present in Figure 3.5) is comprised of cells with intact cytoplasmic membranes and without esterase activity [CFDA$^-$,PI$^-$].

By the end of the batch stage (t = 18 h), the majority of cells were polarized (subpopulation B, 54.54%), 41.58% had their cytoplasmic membrane damaged (subpopulation C) and 3.88% had depolarized mitochondrial membranes (subpopulation A). As feeding rates were increased, from t = 18 h until t = 43.1 h, [DiOC$_6$(3)+PI] staining revealed that although the percentage of cells with permeabilised

cytoplasmic membranes (subpopulation C) decreased significantly, the cells were experiencing stress conditions, as judging by an increase in subpopulation A percentage. The fraction of healthy cells (subpopulation B) remained roughly unchanged, representing 62.21% of the yeast's population at t = 47.9 h. Once the second stage of fed-batch was initiated, the percentage of healthy cells decreased up to 20% (to 41.07% at 65.9 h) and a similar variation in the opposite direction was observed for the cells with depolarized membranes (Subpopulation A, increasing from 31.96% at t = 47.9 to 52.81% at t = 65.9 h). Changing the pH to 5.5 at t = 65.9 h led to a slight increase in subpopulation A, to 56.58%, as subpopulation B decreased to 38.18%. From t = 72.2 h until t = 89.8 h, the residual glucose levels increased from 1.24 $g.L^{-1}$ to 6.69 $g.L^{-1}$, a change that was accompanied by a recovery of subpopulation B to 56.57%. After this time, feeding rates were once again lowered, leading to a drop in the concentration of residual glucose that is accompanied by an increase in the percentage of subpopulation A and a decrease in subpopulation B (from 38.07% to 75.37% and from 56.57% to 18.57%, respectively). From t = 72.2 h forward, subpopulation C remained under 10%.

[CFDA+PI] staining (Figure 4.14b) confirms that cells with permeabilised cytoplasmic membranes (subpopulations E and F) decreased during the first stage of fed-batch culture, remaining low until the end of culturing. During the same time there was an increase in the percentage of subpopulations D and G, however this first one decreased from 81.78% at t = 41.9 h to 13.41% at t = 65.9 h. Subpopulation G increased from 2.06% at t = 18.0 h to 84.39% at t = 65.9 h. Values of both subpopulations oscillated between 30% and 70% through the remainder of the Assay. The behavior of subpopulation G is coincident with the profile of subpopulation A (Figure 4.14a), indicating that the yeast cells were being subjected to some degree of stress. One possibility is that yeast cells were experiencing stress due to the increasing residual glucose concentration as a consequence of the employed feeding rates. However this is not definitive as residual glucose concentration remained under 40 $g.L^{-1}$.

4.2.3. Assay III

4.2.3.1. Culture parameters

The culture conditions in Assay III were the same as for Assay I, except for the supplied carbon source. CPS was used instead of a glucose solution (CPS composition can be found in section 4.1.1). A pH of 5.0 was chosen for the second stage of fed-batch culture based on the outcome of Assays I and II that demonstrated that this pH yielded better results.

Figure 4.15 shows biomass concentration and productivity (a), the natural logarithm of the biomass concentration (b), stirring speed and DO (c), the concentration of residual sugars (d), total carotenoid content and its productivity (e) and fatty acid content and its productivity (f) over time for Assay III.

Batch mode lasted until t = 21.3 h, as represented by the first blue vertical dashed line in Figure 4.15. The first stage of fed-batch mode lasted from this time until t = 48.8 h, time at which the feeding solution was changed by only CPS initiating the second stage of fed-batch mode. This was accompanied by a change in the medium pH, from 4.0 to 5.0, when the culture reached the stationary phase. The

cultivation lasted until t = 67 h, at which time it was stopped because the maximum working volume of the bioreactor was reached. This was a consequence of the higher feeding rates used in this assay, as the total sugars concentration of the CPS used was only approximately one third of the glucose solution concentration used in the previous assays (see section 4.1.1).

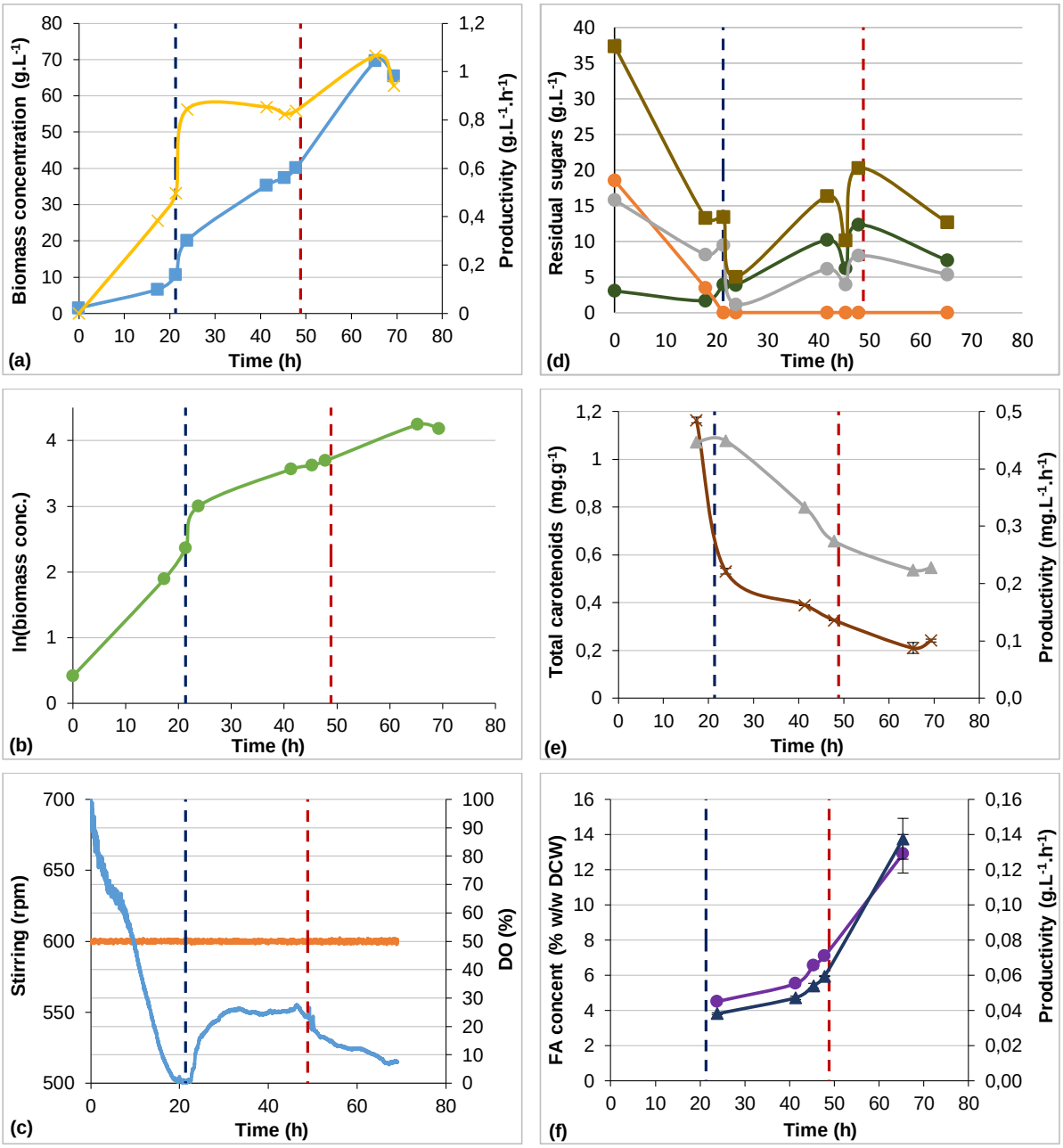

Figure 4.15 – Culture parameters monitored during Assay III. The blue vertical dashed line represents the start of the first stage of fed-batch culture (t = 21.3 h). The red vertical dashed line represents the start of the second stage of fed-batch culture (t = 48.8 h). From top to bottom, left to right: (a), Biomass concentration calculated from OD (■, g.L^{-1}) and biomass productivity (x, g.L^{-1}.h^{-1}); (b), natural logarithm of the biomass concentration (●); (c), stirring speed (■, rpm) and DO (♦, %); (d), concentration of residual sugars (g.L^{-1}), namely glucose (●), fructose (●), sucrose (●) and total sugars (■); (e), total carotenoid content (x, mg.g^{-1} DCW) and total carotenoid productivity (▲, mg.L^{-1}.h^{-1}); (f), fatty acid content (●, % w/w DCW) and productivity (▲, g.L^{-1}.h^{-1}) over time. The black bars represent the standard deviation for each sample.

By the end of the batch phase, biomass concentration had reached 10.61 g.L^{-1}. This value is approximately half of the one that was observed in the two previous Assays where glucose was used

as carbon source. The specific growth rate achieved in this stage was 0.09 h^{-1}. At the end of the first stage of the fed-batch mode the biomass reached a concentration of 40.12 $g.L^{-1}$, again a value that is significantly lower than the one that was achieved in the previous Assays, in a time interval that is comparable to that of Assay II. The final biomass concentration was 65.40 $g.L^{-1}$, having reached a maximum of 69.64 $g.L^{-1}$ at t = 65.3 h. This last value equates to a biomass productivity of 1.07 $g.L^{-1}.h^{-1}$, being the maximum biomass productivity obtained throughout this Assay. The highest increase in both biomass concentration and productivity, considering the time that lasted the assay, was observed after initiating fed-batch mode, with values going from 10.61 $g.L^{-1}$ and 0.50 $g.L^{-1}.h^{-1}$ to 20.14 $g.L^{-1}$ and 0.85 $g.L^{-1}.h^{-1}$, respectively (Figure 4.15a).

Stirring was kept constant at 600 rpm during the entire Assay. Figure 4.15c was constructed by normalizing between 0% and 100% the values of DO recorded throughout the culture. This was necessary because the recorded data presented values between 116% and -80% which obviously cannot be representative of the actual DO values. However, the behavior of DO levels over time still appears to be accurate and is corroborated by data from Figure 4.15b: periods of accentuated growth are coincident with periods at which the DO levels decrease more rapidly, as was observed between t = 0 h and t = 21.3 h and then again between t = 47.8 h and t = 65.3 h. Comparison between the two figures also indicates that actual DO values might not have been as low as depicted: it is unlikely that biomass would increase with rates similar to those of Assays I and II if the culture were under severe oxygen limitation, as indicated by Figure 4.15c.

Figure 4.15d indicates that the culture consumed the available carbon source, as evidenced by the lack of residual glucose in the supernatant of the collected samples. Once glucose was exhausted, at t = 23.83 h, there was a decrease in the levels of residual fructose, suggesting that this carbon source was the most easily assimilated sugar, once glucose was no longer available.

Total carotenoid content diminished constantly throughout this Assay, from 1.16 $mg.g^{-1}$ DCW at t = 17.3 h to 0.21 $mg.g^{-1}$ DCW at t = 65.3 h. A slight rise to 0.24 $mg.g^{-1}$ can be observed at t = 69.3 h. Despite this, the maximum carotenoid productivity (0.45 $mg.L^{-1}.h^{-1}$ at t = 23.8 h) was higher than that found in previous Assays (Figure 4.15e). The behavior of the total carotenoid content over time suggests that the culture was experiencing some degree of oxygen limitation as an adequate aeration is essential for carotenoid production [144].

Fatty acid content increased steadily throughout this Assay, from 4.51% to 12.90%, equating to fatty acid productivities of 0.04 $g.L^{-1}.h^{-1}$ and 0.14 $g.L^{-1}.h^{-1}$, respectively. Still, the highest fatty acid content reached was only approximately half of the maximum obtained in Assay I. However this Assay was interrupted while fatty acid contents were rising, meaning that the maximum content might have reached values similar to those of the previous Assays, if it had been possible to prolong the present one.

Figure 4.16 shows *R. toruloides* fatty acids profiles throughout Assay III.

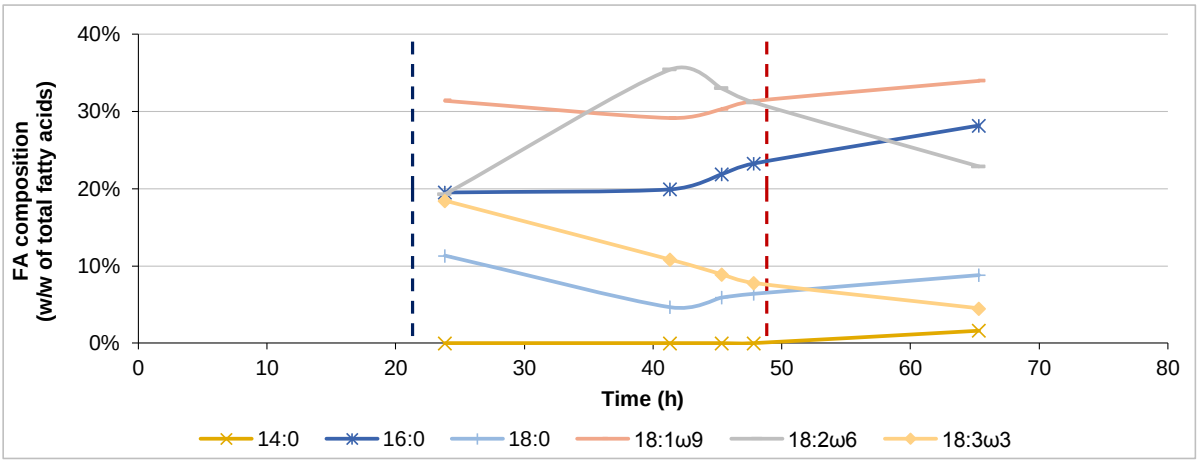

Figure 4.16 – Fatty acid composition in Assay III, quantified as FAMEs. 14:0, myristic acid; 16:0, palmitic acid; 18:0, stearic acid; 18:1ω9, oleic acid, 18:2ω6, linoleic acid; 18:3ω3, linolenic acid. The blue vertical dashed line represents the start of the first stage of fed-batch culture (t = 21.3 h). The red vertical dashed line represents the start of the second stage of fed-batch culture (t = 48.8 h).

Similarly to Assay I, oleic acid was the most abundant representing in average 31.24% w/w of the total fatty acid mass, a value that is within the range published by Sawangkeaw and Ngamprasertsith [29]. However, in this Assay the average linoleic acid percentage of the total fatty acids (28.36% w/w TFA) was higher than in previous assays, and this fatty acid was the second most abundant. Its profile was also different than what was observed in Assay I, increasing through most of the first stage of fed-batch culture rather than decreasing. Near the end of the first stage of fed-batch, and through the second stage, linoleic acid percentage decreased to a value close to the first recorded (22.89% w/w TFA at t = 65.3 h), having reached a maximum of 35.44% w/w TFA at t = 41.3 h. The average value of linolenic acid in this Assay was also higher than in Assay I (10.10% vs. 7.14% w/w TFA), equating to a higher average PUFA content. The average palmitic acid content was above the range published by Sawangkeaw and Ngamprasertsith [29], as was the average linoleic acid content. The average stearic acid content was within the range published by the mentioned authors.

Figure 4.17 shows the percentage of SFAs, PUFAs and MUFAs in the fatty acid content of the biomass. Because of the high percentages of linoleic and linolenic acids, the average PUFA percentage observed in this Assay was significantly higher than in Assay I (38.46% vs. 29.61% w/w TFA). The average SFA and MUFA percentages were 30.30% and 31.24% w/w FTA, respectively. However, at the time at which the maximum fatty acid productivity was achieved (t = 65.3 h), the SFA percentage was approximately the same in both Assays (38.62% w/w TFA in Assay III vs. 38.71% w/w TFA in Assay I). At this time, MUFA and PUFA percentages were higher in the present Assay (33.98% and 27.40% w/w TFA, respectively). These values are similar to those reported by Dias *et al.* [77] for a culture done in the same conditions as Assay I, using a 600 $g.L^{-1}$ glucose solution as the carbon source.

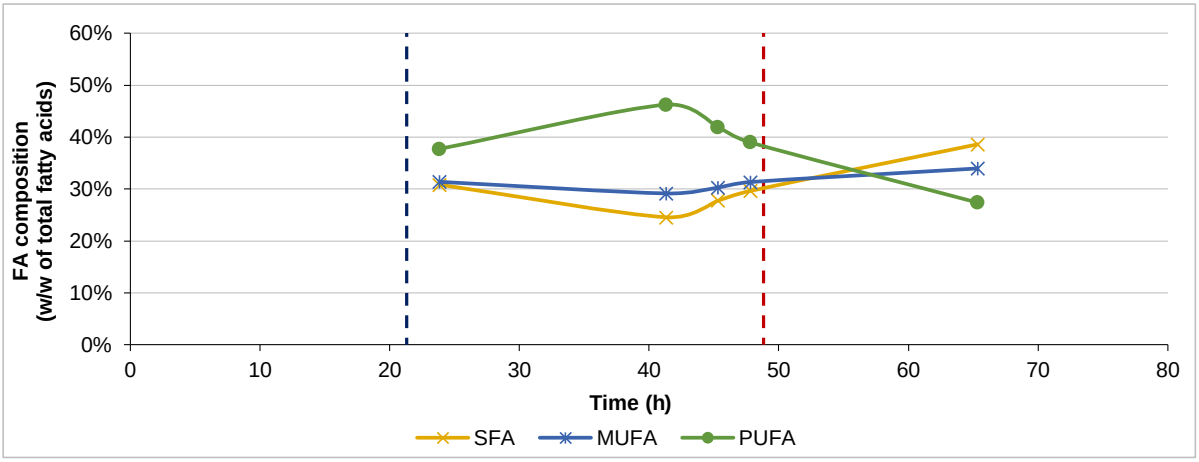

Figure 4.17 – Fatty acid composition in Assay III, quantified as FAMEs. SFA, saturated fatty acids; MUFA, monounsaturated fatty acids; PUFA; polyunsaturated fatty acids. The blue vertical dashed line represents the start of the first stage of fed-batch culture (t = 21.3 h). The red vertical dashed line represents the start of the second stage of fed-batch culture (t = 48.8 h).

4.2.3.2. Cell viability

Figure 4.18 shows the results of [DiOC$_6$(3)+PI] (a) and [CFDA+PI] (b) staining.

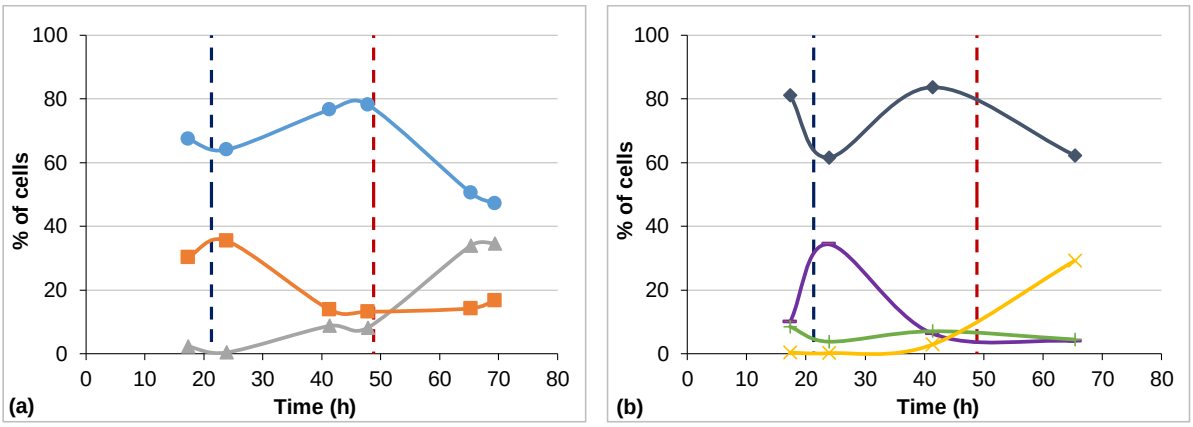

Figure 4.18 – Percentage of cells in each subpopulation, as defined in Figure 3.5, for Assay III. The blue vertical dashed line represents the start of the first stage of fed-batch culture (t = 21.3 h). The red vertical dashed line represents the start of the second stage of fed-batch culture (t = 48.8 h). From left to right: Staining with [DiOC$_6$(3)+PI] (a), subpopulation A (▲) is comprised of cells with depolarized mitochondrial membranes and intact cytoplasmic membranes [DiOC$_6$(3)$^-$,PI$^-$]; Subpopulation B (●) is comprised of cells with polarized mitochondrial membranes and intact cytoplasmic membranes [DiOC$_6$(3)$^+$,PI$^-$]; Subpopulation C (■) is comprised of cells with permeabilised cytoplasmic membrane [DiOC$_6$(3)$^+$,PI$^+$]. Staining with [CFDA+PI] (b), subpopulation D (♦) is comprised of cells with intact cytoplasmic membrane and esterase activity [CFDA$^+$,PI$^-$]; subpopulation E (-) is comprised of cells with permeabilised cytoplasmic membrane that still retain esterase activity [CFDA$^+$,PI$^+$]; subpopulation F (+) is comprised of cells with permeabilised cytoplasmic membranes that do not present esterase activity [CFDA$^-$,PI$^+$]; subpopulation G (x, not present in Figure 3.5) is comprised of cells with intact cytoplasmic membranes and without esterase activity [CFDA$^-$,PI$^-$].

At the end of batch cultivation, the majority of cells (67.37%) were healthy while 30.33% had damaged cytoplasmic membranes. Subpopulation A is virtually nonexistent, with 2.30%. These results are in contrast with those observed in Assay I, wherein a proportion of 32% of healthy cells (subpopulation A) were observed at the end of the batch period. The fact that there are available carbon sources other than glucose at the end of the batch period can help explain why the yeast cells did not appear as being under nutrient starvation conditions, despite the low DO levels. Nevertheless, glucose appears to be the preferred carbon source, as its concentration was always 0 g.L^{-1} during the fed-batch

stage, unlike the remaining carbon sources (fructose and sucrose). Switching the feeding solution to only CPS appeared to have a negative effect on the culture, as there is a significant decrease in subpopulation B, accompanied by a rise in the percentage of subpopulations A and, to a smaller extent, C. By the end of this Assay, subpopulation A represented 34.57% of the culture, B represented 47.21% and C represented 18.22%, indicating that cells were experiencing a higher stress level, comparing to Assay I, where the proportion of healthy cells was almost always higher than 80% during the fed-batch period (Figure 4.10a).

Despite slight differences in the percentage of each cell populations, the results of [CFDA+PI] staining (Figure 4.18b) match the profiles of subpopulations from [$DiOC_6$(3)+PI] staining (Figure 4.18a). The percentage of cells with permeabilised cytoplasmic membrane was highest at the beginning of the fed-batch stage of culture (38.17% at t = 23.8 h), decreasing to under 10% by the end of culture. The percentage of cells belonging to subpopulation D matches that of subpopulation B, increasing during the first stage of fed-batch culture until t = 41.3 h (83.68%), then decreasing until the end of culture (62.29% at t = 65.3 h). In this time period there is an increase in the percentage of subpopulation G that matches the profile of subpopulation A, from 2.90% at t = 41.3 h to 29.25% at t = 65.3 h. This can be a consequence of the exposure of the yeast cells to the inhibitory compounds present in the CPS, coupled with the low DO levels observed at the end of the Assay. Interestingly, this Assay simultaneously presented the highest average percentage of subpopulation D (72.18%) and one of the highest average percentages of subpopulation E (13.67%).

4.2.4. Assay IV

4.2.4.1. Culture parameters

Conditions employed in this Assay were the same as for Assay III. However, CPS was previously concentrated, in order to obtain higher total sugar concentrations, similar to the glucose concentration used during the fed-batch stage of Assays I and II. Final CPS composition can be found in section 4.1.2.

Figure 4.19 shows biomass concentration and productivity (a), the natural logarithm of the biomass concentration (b), stirring speed and DO (c), the concentration of residual sugars (d), total carotenoid content and its productivity (e) and fatty acid content the yeast cells and its productivity (f) over time for Assay IV.

The yeast was cultured in batch mode from t = 0 h to t = 17.8 h (blue vertical traced line), time at which feeding started using a solution containing concentrated CPS and other nutrients. This allowed to prolong the growth phase until t = 65.3 h. The first feeding solution was switched to concentrated CPS at t = 71.8 h (red vertical traced line) and pH was corrected to 5.0 at t = 89.9 h.

Biomass concentration at the end of the batch stage was 25.81 $g.L^{-1}$, corresponding to a biomass productivity of 1.29 $g.L^{-1}.h^{-1}$, the highest recorded in this Assay. The specific growth rate achieved in this stage was 0.13 h^{-1}. By the end of the first stage of fed-batch culture, biomass concentration had risen to 73.76 $g.L^{-1}$ and by the end of the cultivation it dropped to 49.52 $g.L^{-1}$, equating to biomass

productivities of 1.13 h^{-1} and 0.93 h^{-1}, respectively. The maximum biomass concentration was 76.00 $g.L^{-1}$, at t = 93.3 h, during the second stage of fed-batch mode (Figure 4.19 a). This value is higher than the maximum biomass concentration achieved in Assay III, however it is still significantly lower than the maximum obtained in Assay I (118.90 $g.L^{-1}$). Nevertheless, the maximum biomass productivity was identical (1.33 $g.L^{-1}.h^{-1}$ in Assay I).

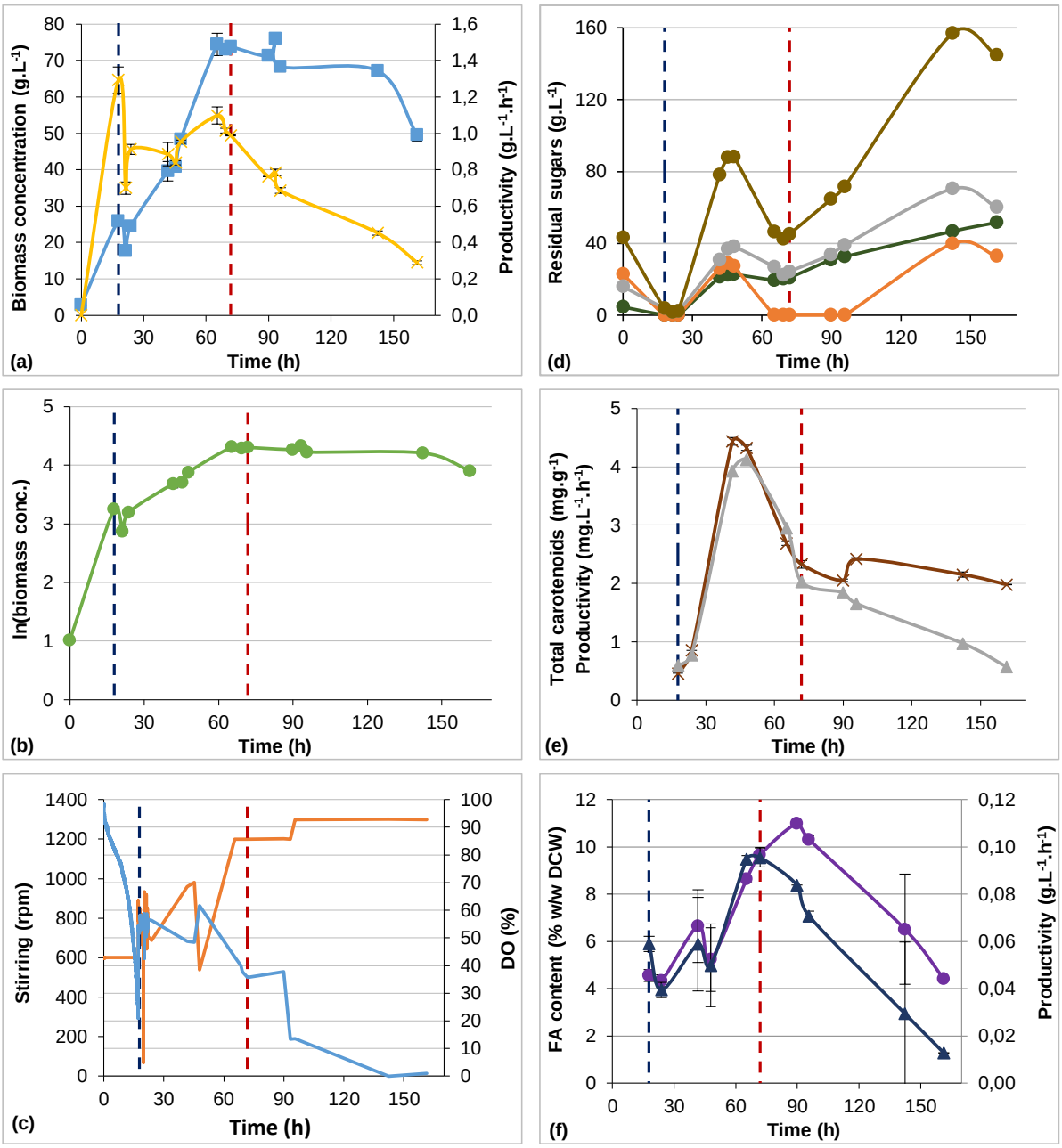

Figure 4.19 – Culture parameters monitored during Assay IV. The blue vertical dashed line represents the start of the first stage of fed-batch culture (t = 17.8 h). The red vertical dashed line represents the start of the second stage of fed-batch culture (t = 71.8 h). From top to bottom, left to right: (a), Biomass concentration calculated from OD (■, $g.L^{-1}$) and biomass productivity (x, $g.L^{-1}.h^{-1}$); (b), natural logarithm of the biomass concentration (●); (c), stirring speed (■, rpm) and DO (♦, %); (d), concentration of residual sugars ($g.L^{-1}$), namely glucose (●), fructose (●), sucrose (●) and total sugars (■); (e), total carotenoid content (x, $mg.g^{-1}$ DCW) and total carotenoid productivity (▲, $mg.L^{-1}.h^{-1}$); (f), fatty acid content (●, % w/w DCW) and productivity (▲, $g.L^{-1}.h^{-1}$) over time. The black bars represent the standard deviation for each sample.

Stirring speed was initially kept constant at 600 rpm. As the culture grew, this speed proved insufficient to maintain adequate DO levels and stirring was made DO-dependent and the set-point for DO was set at 60% oxygen saturation, at t = 17.2 h. The maximum stirring speed was set at 1300 rpm. Unfortunately there was an issue with the data recording software and automatic data logging stopped at t = 21.6 h. Figure 4.19c was constructed from this first set of data until t = 21.6 h and from discrete values recorded manually for the remainder of the Assay. These values indicate that DO levels were kept between 60% and 40% oxygen saturation from t = 23.8 h and t = 68.6 h. From t = 69.3 h onward (beginning of the second stage of fed-batch culture), values decreased to below 40% oxygen saturation. This means that the culture was oxygen deprived during this stage, despite stirring speeds being set at a maximum, 1300 rpm. Weighing precise volumes of CPS and culture medium (at t = 161.3 h) revealed that their densities were 1.256 $g.cm^{-3}$ and 1.163 $g.cm^{-3}$, respectively. Moreover, the CPS used in this Assay appeared to be more viscous than the concentrated glucose solution previously used, although no precise measurements could be made. This raised the question of whether or not using CPS could be negatively impacting oxygen transfer, a possibility that is supported by the DO profile presented in Figure 4.19c: as the initial culture medium, with a higher water content, is replaced by CPS due to successive samples being collected, DO levels dropped despite the increasing stirring speeds. Further studies are needed to conclude if indeed oxygen has a lower solubility in CPS than in water.

Figure 4.19d shows that the residual levels of all three analyzed sugars were low at the end of the batch phase of culturing. However, after being raised at around t = 20 h, the feeding rate utilized led to an accumulation of all three sugars in the cultured broth. Nevertheless, residual glucose concentrations were kept under 40 $g.L^{-1}$. During the second stage of fed-batch of the culture, there was an increase in the concentration of sucrose and fructose, while no residual glucose was detected. After the last adjustment of the feeding rate (t = 95.6 h) there was an increase in the concentration of residual glucose, reaching 39.92 $g.L^{-1}$ at t = 142.3 h. At this time, concentrations of residual fructose and sucrose were 70.41 $g.L^{-1}$ and 46.74 $g.L^{-1}$, respectively, adding to a total residual sugar concentration of 157.07 $g.L^{-1}$. This was only detected after culturing was over because the method used to evaluate residual sugar in real time (Combur-Test® Strips) was only sensitive to glucose, and the concentrations read in the strips fell within the stipulated parameters. Indeed, reductions in biomass concentration (Figure 4.19a), carotenoid content (Figure 4.19e) and fatty acid content (Figure 4.19f) for this time point suggest that the culture could have been inhibited by substrate (sugars) while being simultaneously oxygen deprived.

Despite decreasing significantly from t = 41.7 h until the end of the Assay, maximum total carotenoid content increased 2120% from the values of Assays I and II (Figure 4.7e and Figure 4.11e, respectively) and 282.8% from the value of Assay III (Figure 4.15e). Similarly, carotenoid productivity was 1485% higher in this Assay in comparison with Assay I (Figure 4.7e), 2068% higher in comparison with Assay II (Figure 4.11e) and 758.3% higher in comparison with Assay III (Figure 4.15e). The maximum total carotenoid content was reached at t = 41.7 h with a value of 4.44 $mg.g^{-1}$ and the maximum productivity was recorded in the next analyzed sample (4.12 $mg.L^{-1}.h^{-1}$ at t = 47.8 h). The use of *Rhodosporidium toruloides* or *Rhodotorula glutinis* for the simultaneous production of lipids and

carotenoids is still relatively new so there are not many examples of such experiments in the available literature. This list is further reduced when only cultures using alternative carbon sources are considered. Saenge *et al.* [45] reported a maximum carotenoid productivity of 176.45 $mg.L^{-1}$ in two stage fed-batch cultures using palm oil mill effluent as the carbon source. The same authors published a maximum carotenoid productivity of 1.83 $mg.L^{-1}.h^{-1}$ for fed-batch cultures when using glycerol as the carbon source [39]. Freitas *et al.* [24] mentioned that using CPS as carbon source to grow *R. toruloides* NCYC 921 was beneficial for carotenoid production and reported carotenoid productivities of 9.79 $\mu g.L^{-1}.h^{-1}$ and 3.85 $\mu g.L^{-1}.h^{-1}$ for this microorganism cultured on CPS and sugar cane molasses as carbon sources, respectively. The maximum carotenoid productivity of 4.12 $mg.L^{-1}.h^{-1}$ (equivalent 196.94 $mg.L^{-1}$) achieved in this Assay is thus the highest found in the available literature using *R. toruloides*.

The fatty acid content increased from 4.56% at the end of batch mode to 10.99% attained during the second stage of fed-batch mode (at t = 89.8 h), then decreased to 4.41% by the end of the Assay (Figure 4.19f). Fatty acid content in this Assay was significantly lower than in Assays I and II, indicating that using CPS as a carbon source negatively impacts the yeast fatty acid production and accumulation.

It should be taken into consideration the fact that CPS contains several inhibitory compounds that were not present in the feeding solutions of Assays I and II, and were present in lower concentrations in Assay III. As time passed and more samples were gathered while adding CPS to the bioreactor, the concentrations of these inhibitors increased in the culture broth. These, combined with high concentrations of fructose and sucrose and low oxygenation, explain why biomass concentration and fatty acid content were so severely affected. Despite being higher than in previous Assays, carotenoid content was also affected by these factors towards the end of the cultivation.

Figure 4.20 shows the fatty acids profile during Assay IV.

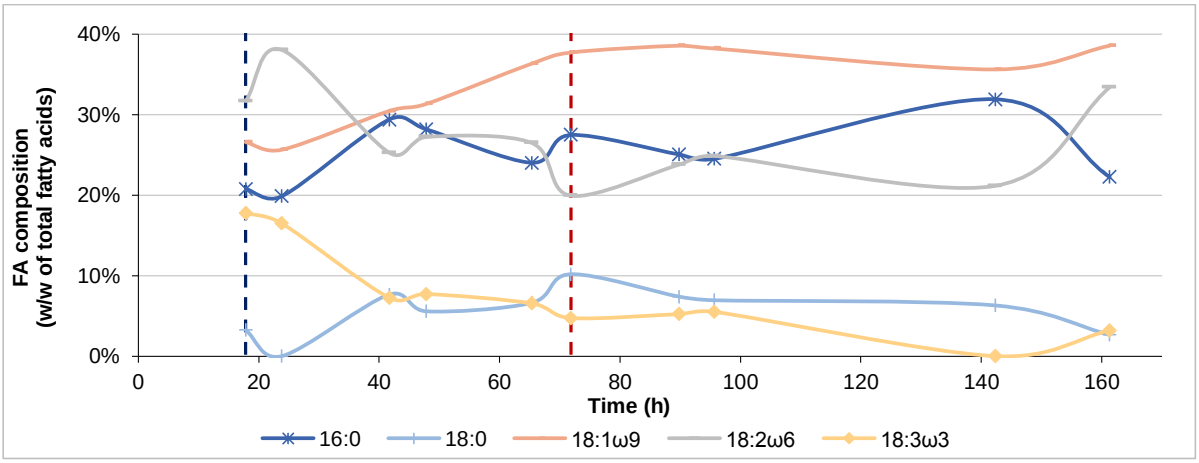

Figure 4.20 – Fatty acid composition in Assay IV, quantified as FAMEs. 16:0, palmitic acid; 18:0, stearic acid; 18:1ω9, oleic acid, 18:2ω6, linoleic acid; 18:3ω3, linolenic acid. The blue vertical dashed line represents the start of the first stage of fed-batch culture (t = 17.8 h). The red vertical dashed line represents the start of the second stage of fed-batch culture (t = 71.8 h).

Despite the lower fatty acid content, fatty acid composition in this Assay was similar to the one observed for Assay III. The most abundant fatty acid was oleic acid, comprising in average 33.89% w/w of the total fatty acids. This value is similar to that observed in Assay I (35.51% w/w TFA) and within the

range published by Sawangkeaw and Ngamprasertsith [29]. The second most abundant fatty acid was linoleic acid, at an average of 27.18% w/w TFA. This figure is similar to that of Assay III (28.36% w/w TFA), higher than the one that was observed in Assay I (22.47% w/w TFA) and within the range published by the abovementioned authors. The SFA present in highest quantity was palmitic acid, comprising in average 25.34% w/w of total fatty acids. This is similar to the results of Assay I (26.48% w/w TFA) and higher than the average of Assay III (22.56% w/w TFA). This value is nearly 10% higher than the interval published by Sawangkeaw and Ngamprasertsith [29]. Stearic acid comprised in average 5.65% w/w of total fatty acids, which is within the published range, while linolenic acid comprised in average 7.44% w/w of total fatty acids, a value that is similar to that of Assay I (7.14% w/w TFA) and lower than in Assay III (10.10% w/w TFA). At the time when the maximum fatty acid productivity was reached (t = 71.8 h), linolenic acid content (4.73% w/w TFA) was approximately the same published by Dias *et al.* [77] (4.50% w/w TFA).

Figure 4.21 shows the percentage of SFAs, PUFAs and MUFAs in the fatty acid content of the biomass.

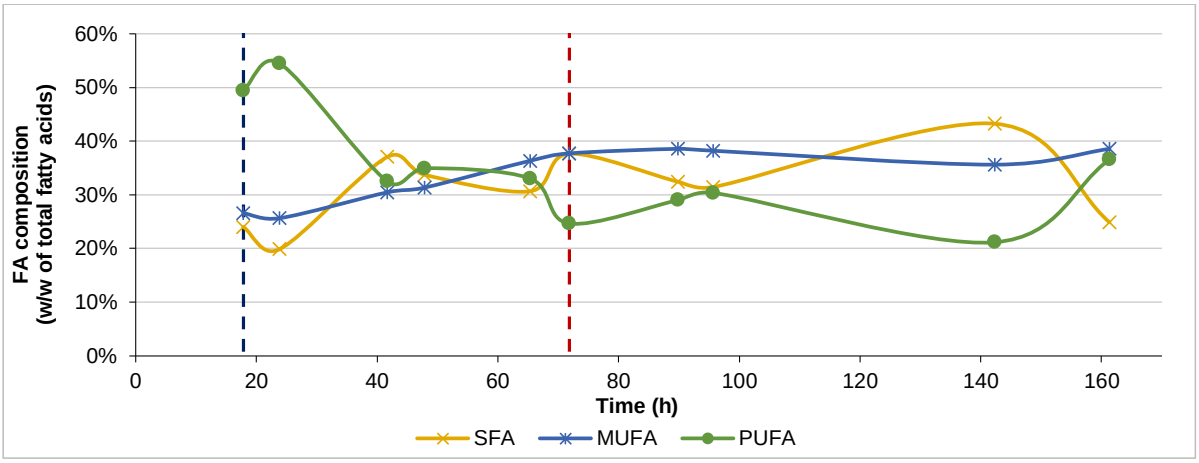

Figure 4.21 – Fatty acid composition in Assay IV, quantified as FAMEs. SFA, saturated fatty acids; MUFA, monounsaturated fatty acids; PUFA; polyunsaturated fatty acids. The blue vertical dashed line represents the start of the first stage of fed-batch culture (t = 17.8 h). The red vertical dashed line represents the start of the second stage of fed-batch culture (t = 71.8 h).

The average SFA, MUFA and PUFA percentages in this Assay were 31.49%, 33.89% and 34.62% w/w TFA, respectively. SFA percentages was thus, in average, lower than what was observed in Assay I and greater than in Assay III. MUFA percentage was also lower than in Assay I and higher than in Assay III, whereas the opposite is true in regards to PUFA percentage. At the time which the highest fatty acid productivity was recorded (t = 71.8 h), SFAs comprised 37.64% w/w of total fatty acids. This value was only about 1% less than what was observed in Assay I (38.71% w/w TFA), the same for Assay III (38.62% w/w TFA). MUFAs and PUFAs comprised 37.71% and 24.65% w/w of total fatty acids, respectively, which are values closer to those observer in Assay I (38.36% and 22.93% w/w TFA).

4.2.4.2. Cell viability

Figure 4.22 shows the results of [$DiOC_6(3)$+PI] (a) and [CFDA+PI] (b) staining for Assay IV.

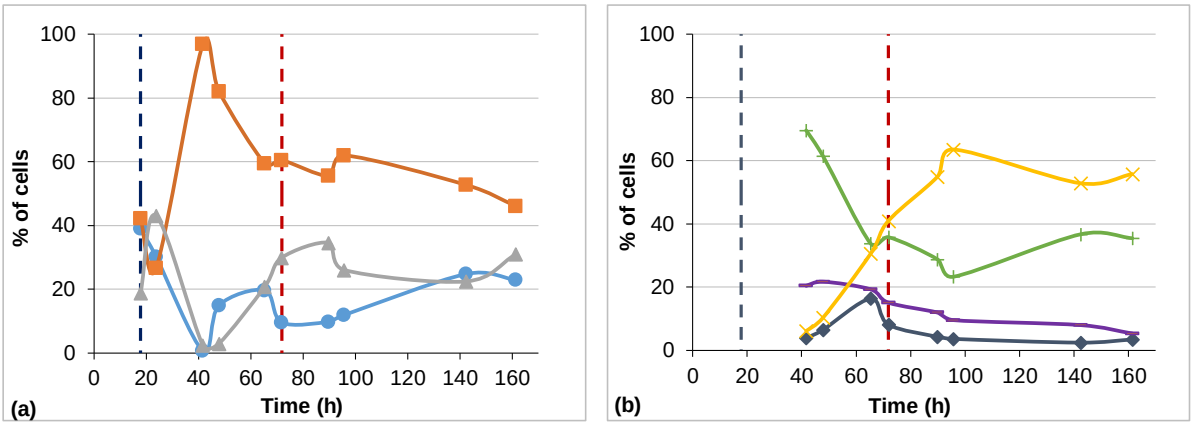

Figure 4.22 – Percentage of cells in each subpopulation, as defined in Figure 3.5, for Assay IV. The blue vertical dashed line represents the start of the first stage of fed-batch culture (t = 17.8 h). The red vertical dashed line represents the start of the second stage of fed-batch culture (t = 71.8 h). From left to right: Staining with [DiOC$_6$(3)+PI] (a), subpopulation A (▲) is comprised of cells with depolarized mitochondrial membranes and intact cytoplasmic membranes [DiOC$_6$(3)$^-$,PI$^-$]; Subpopulation B (●) is comprised of cells with polarized mitochondrial membranes and intact cytoplasmic membranes [DiOC$_6$(3)$^+$,PI$^-$]; Subpopulation C (■) is comprised of cells with permeabilised cytoplasmic membrane [DiOC$_6$(3)$^+$,PI$^+$]. Staining with [CFDA+PI] (b), subpopulation D (♦) is comprised of cells with intact cytoplasmic membrane and esterase activity [CFDA$^+$,PI$^-$]; subpopulation E (-) is comprised of cells with permeabilised cytoplasmic membrane that still retain esterase activity [CFDA$^+$,PI$^+$]; subpopulation F (+) is comprised of cells with permeabilised cytoplasmic membranes that do not present esterase activity [CFDA$^-$,PI$^+$]; subpopulation G (x, not present in Figure 3.5) is comprised of cells with intact cytoplasmic membranes and without esterase activity [CFDA$^-$,PI$^-$].

By the end of the batch stage (t = 17.83 h) healthy cells with polarized membrane (B) and cells with permeabilised membrane (C) represented approximately the same percentage (39.01% and 42.20%, respectively). Cells with depolarized membrane (A) comprised 18.79% of the population. As the feeding rates were increased, from t = 18.83 h until t = 23.83 h, [DiOC$_6$(3)+PI] staining revealed that subpopulations B and C decreased during this period, which was compensated by a rise in subpopulation A, to 43.11%. The feeding rate set at t = 23.83 h was maintained until t = 41.67 h, at which time it was reduced due to evidence that residual glucose levels were rising (Figure 4.19d). During this period there was an unexpected shift in the distribution of the subpopulations, with C comprising 96.93% of all cells and A and B representing 2.37% and 0.70%, respectively. Then the CPS feeding rate was reduced, resulting in a decrease in the subpopulation of cells with damaged cytoplasmic membranes (C). At the end of the first stage of fed-batch culture (t = 71.83 h) healthy cells comprised only 9.58% of the population, with the majority of cells having damaged cytoplasmic membranes (60.51%) or depolarized mitochondrial membranes (29.91%). By the end of the experiment, subpopulation A comprised 30.94% of the total population, B represented 22.93% and C comprised 46.13%. Similarly to Assay III and unlike Assays I and II, the percentage of cells in subpopulation C was significant (after t = 41.5 h it was always higher than 40%) throughout the assay, which might have resulted from the yeast's exposure to high sugar concentrations and inhibitory compounds present in the CPS.

Similarly to [DiOC$_6$(3)+PI] staining, [CFDA+PI] staining (Figure 4.22b) revealed that cells in this assay were experiencing much more adverse conditions than in previous experiments. This is exemplified by the profile of subpopulations that remained below 20% through the entire assay, while the majority of cells that had intact cytoplasmic membrane also displayed reduce esterase activity (subpopulation G). This subpopulation increased from 6.13% at t = 41.7 h to 63.56% at t = 95.7 h,

remaining between 50% and 60% until the end of the experiment. The highest percentage of cells with permeabilised cytoplasmic membrane (90.02%, sum of the percentages of subpopulations E, 20.40%, and F, 69.02%) was observed during the first stage of fed-batch culture (t = 41.7 h). This percentage decreased to 40.79% by the end of the Assay. The low percentages of health cells (subpopulations B and D) observed in this Assay, even when the percentage of cells with permeabilised cytoplasmic membrane (subpopulations C, E and F) decreased, indicates that the cultured cells were experiencing high levels of stress, likely due to oxygen deprivation and exposure to high concentrations of sugars (fructose, glucose and sucrose, plus xylose and arabinose that were not quantified) and inhibitory compounds.

4.2.5. Assay V

4.2.5.1. Culture parameters

Assay V was done with the same set of parameters of Assay I but at a larger scale (50 L bioreactor with 35 L of working volume).

Because this Assay was carried out in a bioreactor that was significantly different than that used in Assays I to IV, there were some issues regarding the control of some culture parameters, in particular those concerning stirring and aeration, because there were no reference values of stirring speeds and aeration rates. During this Assay, the employed stirring speed (150 rpm) and aeration rates (12.5 $L.min^{-1}$) were inadequate and the culture was not being supplied with enough oxygen. There were also issues with the motorization and control of pH because the tube supplying acid to the bioreactor ruptured, irreversibly damaging the acid control pump and the control module (seen on the left of Figure 3.4). The base control pump remained operational. This happened sometime between t = 25.8 h and t = 43.3 h and from this last time onward, pH was adjusted by comparing the value given by the control module and an external pH meter, adjusting the set-point and manually lowering the pH of the culture if necessary.

Figure 4.23 shows biomass concentration and productivity (a), the natural logarithm of the biomass concentration (b), stirring speed and aeration rate (c), the concentration of residual glucose (d), total carotenoid content and its productivity (e) and fatty acid content and its productivity (f) over time for Assay V.

The yeast was cultured in batch mode from t = 0 h to t = 50.2 h (blue vertical traced line), time at which feeding started using a concentrated solution that contained a carbon source (glucose) and other nutrients. The second stage of fed-batch culture was initiated at t = 169.3 h (red vertical traced line) by adding a concentrated glucose solution and the Assay lasted until t = 259.3 h (Figure 4.23).

Biomass concentration at the end of the batch stage was 12.00 $g.L^{-1}$, corresponding to a biomass productivity of 0.21 $g.L^{-1}.h^{-1}$. The specific growth rate achieved in this stage was 0.07 h^{-1}. By the end of the first stage of fed-batch culture, biomass concentration had risen to 30.38 $g.L^{-1}$ and by the end of the fermentation it was at 32.92 $g.L^{-1}$, equating to biomass productivities of 0.17 $g.L^{-1}.h^{-1}$ and 0.12 $g.L^{-1}.h^{-1}$,

respectively. The maximum biomass concentration was 38.29 $g.L^{-1}$, at t = 241.6 h, during the second stage of fed-batch mode. The highest biomass productivity was achieved during batch mode with a value of 0.33 $g.L^{-1}.h^{-1}$ at t = 23.3 h (Figure 4.23a). Both values are significantly lower than those obtained in Assay I and were the lowest recorded in all five Assays.

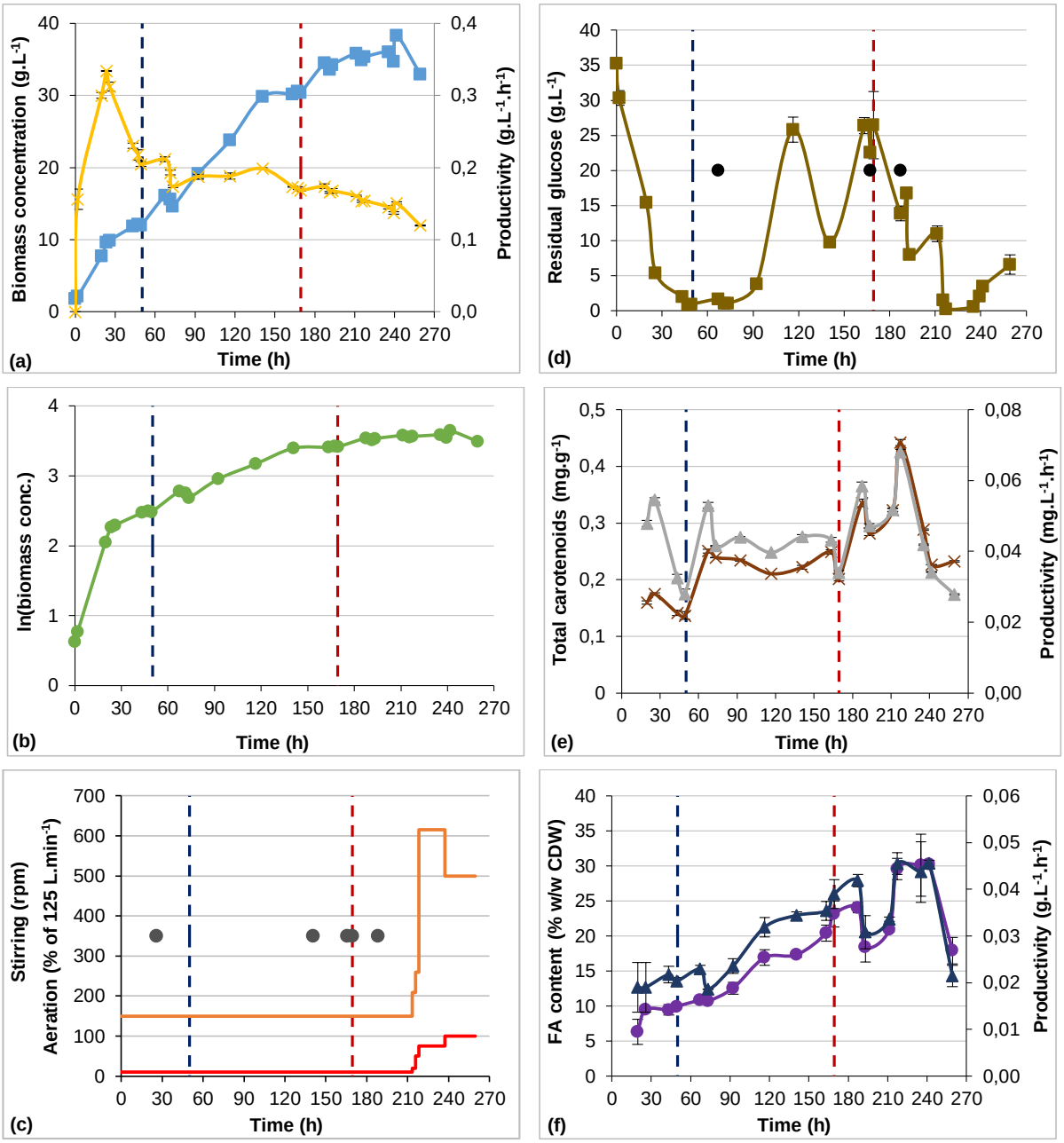

Figure 4.23 – Culture parameters monitored during Assay V. The blue vertical dashed line represents the start of the first stage of fed-batch culture (t = 50.2 h). The red vertical dashed line represents the start of the second stage of fed-batch culture (t = 169.3 h). From top to bottom, left to right: (a), Biomass concentration calculated from OD (■, $g.L^{-1}$) and biomass productivity (x, $g.L^{-1}.h^{-1}$); (b), natural logarithm of the biomass concentration (●); (c), stirring speed (■, rpm) and aeration rate (♦, $L.min^{-1}$), pH corrected either to 4.0 (before the second stage of fed-batch) or 5.0 (during the second stage of fed-batch) (●); (d), concentration of residual glucose (■, $g.L^{-1}$), times at which feeding was interrupted (●); (e), total carotenoid content (x, $mg.g^{-1}$ DCW) and total carotenoid productivity (▲, $mg.L^{-1}.h^{-1}$); (f), fatty acid content (●, % w/w DCW) and productivity (▲, $g.L^{-1}.h^{-1}$) over time. The black bars represent the standard deviation for each sample.

Figure 4.23c shows pH adjustments, stirring and aeration rates. Stirring rate was gradually increased from 150 rpm at t = 213.3 h to 615 rpm at t = 218.3 h, then lowered to 500 rpm at t = 237.3 h

and left at this value through the remainder of the Assay. Stirring rate was reduced because of the strain this was imparting on the equipment. Aeration rates were increased from 12.5 $L.min^{-1}$ to 94 $L.min^{-1}$ from t = 213.3 h to t = 237.3 h, respectively, then to 125 $L.min^{-1}$ to compensate for the decrease in stirring rate.

Glucose concentration in the culture medium was initially 35.29 $g.L^{-1}$. This value decreased significantly during the batch stage of the cultivation, with residual glucose having a concentration of 0.90 $g.L^{-1}$ at t = 49.33 h. Feeding began at t = 50.17 h and afterwards residual glucose levels started to rise, reaching a maximum of 25.82 $g.L^{-1}$ at t = 116.33 h. During this time, feeding was stopped at t = 67.3 h because a fault in the feeding system resulted in the addition of a large amount of feeding solution (NG) to the culture at this time. Feeding was resumed at t = 71.3 h. The feeding rate was reduced at t = 116.3 h, leading to a decrease in residual glucose until t = 140.7 h. At this time the feeding rate was reduced once more and pH was corrected based on the value read on the external pH meter. Until t = 163.3 h residual glucose concentration increased to 26.40 $g.L^{-1}$ and the feeding rate was further reduced, eventually being turned off at t = 167.3 h. Residual glucose concentration was successfully kept at or under 15 $g.L^{-1}$ during the second stage of fed-batch culture (Figure 4.23d).

Despite the above mentioned setbacks, carotenoid content was generally higher in this Assay than in Assays I and II that also used glucose as carbon source. The low carotenoid productivity was due to lower biomass concentrations and, consequently, its productivity. A maximum carotenoid content of 0.44 $mg.g^{-1}$ was reached at t = 217.3 h, equating to a productivity of 0.07 $mg.L^{-1}.h^{-1}$ which was also the maximum obtained (Figure 4.23e).

The maximum fatty acid content was higher in this Assay than in the remaining assays, reaching 30.24% at t = 241.6 h. Fatty acid productivity was also compromised by the low biomass concentration and productivity, reaching a maximum of only 0.05 $g.L^{-1}.h^{-1}$ also at t = 241.6 h (Figure 4.23f).

Figure 4.24 shows the distribution of the fatty acids comprising the total fatty acid content presented in Figure 4.23f. Perhaps one the most interesting aspects about this Assay is the diversity of synthesized fatty acids, different from the fatty acids detected in previous assays. While myristic, palmitic, palmitoleic, stearic, oleic, linoleic and linolenic acids had been observed in previous experiments, in Assay V myristoleic, arachidic, behenic and lignoceric acids were also detected, even in low quantities (in average, less than 1% w/w of total fatty acids, each). Also interesting is the way the fatty acid composition varied through the Assay, in particular regarding oleic acid content. While in previous Assays the average oleic acid percentage was between 30% and 40% w/w of total fatty acids, in this Assay the average composition of total fatty acids was 52.28% w/w TFA and reached a maximum of 69.71% w/w TFA at t = 67.3 h. The average oleic acid percentage was higher than the interval reported by Sawangkeaw and Ngamprasertsith [29], as was the average palmitic acid percentage (18.38% w/w TFA). The average stearic acid percentage (21.76% w/w TFA) was within the reported interval for this fatty acid while the average linoleic acid percentage was below its reported interval. Average myristic, myristoleic, palmitoleic, linolenic, arachidic, behenic and lignoceric acid percentages are not reported by these authors.

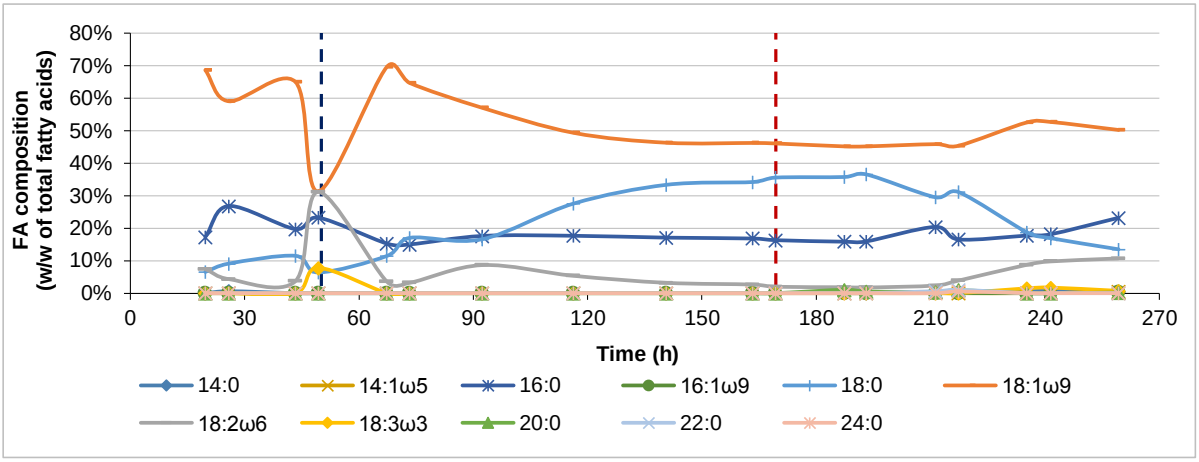

Figure 4.24 – Fatty acid composition in Assay V, quantified as FAMEs. 14:0, myristic acid; 14:1ω5, myristoleic acid; 16:0, palmitic acid; 16:1ω9, palmitoleic acid; 18:0, stearic acid; 18:1ω9, oleic acid, 18:2ω6, linoleic acid; 18:3ω3, linolenic acid; 20:0, arachidic acid; 22:0, behenic acid; 24:0, lignoceric acid. The blue vertical dashed line represents the start of the first stage of fed-batch culture (t = 50.2 h). The red vertical dashed line represents the start of the second stage of fed-batch culture (t = 169.3 h).

Figure 4.25 shows the percentage of SFAs, PUFAs and MUFAs of total fatty acid contents.

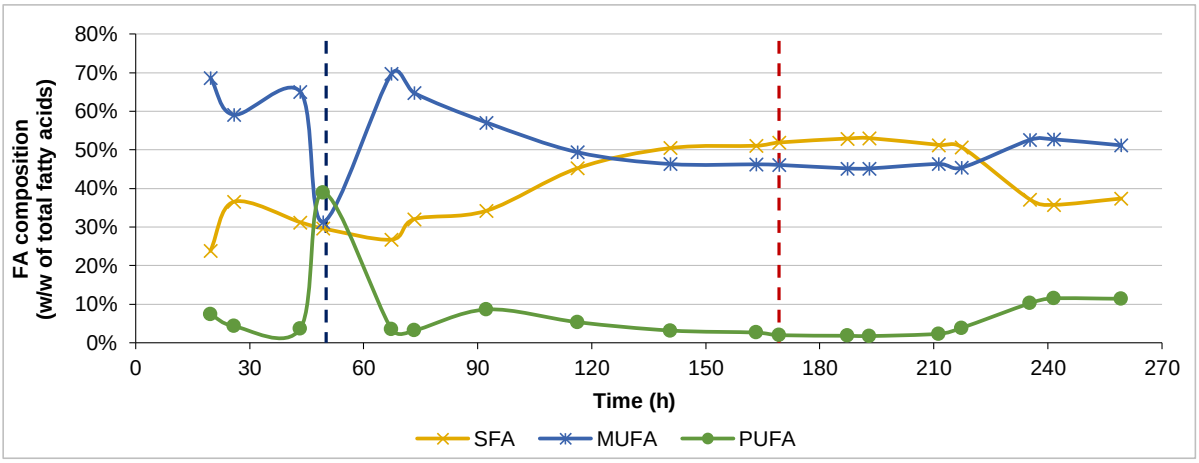

Figure 4.25 – Fatty acid composition in Assay V, quantified as FAMEs. SFA, saturated fatty acids; MUFA, monounsaturated fatty acids; PUFA; polyunsaturated fatty acids. The blue vertical dashed line represents the start of the first stage of fed-batch culture (t = 50.2 h). The red vertical dashed line represents the start of the second stage of fed-batch culture (t = 169.3 h).

Because of the high oleic acid percentage, the overall MUFA proportion was higher than in any of the previous Assays (52.36% w/w TFA). The average SFA percentage was 40.64% w/w TFA, also higher than in previous cultivations. The average PUFA percentage was the lowest observed throughout this work, comprising just 7.00% w/w of total fatty acids. At the time which the maximum fatty acid productivity was observed (t = 241.6 h), SFAs, MUFAs and PUFAs comprised 35.77%, 52.72% and 11.51% w/w of total fatty acids, respectively. Again, this means that the fatty acids produced in this Assay would be more suitable for biodiesel production than those observed for previous Assays, due to the low PUFA percentage.

4.2.5.2. Cell viability

Figure 4.26 shows the results of [$DiOC_6(3)$+PI] (a) and [CFDA+PI] (b) staining for Assay V.

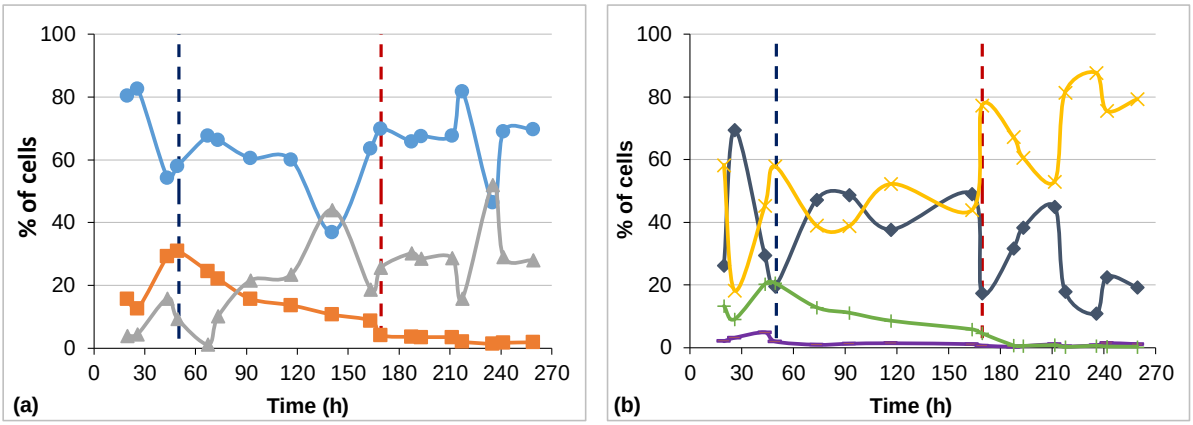

Figure 4.26 – Percentage of cells in each subpopulation, as defined in Figure 3.5, for Assay V. The blue vertical dashed line represents the start of the first stage of fed-batch culture (t = 50.2 h). The red vertical dashed line represents the start of the second stage of fed-batch culture (t = 169.3 h). From left to right: Staining with [DiOC$_6$(3)+PI] (a), subpopulation A (▲) is comprised of cells with depolarized mitochondrial membranes and intact cytoplasmic membranes [DiOC$_6$(3)$^-$,PI$^-$]; Subpopulation B (●) is comprised of cells with polarized mitochondrial membranes and intact cytoplasmic membranes [DiOC$_6$(3)$^+$,PI$^-$]; Subpopulation C (■) is comprised of cells with permeabilised cytoplasmic membrane [DiOC$_6$(3)$^+$,PI$^+$]. Staining with [CFDA+PI] (b), subpopulation D (♦) is comprised of cells with intact cytoplasmic membrane and esterase activity [CFDA$^+$,PI$^-$]; subpopulation E (-) is comprised of cells with permeabilised cytoplasmic membrane that still retain esterase activity [CFDA$^+$,PI$^+$]; subpopulation F (+) is comprised of cells with permeabilised cytoplasmic membranes that do not present esterase activity [CFDA$^-$,PI$^+$]; subpopulation G (x, not present in Figure 3.5) is comprised of cells with intact cytoplasmic membranes and without esterase activity [CFDA$^-$,PI$^-$].

At t = 19.7 h the majority of cells (80.39%) belonged to subpopulation B. Subpopulations A and C comprised 3.94% and 15.64% of the cells, respectively. A comparison between Figure 4.26a and Figure 4.23d perfectly illustrates the relationship between the percentage of cells in each subpopulation and the availability of the carbon source: from t = 19.7 h until t = 49.3 h (just before the beginning of the fed-batch phase, at t = 50.2 h) there is an increase in subpopulations A and C (to 31.04% and 9.36%, respectively), accompanied by a decrease in subpopulation B (to 58.07%); this was coincident with a continued decrease in the concentration of residual glucose, meaning that the available carbon source was being exhausted and the culture was starting to become starved of this nutrient. Once fed-batch regimen was initiated, subpopulation C decreased steadily throughout the Assay, comprising only 1.87% of the yeast population at the end of culturing.

Similarly to previous experiments, the results of [CFDA+PI] staining (Figure 4.26b) reinforce and confirm the results of [DiOC$_6$(3)+PI] staining. The percentage of cells with permeabilised cytoplasmic membrane (subpopulations E and F) increased through the batch stage of cultivation as the biomass concentration increased and cells became nutrient deprived, from 15.34% at t = 19.7 h to 22.58% at t = 49.3 h. Subpopulation E remained under 5% during the entirety of the Assay, while subpopulation F steadily decreased from t = 49.3 h onward, comprising 0.28% of cells at the end of the experiment. Despite varying significantly during the culture, the tendency of subpopulation G was to rise as the Assay progressed, from 18.23% at t = 25.8 h to 79.37% at t = 259.3 h. Inversely, subpopulation D decreased through the culture, from 69.54% to 19.25% during the same time frame. This indicates that the yeast cells were under stress during this Assay, although the adverse conditions did not compromise cell viability, as evidence by Figure 4.23.

4.2.6. Comparison

The summarized results of Assays I through V are present in Table 4.2.

Comparison between Assays I and II reveals that there maximum biomass concentration achieved was 20.03% greater in the first Assay. In both instances the maximum biomass concentration was reached during the second stage of fed-batch culture, therefore some importance can be attributed to the different pH used in these Assays. Assay II presented a higher maximum biomass productivity, however this value was achieved during the first stage of fed-batch culture in both instances, when culture conditions were the same. In regards to biomass concentration, results of Assay I were 11.64% higher than those reported by Li *et al.* [75] for a cultivation done in a 15 L bioreactor operating in fed-batch mode, using glucose as the carbon source, and approximately 6.5% lower than the results published by both Zhao *et al.* [80] and Dias *et al.* [77], for cultivations performed with similar conditions as those of Assay I.

In Assays III and IV both the maximum biomass concentrations and the maximum biomass productivities were lower than those observed for Assays I and II. Assays III and IV also presented higher percentages of cells with either depolarized or permeabilised membranes through the culture, meaning that conditions were less favorable than in previous Assays. This can be partially attributed to the CPS, because of the inhibitory compounds present in it, however in both Assays the culture was subjected to oxygen limitation. This factor cannot be disregarded when analyzing why cellular growth was impaired. Further studies are needed to conclude if oxygen limitation was indeed the main factor behind the lower biomass concentrations and productivities or if this is in fact due to the use of CPS as the carbon source. If the latter situation is true, then using CPS preparation strategies that do not require heating in the sugars extraction step from the carob pulp or to sterilize the CPS might yield better results, as it is expected that lower proportion of inhibitory compounds are released, under these conditions. In comparison with other works that used alternative carbon sources (such as glycerol, sugar cane molasses or a palm oil mill effluent), Assay IV yielded far greater biomass concentrations [24,39,45].

Despite using the same set of conditions as Assay I and as published by Dias *et al.* [77], Assay V yielded lower biomass concentrations than these (67.80% lower than the one observed for Assay I and 69.85% lower than the biomass concentration reported by Dias *et al.* [77]). However, this Assay encountered a series of setbacks that severely affected its outcome, from aeration monitoring problems to complications with culture pH monitoring and controlling, so these results cannot be considered definitive. The way the cultured progressed suggests that this two-stage culturing technique can indeed be scaled up and there should be further improvements to this process.

In regards to carotenoid production, results show that using CPS as the carbon source, in opposition to glucose, greatly increases this parameter. Carotenoid content and productivity increased dramatically from Assay I to Assay IV, from 0.20 $mg.g^{-1}$ DCW and 0.26 $mg.L^{-1}.h^{-1}$ to 4.44 $mg.g^{-1}$ DCW and 4.12 $mg.L^{-1}.h^{-1}$, respectively. The carotenoid productivity observed for Assay IV is the highest in the available literature, approximately 23% higher than the highest reported productivity in the works by Saenge's team [39,45]. Interestingly and despite its problems, Assay V was also a success in this aspect

as the maximum carotenoid productivity increased 120.00% relative to the value of Assay I and 51.72% comparing to the value of the work by Dias *et al.* [77], obtained with the same experimental setup but using a smaller bioreactor (5 L working volume).

Table 4.2 – Summarized results of Assays I through V. Accented values are the highest for each parameter. † - Average 18:3ω3 is within EN 14214 specifications, however there were time at which its content was > 12%.

		Assay I	Assay II	Assay III	Assay IV	Assay V
pH		4.0 → 5.0	4.0 → 5.5	4.0 → 5.0	4.0 → 5.0	4.0 → 5.0
Scale		Laboratory (5 L)	Laboratory (5 L)	Laboratory (5 L)	Laboratory (5 L)	Pilot (35 L)
Carbon source		Glucose	Glucose	CPS	Concentrated CPS	Glucose
Max. biomass concentration ($g.L^{-1}$)		**118.90** (t = 186.0 h)	95.08 (t = 89.8 h)	69.94 (t = 65.3 h)	76.00 (t = 93.3 h)	38.29 (t = 241.6 h)
Max. biomass productivity ($g.L^{-1}.h^{-1}$)		1.33 (t = 22.0 h)	**1.52** (t = 21.9 h)	1.06 (t = 65.3 h)	1.29 (t = 17.8 h)	0.33 (t = 23.3 h)
Max. carotenoid content ($mg.g^{-1}$ DCW)		0.20 (t = 48.5 h)	0.20 (t = 185.9 h)	1.16 (t = 17.3 h)	**4.44** (t = 41.7 h)	0.44 (t = 217.3 h)
Max. carotenoid productivity ($mg.L^{-1}.h^{-1}$)		0.26 (t = 48.5 h)	0.19 (t = 65.9 h)	0.48 (t = 23.8 h)	**4.12** (t = 47.8 h)	0.07 (t = 217.3 h)
Max. fatty acid content (% w/w DCW)		24.25 (t = 66.0 h)	25.76 (t = 163.7 h)	12.90 (t = 65.3 h)	10.99 (t = 89.8 h)	**30.24** (t = 241.6 h)
Max. fatty acid productivity ($g.L^{-1}.h^{-1}$)		**0.29** (t = 72.0 h)	0.27 (t = 65.9 h)	0.14 (t = 65.3 h)	**0.10** (t = 71.8 h)	0.05 (t = 241.6 h)
Total fatty acid average composition (% w/w)	**SFA**	34.62	35.17	30.30	31.49	**40.64**
	MUFA	35.77	34.83	31.24	33.89	**52.36**
	PUFA	29.61	30.00	**38.46**	34.62	7.00
	18:3ω3	7.14	6.17	**10.10**	7.44	0.65
Average subpopulation (%)	**A**	10.22	**42.23**	14.72	23.20	21.75
	B	**74.13**	46.63	63.98	18.35	64.96
	C	15.47	8.87	20.64	**58.45**	11.42
	D	34.47	53.18	**72.18**	6.07	33.18
	E	2.40	3.12	13.67	**13.91**	1.43
	F	6.78	2.28	5.97	**40.62**	6.87
	G	56.35	41.42	8.18	39.40	**58.52**
EN 14214 requirements		Fulfilled	Fulfilled	Failed†	Fulfilled	Fulfilled

Concerning fatty acid content and productivity, again Assay V presented interesting results. This Assay achieved the highest yeast fatty acid content, at 30.24% w/w, which is a 24.70% increase over the maximum fatty acid content of Assay I. This result might be a consequence of the oxygen limitation experienced by the culture during this Assay as the yeast's metabolism shifts from division and population growth to the accumulation of storage materials. A similar result can be observed in the work of Dias *et al.* [77], as their highest fatty acid content (27.88% w/w DCW) was achieved in an experiment where the culture suffered oxygen limitation. Results of Assays I and II concerning fatty acid content, were similar to those published by Dias *et al.* [77]. However, because of lower biomass productivities, fatty acid productivities in Assays III and V were severely affected, being 51.72% and 82.76% lower than those observed for Assays I. The lowest fatty acid content was observed in Assay IV (10.99% w/w DCW), likely due to the presence of high concentrations of inhibitory compounds present in the culture medium.

As mentioned in section 1.3, biodiesel production from oleaginous microbial cultures is far from becoming economically viable, hence the concomitant production of carotenoids and fatty acids is crucial to achieve this goal. Because carotenoids are the products with the higher added value, cells should be harvested when carotenoid productivity is maximum. Consequently, the resulting biodiesel would be produced from the fatty acids accumulated at the time the highest carotenoid productivity was reached. This means that, despite its lower biomass productivity and fatty acid content, Assay IV produced the biomass with potentially the highest value as its carotenoid content was the highest, among the other Assays. Table 4.3 presents the SFA, MUFA, PUFA and linolenic acid percentages of the yeast cells, at the corresponding time at which the highest carotenoid productivity was attained, for each Assay, to determine if the fatty acid composition met the specifications of the European Standard EN 14214 that defines the biodiesel characteristics.

Table 4.3 – SFA, MUFA, PUFA and linolenic acid contents as % w/w of total fatty acids at the time of the maximum carotenoid productivity for each performed Assay. Accented values are the highest for each parameter.

	Assay I	Assay II	Assay III	Assay IV	Assay V
SFA (% w/w)	38.74	36.27	30.85	33.74	**50.73**
MUFA (% w/w)	37.21	37.49	31.40	31.33	**45.40**
PUFA (% w/w)	24.05	26.24	**37.75**	34.94	3.87
18:3ω3 (% w/w)	5.41	4.68	**18.46**	7.71	0.00
EN 14214 requirements	Fulfilled	Fulfilled	Failed	Fulfilled	Fulfilled

As already stated, European Standard EN 14214 dictates that biodiesel must not contain linolenic acid methyl ester over 12% w/w and must not contain PUFA derived methyl esters with four or more unsaturations over 1% w/w [42]. There are, of course, other criteria, however these two are the ones that more directly relate to the raw material used to produce the biodiesel. In this sense, results from Table 4.2 and Table 4.3 show that the fatty acids produced in Assays I, II, IV and V would yield biodiesels that would meet EN 14214, while biodiesel produced from the fatty acids of Assay III would fail the requirements on account of the percentage of linolenic acid. Fatty acids with four or more unsaturations were not observed in any of the Assays.

5 Conclusions and future prospects

The main goal of the present work was to evaluate the possibility of using CPS as the carbon source to develop *Rhodosporidium toruloides* NCYC 921 fed-batch cultures in a benchtop bioreactor and in a pilot scale bioreactor, for the simultaneous synthesis of carotenoids and lipids, towards biodiesel production. Besides this, three other objectives were set: (i) to evaluate the response of *R. toruloides* NCYC 921 when cultured in a two-stage fed-batch system, with the second stage at pH 5.5, while ensuring the culture did not suffer from oxygen limitation, a work that was lacking in the literature; (ii) to evaluate the possibility of scaling-up *R. toruloides* NCYC 921 fed-batch cultures, using the conditions published by Dias *et al.* [77] in a work framed within the same project were the present work is inserted; (iii) to determine how carob pulp storage conditions and sugar extraction techniques affect CPS composition.

Regarding the main objective, assays carried out using CPS as the carbon source revealed that this is a suitable substrate to grow *R. toruloides* NCYC 921, despite cell viability being somewhat compromised. Furthermore, these assays revealed that carotenoid productivity greatly benefited from the use of CPS, as carotenoid content and productivity in the best of these assays were significantly higher than the values that can currently be found in the available literature (4.12 $mg.L^{-1}.h^{-1}$). Fatty acid content and productivity were comparable to the assays where glucose was used as the carbon source and are similar to other values found in the literature. However, both cultures done with CPS suffered from oxygen limitation, an issue that several authors have found to be determinant in the outcome of *R. toruloides* cultivations, regarding carotenoid production. This was due to an incorrect control of stirring speed, resulting from equipment failure.

Using a pH of 5.5 for the second stage of cultivation was found to yield less preferable results, despite several authors having mentioned this pH to be optimal for *R. toruloides* cultivations.

Using the strategy that was found to yield the best results (two-stage fed-batch culture, first at a pH of 4.0 then at 5.0, using a 600 $g.L^{-1}$ glucose solution as carbon source), the cultivation was successfully scaled up to a 50 L bioreactor (35 L working volume). However, there were several issues with the used equipment and both DO and pH levels were not adequately monitored and controlled. This greatly compromised biomass productivity, in turn leading to lower fatty acid and carotenoid productivities. Despite these issues, this experiment registered the highest fatty acid content amongst all performed assays and the lowest PUFA and linolenic acid contents, therefore this strategy should be pursued.

The conditions under which carob pulp is stored was found to have an impact on the composition of CPS as carob pulp kept refrigerated in airtight containers had more extractable sugars than carob pulp kept in the laboratory at room temperature, despite this latter having a larger surface area. It was also found that the extraction procedure used to prepare CPS for the cultivations was not the most adequate, regarding the extraction efficiency. A technique that uses higher water to carob pulp ratios in combination with heating was found to extract more sugars from the carob pulp, while increasing CPS

productivity. This result is consistent with others found in the available literature. The employed method had, however, a lower energy requirement which aids in an overall process cost reduction. Additionally, by not using heating during extraction, the amounts of inhibitory compounds in the CPS is minimized. The method by which CPS was sterilized (autoclaving) led to the degradation of a significant part of the extracted sugars, either by caramelization or via the formation of HMF and furfural. Therefore, alternative means of sterilizing the CPS that to not require heating (e.g. filtration) might have yielded better results in regards to cell viability in the cultures that used CPS as the carbon source.

Because of the unforeseen problems that occurred during this work, some of the results should be consolidated by repeating specific assays. Assay IV should be repeated, changing the necessary parameters to ensure that there is no oxygen limitation. Furthermore, the results of CPS analysis should be taken into consideration, meaning that, when repeating this assay, the CPS should be prepared with carob pulp stored under controlled conditions and the extraction should be done with techniques that employ higher water to carob pulp ratios. Other methods of sterilizing the CPS should be investigated in order to reduce the amount of inhibitory compounds added to the culture medium. The physical characteristics of the CPS used in Assay IV might have further contributed to the lower biomass productivity in the sense that oxygen transfer might have been impaired. Future cultures could benefit from the use of a CPS with a total sugar concentration between the one of Assay III and Assay IV, i.e. 350 $g.L^{-1}$ to 450 $g.L^{-1}$ of total sugars, which should ensure manageable feeding rates. Regarding Assay V, it should also be repeated, correcting the operational parameters that were found to be inadequate in the present experiment.

Finally, the possibility of scaling up *R. toruloides* cultures using CPS as the carbon source should be evaluated, based on the results of Assays IV and V.

Throughout the assays, FC proved to be an invaluable technique as it allowed to monitor cellular viability and total carotenoid content in next-to-real time, in turn allowing expedited corrections of the employed culture parameters if necessary.

6 References

[1] Pasten, C. and Santamarina, J. C., Energy and quality of life. Energy Policy, 2012. **49**: p. 468-76.

[2] U.S. Energy Information Administration, *International Energy Outlook 2014: World Petroleum and Other Liquid Fuels*. 2014, U.S. Energy Information Administration.

[3] Atabani, A. E., Silitonga, A. S., Badruddin, I. A., Mahlia, T. M. I.*, et al.*, A comprehensive review on biodiesel as an alternative energy resource and its characteristics. Renewable and Sustainable Energy Reviews, 2012. **16**(4): p. 2070-93.

[4] Kafuku, G. and Mbarawa, M., Biodiesel production from *Croton megalocarpus* oil and its process optimization. Fuel, 2010. **89**(9): p. 2556-60.

[5] Ahmad, A. L., Yasin, N. H. M., Derek, C. J. C., and Lim, J. K., Microalgae as a sustainable energy source for biodiesel production: A review. Renewable and Sustainable Energy Reviews, 2011. **15**(1): p. 584-93.

[6] Sharma, Y. C. and Singh, B., Development of biodiesel: Current scenario. Renewable and Sustainable Energy Reviews, 2009. **13**(6-7): p. 1646-51.

[7] British Petroleum, *BP Statistical Review of World Energy 2014*. 2014.

[8] Timilsina, G. R. and Shrestha, A., How much hope should we have for biofuels? Energy, 2011. **36**(4): p. 2055-69.

[9] Naik, S. N., Goud, V. V., Rout, P. K., and Dalai, A. K., Production of first and second generation biofuels: A comprehensive review. Renewable and Sustainable Energy Reviews, 2010. **14**(2): p. 578-97.

[10] Nogueira, L. A. H., Does biodiesel make sense? Energy, 2011. **36**(6): p. 3659-66.

[11] Nigam, P. S. and Singh, A., Production of liquid biofuels from renewable resources. Progress in Energy and Combustion Science, 2011. **37**(1): p. 52-68.

[12] Council Directive 2009/28/EC of 23 April 2009 on the promotion of the use of energy from renewable sources and amending and subsequently repealing Directives 2001/77/EC and 2003/30/EC. Official Journal of the European Union, 2009. **L140**: p. 16-62.

[13] *Plano Nacional de Acção para as Energias Renováveis ao Abrigo da Directiva 2009/28/CE : (de acordo com o modelo estabelecido pela Decisão da Comissão de 30.6.2009) : versão final [National Plan of Action for Renewable Energies under Directive 2009/28/CE : (in accordance with the model established by the Decision of the Commission of 30.6.2009) : final version]*, República Portuguesa, Editor. 2010: Lisbon, Portugal.

[14] da Silva, T. L., Roseiro, J. C., and Reis, A., Applications and perspectives of multi-parameter flow cytometry to microbial biofuels production processes. Trends in Biotechnology, 2012. **30**(4): p. 225-32.

[15] McCormick, R. L., Alleman, T., Williams, A., Coy, Y.*, et al.*, *Status and Issues for Biodiesel in the United States. A Discussion Paper for Clean Cities Coalitions and Stakeholders to Develop Strategies for the Future*. 2009, National Renewable Energy Laboratory. p. 26.

[16] Cobuloglu, H. I. and Büyüktahtakın, İ. E., Food vs. biofuel: An optimization approach to the spatio-temporal analysis of land-use competition and environmental impacts. Applied Energy, 2015. **140**: p. 418-34.

[17] Chen, H.-G. and Zhang, Y. H. P., New biorefineries and sustainable agriculture: Increased food, biofuels, and ecosystem security. Renewable and Sustainable Energy Reviews, 2015. **47**: p. 117-32.

[18] Carriquiry, M. A., Du, X., and Timilsina, G. R., Second generation biofuels: Economics and policies. Energy Policy, 2011. **39**(7): p. 4222-34.

[19] Thompson, W. and Meyer, S., Second generation biofuels and food crops: Co-products or competitors? Global Food Security, 2013. **2**(2): p. 89-96.

[20] Schenk, P. M., Thomas-Hall, S. R., Stephens, E., Marx, U. C.*, et al.*, Second Generation Biofuels: High-Efficiency Microalgae for Biodiesel Production. BioEnergy Research, 2008. **1**(1): p. 20-43.

[21] Meng, X., Yang, J., Xu, X., Zhang, L.*, et al.*, Biodiesel production from oleaginous microorganisms. Renewable Energy, 2009. **34**(1): p. 1-5.

[22] Zhang, Z., Zhang, X., and Tan, T., Lipid and carotenoid production by *Rhodotorula glutinis* under irradiation/high-temperature and dark/low-temperature cultivation. Bioresource Technology, 2014. **157**: p. 149-53.

[23] Schneider, T., Graeff-Hönninger, S., French, W. T., Hernandez, R.*, et al.*, Lipid and carotenoid production by oleaginous red yeast *Rhodotorula glutinis* cultivated on brewery effluent. Energy, 2013. **61**: p. 34-43.

[24] Freitas, C., Parreira, T. M., Roseiro, J., Reis, A.*, et al.*, Selecting low-cost carbon sources for carotenoid and lipid production by the pink yeast *Rhodosporidium toruloides* NCYC 921 using flow cytometry. Bioresource Technology, 2014. **158**: p. 355-9.

[25] Noraini, M. Y., Ong, H. C., Badrul, M. J., and Chong, W. T., A review on potential enzymatic reaction for biofuel production from algae. Renewable and Sustainable Energy Reviews, 2014. **39**: p. 24-34.

[26] Jacob, A., Xia, A., and Murphy, J. D., A perspective on gaseous biofuel production from micro-algae generated from CO2 from a coal-fired power plant. Applied Energy, 2015. **148**: p. 396-402.

[27] Allen, E., Wall, D. M., Herrmann, C., and Murphy, J. D., Investigation of the optimal percentage of green seaweed that may be co-digested with dairy slurry to produce gaseous biofuel. Bioresource Technology, 2014. **170**: p. 436-44.

[28] Ho, S. H., Huang, S. W., Chen, C. Y., Hasunuma, T.*, et al.*, Bioethanol production using carbohydrate-rich microalgae biomass as feedstock. Bioresource Technology, 2013. **135**: p. 191-8.

[29] Sawangkeaw, R. and Ngamprasertsith, S., A review of lipid-based biomasses as feedstocks for biofuels production. Renewable and Sustainable Energy Reviews, 2013. **25**: p. 97-108.

[30] Ratledge, C., Regulation of lipid accumulation in oleaginous micro-organisms. Biochemical Society Transactions, 2002. **30**: p. 1047-50.

[31] Alvarez, H. M. and Steinbuchel, A., Triacylglycerols in prokaryotic microorganisms. Applied Microbiology and Biotechnology, 2002. **60**(4): p. 367-76.

[32] Papanikolaou, S., Sarantou, S., Komaitis, M., and Aggelis, G., Repression of reserve lipid turnover in *Cunninghamella echinulata* and *Mortierella isabellina* cultivated in multiple-limited media. Journal of Applied Microbiology, 2004. **97**(4): p. 867-75.

[33] Papanikolaou, S., Komaitis, M., and Aggelis, G., Single cell oil (SCO) production by *Mortierella isabellina* grown on high-sugar content media. Bioresource Technology, 2004. **95**(3): p. 287-91.

[34] Ratledge, C., Single cell oils - have they a biotechnological future? Trends in Biotechnology, 1993. **11**(7): p. 278-84.

[35] Stansell, G. R., Gray, V. M., and Sym, S. D., Microalgal fatty acid composition: implications for biodiesel quality. Journal of Applied Phycology, 2011. **24**(4): p. 791-801.

[36] Belarbi, E. H., Molina, E., and Chisti, Y., A process for high yield and scaleable recovery of high purity eicosapentaenoic acid esters from microalgae and fish oil. Enzime and Microbial Technology, 2000. **26**: p. 516-29.

[37] *A Guide to IUPAC Nomenclature of Organic Compounds*, ed. R. Panico, W.H. Powell, and J.C. Richer. 1993: IUPAC/Blackwell Science.

[38] Girio, F. M., Fonseca, C., Carvalheiro, F., Duarte, L. C.*, et al.*, Hemicelluloses for fuel ethanol: A review. Bioresource Technology, 2010. **101**(13): p. 4775-800.

[39] Saenge, C., Cheirsilp, B., Suksaroge, T. T., and Bourtoom, T., Potential use of oleaginous red yeast *Rhodotorula glutinis* for the bioconversion of crude glycerol from biodiesel plant to lipids and carotenoids. Process Biochemistry, 2011. **46**(1): p. 210-8.

[40] Yang, X., Jin, G., Gong, Z., Shen, H.*, et al.*, Recycling biodiesel-derived glycerol by the oleaginous yeast *Rhodosporidium toruloides* Y4 through the two-stage lipid production process. Biochemical Engineering Journal, 2014. **91**: p. 86-91.

[41] Meireles, B. A. and Pereira, V. L. P., Synthesis of Bio-Additives: Transesterification of Ethyl Acetate with Glycerol using Homogeneous or Heterogeneous Acid Catalysts. Journal of the Brazilian Chemical Society, 2013. **24**(1): p. 17-25.

[42] Jääskeläinen, H. *Biodiesel Standards & Properties*. [cited 2015 May 31]; Available from: https://www.dieselnet.com/tech/fuel_biodiesel_std.php#spec.

[43] Worldwatch Institute, *Biofuels for transportation: Global Potential and Implications for Sustainable Agriculture and Energy in the 21st Century*. 2006, Worldwatch Institute: Washington DC.

[44] Pate, R. and Hightower, M., *Overview of Biofuels from the Energy-Water Nexus Perspective and the Promise and Challenge of Algae as Biofuel Feedstock*. 2008, Energy, Resources and Systems Analysis Center, Sandia National Laboratories: Albuquerque, NM.

[45] Saenge, C., Cheirsilp, B., Suksaroge, T. T., and Bourtoom, T., Efficient Concomitant Production of Lipids and Carotenoids by Oleaginous Red Yeast *Rhodotorula glutinis* Cultured in Palm Oil Mill Effluent and Application of Lipids for Biodiesel Production. Biotechnology and Bioprocess Engineering, 2011. **16**(1): p. 23-33.

[46] Grama, B. S., Chader, S., Khelifi, D., Stenuit, B.*, et al.*, Characterization of fatty acid and carotenoid production in an Acutodesmus microalga isolated from the Algerian Sahara. Biomass and Bioenergy, 2014. **69**: p. 265-75.

[47] Vachali, P., Bhosale, P., and Bernstein, P. S., *Microbial Carotenoids*, in *Microbial Carotenoids From Fungi*, J.-L. Barredo, Editor. 2012, Humana Press.

[48] Perera, C. O. and Yen, G. M., Functional Properties of Carotenoids in Human Health. International Journal of Food Properties, 2007. **10**(2): p. 201-30.

[49] Nells, H. J. and De Leenheer, A. P., Microbial sources of carotenoid pigments used in foods and feeds. Journal of Applied Bacteriology, 1991. **70**: p. 181-91.

[50] American Cancer Society. *Vitamin A, Retinoids, and Provitamin A Carotenoids*. 2012 [cited 2015 April 10]; Available from: http://www.cancer.org/treatment/treatmentsandsideeffects/complementaryandalternativemedicine/herbsvitaminsandminerals/vitamin-a-and-beta-carotene.

[51] *Carotenoids: Volume 5: Nutrition and Health*. 2009: Birkhäuser Verlag.

[52] Linnewiel-Hermoni, K., Khanin, M., Danilenko, M., Zango, G.*, et al.*, The anti-cancer effects of carotenoids and other phytonutrients resides in their combined activity. Archives of Biochemistry and Biophysics, 2015.

[53] Peto, R., Doll, R., Buckley, J. D., and Sporn, M. B., Can dietary beta-carotene materially reduce human cancer rates? Nature, 1981. **290**: p. 201-8.

[54] Sluijs, I., Cadier, E., Beulens, J. W., van der, A. D.*, et al.*, Dietary intake of carotenoids and risk of type 2 diabetes. Nutrition, Metabolism, and Cardiovascular Diseases, 2015. **25**(4): p. 376-81.

[55] Zoz, L., Carvalho, J. C., Soccol, V. T., Casagrande, T. C.*, et al.*, Torularhodin and Torulene: Bioproduction, Properties and Prospective Applications in Food and Cosmetics - a Review. Brazilian Archives of Biology and Technology, 2015. **58**(2): p. 278-88.

[56] De Carvalho, J. C., Cardoso, L. C., Ghiggi, V., Woiciechowski, A. L.*, et al.*, *Microbial Pigments*, in *Biotransformation of Wast Biomass into High Value Biochemicals*, K.S. Brar, G.S. Dhillon, and C.R. Soccol, Editors. 2014, Springer. p. 73-97.

[57] Maldonade, I. R., Rodriguez-Amaya, D. B., and Scamparini, A. R. P., Carotenoids of yeasts isolated from the Brazilian ecosystem. Food Chemistry, 2008. **107**(1): p. 145-50.

[58] European spending on carotenoids to pass $400 M mark by 2010. Focus on Pigments, 2004. **2004**(5): p. 3.

[59] Cardenas-Toro, F. P., Alcázar-Alay, S. C., Coutinho, J. P., Godoy, H. T.*, et al.*, Pressurized liquid extraction and low-pressure solvent extraction of carotenoids from pressed palm fiber: Experimental and economical evaluation. Food and Bioproducts Processing, 2015. **94**: p. 90-100.

[60] Zaghdoudi, K., Pontvianne, S., Framboisier, X., Achard, M.*, et al.*, Accelerated solvent extraction of carotenoids from: Tunisian Kaki (Diospyros kaki L.), peach (Prunus persica L.) and apricot (Prunus armeniaca L.). Food Chemistry, 2015. **184**: p. 131-9.

[61] Strati, I. F., Gogou, E., and Oreopoulou, V., Enzyme and high pressure assisted extraction of carotenoids from tomato waste. Food and Bioproducts Processing, 2015. **94**: p. 668-74.

[62] Strati, I. F. and Oreopoulou, V., Recovery of carotenoids from tomato processing by-products – a review. Food Research International, 2014. **65**: p. 311-21.

[63] Wang, C. C., Chang, S. C., Inbaraj, B. S., and Chen, B. H., Isolation of carotenoids, flavonoids and polysaccharides from Lycium barbarum L. and evaluation of antioxidant activity. Food Chemistry, 2010. **120**(1): p. 184-92.

[64] *Carotenoids: Volume 2: Synthesis*. 1996: Birkhäuser Verlag.

[65] Kaiser, P., Surmann, P., Vallentin, G., and Fuhrmann, H., A small-scale method for quantitation of carotenoids in bacteria and yeasts. Journal of Microbiological Methods, 2007. **70**(1): p. 142-9.

[66] Luengo, E., Condón-Abanto, S., Condón, S., Álvarez, I.*, et al.*, Improving the extraction of carotenoids from tomato waste by application of ultrasound under pressure. Separation and Purification Technology, 2014. **136**: p. 130-6.

[67] Goto, M., Kanda, H., Wahyudiono, and Machmudah, S., Extraction of carotenoids and lipids from algae by supercritical CO_2 and subcritical dimethyl ether. The Journal of Supercritical Fluids, 2015. **96**: p. 245-51.

[68] Li, Y., Fabiano-Tixier, A. S., Tomao, V., Cravotto, G.*, et al.*, Green ultrasound-assisted extraction of carotenoids based on the bio-refinery concept using sunflower oil as an alternative solvent. Ultrasonics sonochemistry, 2013. **20**(1): p. 12-8.

[69] Moline, M., Libkind, D., and van Broock, M., *Production of Torularhodin, Torulene, and β-Carotene by Rhodotorula Yeasts*, in *Microbial Carotenoids From Fungi: Methods and Protocols*, J.-L. Barredo, Editor. 2012, Springer Science+Business Media: New York. p. 275-83.

[70] Freitas, C., Nobre, B., Gouveia, L., Roseiro, J.*, et al.*, New at-line flow cytometric protocols for determining carotenoid content and cell viability during *Rhodosporidium toruloides* NCYC 921 batch growth. Process Biochemistry, 2014. **49**(4): p. 554-62.

[71] Zhu, Z., Zhang, S., Liu, H., Shen, H.*, et al.*, A multi-omic map of the lipid-producing yeast *Rhodosporidium toruloides.* Nature Communications, 2012. **3**: p. 1112.

[72] UniProt Consortium. *Rhodosporidium toruloides (Yeast) (Rhodotorula gracilis) (SPECIES)*. 2015 [cited 2015 April 27]; Available from: http://www.uniprot.org/taxonomy/5286.

[73] Ratledge, C. and Hall, M. J., Accumulation of Lipid by *Rhodotorula glutinis* in Continuous Culture. Biotechnology Letters, 1979. **1**(3): p. 115-20.

[74] Yoon, S. H. and Rhee, J. S., Lipid from Yeast Fermentation: Effects of Cultural Conditions on Lipid Production and Its Characteristics of *Rhodotorula glutinis.* Journal of the American Oil Chemists' Society, 1983. **60**(7): p. 1281-6.

[75] Li, Y., Zhao, Z. K., and Bai, F., High-density cultivation of oleaginous yeast *Rhodosporidium toruloides* Y4 in fed-batch culture. Enzyme and Microbial Technology, 2007. **41**(3): p. 312-17.

[76] Pan, J. G., Kwak, M. Y., and Rhee, J. S., High density cell culture of *Rhodotorula glutinis* using oxygen-enriched air. Biotechnology Letters, 1986. **8**(10): p. 715-8.

[77] Dias, C., Sousa, S., Caldeira, J., Reis, A.*, et al.*, New dual-stage pH control fed-batch cultivation strategy for the improvement of lipids and carotenoids production by the red yeast *Rhodosporidium toruloides* NCYC 921. Bioresource Technology, 2015. **189**: p. 309-18.

[78] Ratledge, C. and Hall, M. J., Oxygen Demand by Lipid-Accumulating Yeasts in Continuous Culture. Applied and Environmental Microbiology, 1977. **34**(2): p. 230-1.

[79] Silva, C. I. S., *Otimização das condições de cultivo da levedura Rhodosporidium toruloides NCYC 921 para produção de lípidos e carotenóides em frascos agitados [Optimization of conditions for culturing Rhodosporidium toruloides NCYC 921 in shake flasks for the production of lipids and carotenoids]*, in *Food Engineering*. 2015, Instituto Superior de Agronomia: Lisbon. p. 65.

[80] Zhao, X., Hu, C., Wu, S., Shen, H.*, et al.*, Lipid production by *Rhodosporidium toruloides* Y4 using different substrate feeding strategies. Journal of Industrial Microbiology & Biotechnology, 2011. **38**(5): p. 627-32.

[81] Wiebe, M. G., Koivuranta, K., Penttilä, M., and Ruohonen, L., Lipid production in batch and fed-batch cultures of *Rhodosporidium toruloides* from 5 and 6 carbon carbohydrates. BMC Biotechnology, 2012. **12**(26).

[82] Frengova, G. I. and Beshkova, D. M., Carotenoids from *Rhodotorula* and *Phaffia*: yeasts of biotechnological importance. Journal of Industrial Microbiology & Biotechnology, 2009. **36**(2): p. 163-80.

[83] National Collection of Yeast Cultures. *NCYC 921. Rhodosporidium toruloides*. 2015 [cited 2015 May 26]; Available from: https://catalogue.ncyc.co.uk/rhodosporidium-toruloides-921.

[84] Riggs, J. B. and Karim, M. N., *Introduction to Chemical and Bio-Process Control*, in *Chemical and Bio-Process Control. Third Edition*. 2007, Pearson Education International: Boston, MA.

[85] Teixeira, J. A., Fonseca, M. M. d., and Vicente, A. A., *Geometrias e Modos de Operação [Geometry and Modes of Operation]*, in *Reactores Biológicos. Fundamentos e Aplicações [Biological Reactors. Fundamentals and Applications]*, M.M.d. Fonseca and J.A. Teixeira, Editors. 2007, LIDEL - Edições Técnicas Lda.: Lisbon, Portugal.

[86] Weusthuis, R. A., Pronk, J. T., van den Broek, P. J., and van Dijken, J. P., Chemostat Cultivation as a Tool for Studies on Sugar Transport in Yeasts. Microbiological Reviews, 1994. **58**(4): p. 616-30.

[87] Doran, P. M., *Reactor Engineering*, in *Bioprocess Engineering Principles*. 1995, Elsevier Science & Technology Books.

[88] Pinheiro, H. M. and Lourenço, N. D., *Reactores de Tratamento Aeróbio [Reactors for Aerobic Treatment]*, in *Reactores Biológicos. Fundamentos e Aplicações [Biological Reactors. Fundamentals and Applications]*, M.M.d. Fonseca and J.A. Teixeira, Editors. 2007, LIDEL - Edições Técnicas Lda.: Lisbon, Portugal.

[89] Battle, I. and Tous, J., *Carob Tree (Ceratonia siliqua L.)*. 1997, Via Delle Sette Chiese 14200145 Rome, Italy: International Plant Genetic Resources Institute.

[90] Turhan, I., Bialka, K. L., Demirci, A., and Karhan, M., Ethanol production from carob extract by using *Saccharomyces cerevisiae.* Bioresource Technology, 2010. **101**(14): p. 5290-6.

[91] Sánchez, S., Lozano, L. J., Godínez, C., Juan, D.*, et al.*, Carob pod as a feedstock for the production of bioethanol in Mediterranean areas. Applied Energy, 2010. **87**(11): p. 3417-24.

[92] Bahloul, A., Khlifa, M., Kitane, S., Lakhtib, I.*, et al.*, Effect of Water Treatment and Optimization of Extraction Applied to the Carob Pulp. Asian Journal of Engineering and Technology, 2013. **1**(3): p. 84-93.

[93] Yousif, A. K. and Alghzawi, H. M., Processing and characterization of carob powder. Food Chemistry, 2000. **69**: p. 283-7.

[94] Karkacier, M. and Artik, N., Determination of physical properties, chemical composition and extraction conditions of carob bean (*Ceratonia siliqua* L.). Gida, 1995. **20**(3): p. 131-6.

[95] Turhan, I., Tetik, N., Aksu, M., Karhan, M.*, et al.*, Liquid-solid extraction of soluble solids and total phenolic compounds of carob bean (*Ceratonia siliqua* L.). Journal of Food Process Engineering, 2006. **29**(5): p. 498-507.

[96] Larsson, S., Palmqvist, E., Hahn-Hägerdal, B., Tengborg, C.*, et al.*, The generation of fermentation inhibitors during dilute acid hydrolysis of softwood. Enzyme and Microbial Technology, 1999. **24**: p. 151-9.

[97] Keating, J. D., Panganiban, C., and Mansfield, S. D., Tolerance and adaptation of ethanologenic yeasts to lignocellulosic inhibitory compounds. Biotechnol Bioeng, 2006. **93**(6): p. 1196-206.

[98] Palmqvist, E. and Hahn-Hägerdal, B., Fermentation of lignocellulosic hydrolysates. I: inhibition and detoxification. Bioresource Technology, 2000. **74**: p. 17-24.

[99] Palmqvist, E. and Hahn-Hägerdal, B., Fermentation of lignocellulosic hydrolysates. II: inhibitors and mechanisms of inhibition. Bioresource Technology, 2000. **74**: p. 25-33.

[100] Robertson, S. *What is Flow Cytometry?* 2014 [cited 2015 March 20]; Available from: http://www.news-medical.net/health/What-is-Flow-Cytometry.aspx.

[101] Díaz, M., Herrero, M., García, L. A., and Quirós, C., Application of flow cytometry to industrial microbial bioprocesses. Biochemical Engineering Journal, 2010. **48**(3): p. 385-407.

[102] Cutzu, R., Clemente, A., Reis, A., Nobre, B.*, et al.*, Assessment of β-carotene content, cell physiology and morphology of the yellow yeast *Rhodotorula glutinis* mutant 400A15 using flow cytometry. Journal of Industrial Microbiology & Biotechnology, 2013. **40**(8): p. 865-75.

[103] Nelson, D. L. and Cox, M. M., *Biological Membranes and Transport*, in *Principles of Biochemistry*. 2008, W. H. Freeman and Company: New York.

[104] Nelson, D. L. and Cox, M. M., *Oxidative Phosphorylation and Photophosphorylation*, in *Principles of Biochemistry*. 2008, W. H. Freeman and Company: New York.

[105] Dinsdale, M. G., Lloyd, D., and Jarvis, B., Yeast vitality during cider fermentation: two approaches to the measurement of membrane potential. Journal of the Institute of Brewing, 1995. **101**: p. 453-8.

[106] Life Technologies. *DiOC6(3) (3,3'-Dihexyloxacarbocyanine Iodide)*. 2015 [cited 2015 March 31]; Available from: https://www.lifetechnologies.com/order/catalog/product/D273.

[107] Shapiro, H. M., Microbial analysis at the single-cell level: tasks and techniques. Journal of Microbiological Methods, 2000. **42**: p. 3-16.

[108] Parthulsot, N., Catala, P., Lemarchand, K., Baudart, J.*, et al.*, Evaluation of ChemChrome V6 for bacterial viability assessment in waters. Journal of Applied Microbiology, 2000. **89**(2): p. 370-80.

[109] Jepras, R. I., Carter, J., Pearson, C., Paul, F. E.*, et al.*, Development of a Robust Flow Cytometric Assay for Determining Numbers of Viable Bacteria. Applied and Environmental Microbiology, 1995. **61**(7): p. 2696-701.

[110] Malacrino, P., Zapparoli, G., Torriani, S., and Dellaglio, F., Rapid detection of viable yeasts and bacteria in wine by flow cytometry. Journal of Microbiological Methods, 2001. **45**: p. 127-34.

[111] Diaper, J. P. and Edwards, C., The use of fluorogenic esters to detect viable bacteria by flow cytometry. Journal of Applied Bacteriology, 1994. **77**: p. 221-8.

[112] Hoefel, D., Grooby, W. L., Monis, P. T., Andrews, S.*, et al.*, A comparative study of carboxyfluorescein diacetate and carboxyfluorescein diacetate succinimidyl ester as indicators of bacterial activity. Journal of Microbiological Methods, 2003. **52**: p. 379-88.

[113] Vives-Rego, J., Lebaron, P., and Nebe-von Caron, G., Current and future applications of flow cytometry in aquatic microbiology. FEMS Microbiology Reviews, 2000. **24**: p. 429-48.

[114] López-Amorós, R., Castel, S., Comas-Riu, J., and Vives-Rego, J., Assessment of *E. coli* and *Salmonella* Viability and Starvation by Confocal Laser Microscopy and Flow Cytometry Using Rhodamine 123, DiBAC4(3), Propidium Iodide, and CTC. Cytometry, 1997. **29**(4): p. 298-305.

[115] Lebaron, P., Catala, P., and Parthulsot, N., Effectiveness of SYTOX Green Stain for Bacteria Viability Assessment. Applied and Environmental Microbiology, 1998. **64**(7): p. 2697-700.

[116] Zuliani, T., Duval, R., Jayat, C., Schnebert, S.*, et al.*, Sensitive and Reliable JC-1 and TOTO-3 Double Staining to Assess Mitochondrial Transmembrane Potential and Plasma Membrane Integrity: Interest for Cell Death Investigations. Cytometry A, 2003. **54**(2): p. 100-8.

[117] Looser, V., Hammes, F., Keller, M., Berney, M.*, et al.*, Flow-Cytometric Detection of Changes in the Physiological State of *E. coli* Expressing a Heterologous Membrane Protein During Carbon-Limited Fedbatch Cultivation. Biotechnology and Bioengineering, 2005. **92**(1): p. 69-78.

[118] Shi, L., Gunther, S., Hubschmann, T., Wick, L. Y.*, et al.*, Limits of Propidium Iodide as a Cell Viability Indicator for Environmental Bacteria. Cytometry A, 2007. **71**(8): p. 592-8.

[119] Melin, P., Hakansson, S., Eberhard, T. H., and Schnurer, J., Survival of the biocontrol yeast *Pichia anomala* after long-term storage in liquid formulations at different temperatures, assessed by flow cytometry. Journal of Applied Microbiology, 2006. **100**(2): p. 264-71.

[120] Juzwa, W. and Czaczyk, K., Flow Cytometry Analysis of Microbial Contamination in Food Industry Technological Lines - Inital Study. ACTA Scientiarum Polonorum Technologia Alimentaria, 2012. **11**(2): p. 111-9.

[121] Muro, M., Izumi, K., Imai, T., Ogawa, Y.*, et al.*, Yeast Cell Cycle During Fermentation and Beer Quality. Journal of the American Society of Brewing Chemists, 2006. **64**(3): p. 151-4.

[122] Kuřec, M., Baszczyňski, M., Lehnert, R., Mota, A.*, et al.*, Flow Cytometry for Age Assessment of a Yeast Population and its Application in Beer Fermentations. Journal of the Institute of Brewing, 2009. **115**(3): p. 253-8.

[123] Bruetschy, A., Laurent, M., and Jacquet, R., Use of flow cytometry in oenology to analyse yeasts. Letters in Applied Microbiology, 1994. **18**: p. 343-5.

[124] Lloyd, D., Moran, C. A., Suller, M. T. E., and Dinsdale, M. G., Flow Cytometric Monitoring of Rhodamine 123 and a Cyanine Dye Uptake by Yeast During Cider Fermentation. Journal of the Institute of Brewing, 1996. **102**: p. 251-9.

[125] Pina-Vaz, C., Sansonetty, F., Rodrigues, A. G., Costa-de-Oliveira, S.*, et al.*, Susceptibility to fluconazole of *Candida* clinical isolates determined by FUN-1 staining with flow cytometry and epifluorescence microscopy. Journal of Medical Microbiology, 2001. **50**(4): p. 375-82.

[126] Pinto, E., Queiroz, M. J., Vale-Silva, L. A., Oliveira, J. F.*, et al.*, Antifungal activity of synthetic di(hetero)arylamines based on the benzo[*b*]thiophene moiety. Bioorganic & Medicinal Chemistry, 2008. **16**(17): p. 8172-7.

[127] Wood, D. N., Chaussee, M. A., Chaussee, M. S., and Buttaro, B. A., Persistence of *Streptococcus pyogenes* in Stationary-Phase Cultures. Journal of Bacteriology, 2005. **187**(10): p. 3319-28.

[128] Berney, M., Hammes, F., Bosshard, F., Weilenmann, H. U.*, et al.*, Assessment and Interpretation of Bacterial Viability by Using the LIVE/DEAD BacLight Kit in Combination With Flow Cytometry. Applied and Environmental Microbiology, 2007. **73**(10): p. 3283-90.

[129] Hoefel, D., Monis, P. T., Grooby, W. L., Andrews, S.*, et al.*, Profiling bacterial survival through a water treatment process and subsequent distribution system. Journal of Applied Microbiology, 2005. **99**(1): p. 175-86.

[130] Foladori, P., Bruni, L., Tamburini, S., and Ziglio, G., Direct quantification of bacterial biomass in influent, effluent and activated sludge of wastewater treatment plants by using flow cytometry. Water Research, 2010. **44**(13): p. 3807-18.

[131] Srienc, F., Cytometric data as the basis for rigorous models of cell population dynamics. Journal of Biotechnology, 1999. **71**: p. 233-8.

[132] Davey, H. M. and Winson, M. K., Using Flow Cytometry to Quantify Microbial Heterogeneity. Current Issues in Molecular Biology, 2003. **5**(1): p. 9-15.

[133] Cipollina, C., Vai, M., Porro, D., and Hatzis, C., Towards understanding of the complex structure of growing yeast populations. Journal of Biotechnology, 2007. **128**(2): p. 393-402.

[134] Camacho, F. G., Belarbi, E. H., García, M. C. C., Mirón, A. S.*, et al.*, Shear effects on suspended marine sponge cells. Biochemical Engineering Journal, 2005. **26**(2-3): p. 115-21.

[135] Alcon, A., Santos, V. E., Casas, J. A., and García-Ochoa, F., Use of flow cytometry for growth structured kinetic model development. Application to *Candida bombicola* growth. Enzyme and Microbial Technology, 2004. **34**(5): p. 399-406.

[136] Quiros, C., Herrero, M., Garcia, L. A., and Diaz, M., Quantitative Approach to Determining the Contribution of Viable-but-Nonculturable Subpopulations to Malolactic Fermentation Processes. Applied and Environmental Microbiology, 2009. **75**(9): p. 2977-81.

[137] Garcia-Ochoa, F., Santos, V. E., and Alcon, A., Structured kinetic model for *Xanthomonas campestris* growth. Enzyme and Microbial Technology, 2004. **34**(6): p. 583-94.

[138] Zhao, X., Peng, F., Du, W., Liu, C.*, et al.*, Effects of some inhibitors on the growth and lipid accumulation of oleaginous yeast *Rhodosporidium toruloides* and preparation of biodiesel by enzymatic transesterification of the lipid. Bioprocess and Biosystems Engineering, 2012. **35**(6): p. 993-1004.

[139] Miller, G. L., Use of Dinitrosalicylic Acid Reagent for Determination of Reducing Sugar. Analytical Chemistry, 1959. **31**(3): p. 426-8.

[140] Lepage, G. and Roy, C. C., Direct transesterificação of all classes of lipids in a one-step reaction. Journal of Lipid Research, 1986. **27**(1): p. 114-20.

[141] Sousa, A. S. S., *Produção microbiana de lípidos e carotenóides em culturas da levedura Rhodosporidium toruloides NCYC 921 desenvolvidas em regime semi-descontínuo [Microbial production of lipids and carotenoids in Rhodosporidium toruloides NCYC 921 cultures developed in fed-batch mode]*, in *Biological Engineering*. 2014, Instituto Superior Técnico: Lisbon, Portugal.

[142] Parreira, T. M., *Otimização do processo de produção de lípidos e carotenóides a partir da biomassa da levedura Rhodotorula glutinis NRRL Y-1091 [Optimization of the production process*

of lipids and carotenoids from Rhodotorula glutinis NRRL Y-1091 biomass], in *Food Engineering*. 2014, Instituto Superior de Agronomia: Lisbon, Portugal.

[143] Gírio, F. M., Carvalheiro, F., Duarte, L. C., and Bogel-Łukasik, R., *Deconstruction of the Hemicellulose Fraction from Lignocellulosic Materials into Simple Sugars*, in *D-Xylitol. Fermentative Production, Application and Commercialization.*, S.S. da Silva and A.K. Chandel, Editors. 2012, Springer Berlin Heidelberg. p. 3-37.

[144] Mata-Goméz, L. C., Montañez, J. C., Méndez-Zavala, A., and Aguilar, C. N., Biotechnological production of carotenoids by yeasts: an overview. Microbial Cell Factories, 2014. **13**(12): p. 1-11.

Annex I – Chemical reagents

The reagents used in this work, their molar mass, chemical formula, purity, brand and application are listed in Table A.1.

Table A.1 – Chemical reagents used in this work. A, assays; CE, carotenoids extraction; CM, culture medium; FC, flow cytometry; HPLC, high performance liquid chromatography; NG, nutrient solution; RG, residual glucose; SM, slant medium; TR, transesterification reaction.

Name	MM ($g.mol^{-1}$)	Chemical formula	Purity	Brand	Application
3,3'-Dihexyloxacarbocyanine iodide	572.23	$C_{29}H_{37}IN_2O_2$	-	Invitrogen	FC
3,5-Dinitrosalisilic acid	228.12	$C_7H_6O_5 \cdot H_2O$	-	Merck	RG
Acetone	58.08	CH_3COCH_3	99.5%	Merck	CE
Acetonitrile	41.05	C_2H_3N	-	Carlo Erba	HPLC
Acetyl chloride	78.50	C_2H_3ClO	98.5%	Panreac	TR
Aluminum chloride, hexahydrate	241.45	$AlCl_3 \cdot 6H_2O$	97.0%	Merck	CM
Ammonium sulfate	132.14	$(NH_4)_2SO_4$	99.0%	Panreac	CM
Calcium chloride, dihydrate	147.02	$CaCl_2 \cdot 2H_2O$	99.5%	Merck	CM
Calcium Titriplex®, dihydrate	410.31	$C_{10}H_{12}CaN_2Na_2O_8 \cdot 2H_2O$	98.0%	Merck	HPLC
Cobalt chloride	129.84	$CoCl_2$	99.0%	Fluka	CM
Copper chloride, dihydrate	170.48	$CuCl_2 \cdot 2H_2O$	99.0%	Merck	CM
D-Glucose, anhydrous	180.16	$C_6H_{12}O_6$	99.5%	Pronolab	CM; NG; RG; HPLC
Dimethyl sulfoxide	78.13	C_2H_6OS	-	Riedel-de-Haën	CE; FC
Disodium hydrogen phosphate	141.96	Na_2HPO_4	99.0%	Panreac	CM
Ethyl acetate	88.00	$C_4H_8O_2$	-	Carlo Erba	HPLC
Fructose	180.16	$C_6H_{12}O_6$	99.5%	Fagron	HPLC
Hydrochloric acid	36.45	HCl	37.0%	Merck	A
Iron(II) sulfate, heptahydrate	278.02	$FeSO_4 \cdot 7H_2O$	99.5%	Merck	CM
Magnesium sulfate, heptahydrate	246.48	$MgSO_4 \cdot 7H_2O$	99.5%	Merck	CM; NG
Malt extract agar	-	-	-	Himedia	SM
Manganese sulfate, heptahydrate	277.11	$MnSO_4 \cdot 7H_2O$	99.0	-	CM
Methanol	32.04	CH_3OH	99.8%	Merck	HPLC; TR
Monopotassium phosphate	136.09	KH_2PO_4	99.0%	Panreac	CM
n-Heptane	100.21	C_7H_{16}	99.0%	Merck	TR
n-Hexane	86.18	C_6H_{14}	99.5%	Fisher Chemical	CE
Petroleum ether (40 °C – 60 °C)	-	$(CH_3)_3COCH_3$	-	Fisher Chemical	CE
Petroleum ether (80 °C – 100 °C)	-	$(CH_3)_3COCH_3$	-	Fisher Chemical	TR
Polypropylene glycol	-	-	-	Prolab	A
Potassium sodium tartrate	282.23	$KNaC_4H_4O_6 \cdot 4H_2O$	99.0%	Panreac	RG
Propidium iodide	668.4	$C_{27}H_{34}I_2N_4$	-	Invitrogen	FC
Sodium chloride	58.44	NaCl	99.5%	Pronolab	CE

Table A.1 (continuation) – Chemical reagents used in this work. A, assays; CE, carotenoids extraction; CM, culture medium; FC, flow cytometry; HPLC, high performance liquid chromatography; NG, nutrient solution; RG, residual glucose; SM, slant medium; TR, transesterification reaction.

Name	MM ($g.mol^{-1}$)	Chemical formula	Purity	Brand	Application
Sodium hydroxide	39.99	NaOH	-	José M. Vaz Pereira	A
Sodium molybdate, dihydrate	241.95	$Na_2MoO_4 \cdot 2H_2O$	99.5%	Merck	CM
Sodium sulfate, anhydrous	142.04	Na_2SO_4	99.0%	Merck	RT; CE
Sucrose	342.30	$C_{12}H_{22}O_{11}$	99.5%	Mikrobiologie	HPLC
Sulfuric acid	98.08	H_2SO_4	97.0%	Merck	HPLC
Triethylamine	101.10	$N(CH_2CH_3)_3$	89.5%	Panreac	HPLC
Yeast extract	-	-	-	BD	CM; NG
Zinc sulfate, heptahydrate	287.55	$ZnSO_4 \cdot 7H_2O$	99.5%	M&B	CM